WORKSHOP HOSTED BY FRAGBLAST 10 — THE 10TH INTERNATIONAL SYMPOSIUM ON ROCK FRAGMENTATION BY BLASTING, NEW DELHI, INDIA, 24–25 NOVEMBER 2012

Performance of Explosives and New Developments

Editors

Bibhu Mohanty
Department of Civil Engineering and Lassonde Institute of Mining, University of Toronto, Toronto, Canada

Vinay Kumar Singh
Northern Coalfields Limited, Singrauli, India

Downloaded by [Visvesvaraya Technological University (VTU Consortium)] at 21:50 01 March 2016

CRC Press
Taylor & Francis Group
Boca Raton London New York Leiden

CRC Press is an imprint of the
Taylor & Francis Group, an **informa** business

A BALKEMA BOOK

Downloaded by [Visvesvaraya Technological University (VTU Consortium)] at 21:50 01 March 2016

CRC Press/Balkema is an imprint of the Taylor & Francis Group, an informa business

© 2013 Taylor & Francis Group, London, UK

Typeset by V Publishing Solutions Pvt Ltd., Chennai, India
Printed and bound in Great Britain by CPI Group (UK) Ltd, Croydon, CR0 4YY

All rights reserved. No part of this publication or the information contained herein may be reproduced, stored in a retrieval system, or transmitted in any form or by any means, electronic, mechanical, by photocopying, recording or otherwise, without written prior permission from the publisher.

Although all care is taken to ensure integrity and the quality of this publication and the information herein, no responsibility is assumed by the publishers nor the author for any damage to the property or persons as a result of operation or use of this publication and/or the information contained herein.

Published by: CRC Press/Balkema
P.O. Box 447, 2300 AK Leiden, The Netherlands
e-mail: Pub.NL@taylorandfrancis.com
www.crcpress.com – www.taylorandfrancis.com

ISBN: 978-0-415-62142-7 (Hbk + CD-ROM)
ISBN: 978-0-203-38770-2 (eBook)

Performance of Explosives and New Developments – Mohanty & Singh (Eds)
© 2013 Taylor & Francis Group, London, ISBN 978-0-415-62142-7

Table of contents

Downloaded by [Visvesvaraya Technological University (VTU Consortium)] at 21:50 01 March 2016

Downloaded by [Visvesvaraya Technological University (VTU Consortium)] at 21:50 01 March 2016

Performance of Explosives and New Developments – Mohanty & Singh (Eds)
© 2013 Taylor & Francis Group, London, ISBN 978-0-415-62142-7

Preface

Downloaded by [Visvesvaraya Technological University (VTU Consortium)] at 21:50 01 March 2016

This volume is part of a continuing series of workshops that are normally held in conjunction with the International Symposium on Rock Fragmentation by Blasting (FRAGBLAST), held at 3–4 year intervals. Whereas the main symposium is directed at the latest research and developments in the field of rock fragmentation, the workshops are geared more towards practitioners in the field. As this volume illustrates, there is considerable scope for improvement in the outcome of any blasting operation when accompanied by basic understanding and applications of the principles of blasting science and technology. The main objective is to sensitize the practitioner to critically examine the various empirical approaches in blasting which may be of long use, but lack any sound physical basis. On the other hand, where the empirical approaches have proven of value, significant additional improvement can be achieved through better understanding of the underlying process. The overwhelming message is that none of the components involved in a blasting operation should be treated in isolation, as they are all inter-linked. Fragmentation of rock by blasting represents the first stage in the size reduction process which is essential to liberation of valuable minerals and metals. Therefore, understanding the performance of the explosive and initiators under actual field conditions, and critical assessment of the blast results afterwards are central to effective blast design, improved productivity, and novel applications.

B. Mohanty
University of Toronto, Toronto, Canada

V.K. Singh
Northern Coalfields Limited, Singrauli, India

Performance of Explosives and New Developments – Mohanty & Singh (Eds)
© 2013 Taylor & Francis Group, London, ISBN 978-0-415-62142-7

Organising Institution

CSIR - Central Institute of Mining & Fuel Research
(Council of Scientific & Industrial Research)
Dhanbad, India

Downloaded by [Visvesvaraya Technological University (VTU Consortium)] at 21:50 01 March 2016

Performance of Explosives and New Developments – Mohanty & Singh (Eds)
© 2013 Taylor & Francis Group, London, ISBN 978-0-415-62142-7

Committees

Downloaded by [Visvesvaraya Technological University (VTU Consortium)] at 21:50 01 March 2016

PATRONS

- Prof. Samir K. Brahmachari, *Director General, CSIR and Secretary, DSIR, New Delhi*
- Mr. Partho S. Bhattacharyya, *Chairman, CSIR-CIMFR, Research Council, Dhanbad*
- Mr. Satish Puri, *Director General of Mines Safety, DGMS, Dhanbad*
- Mr. S. Narsing Rao, *Chairman-cum-Managing Director, Coal India Limited, Kolkata*

CHAIRMAN ORGANISING COMMITTEE

- Dr. Amalendu Sinha, *Director, CSIR-CIMFR, Dhanbad*

ORGANISING SECRETARY & CONVENOR

- Dr. Pradeep K. Singh, *Senior Principal Scientist, CSIR-CIMFR, Dhanbad*

INTERNATIONAL ORGANISING COMMITTEE

Prof. W.L. Fourney	*University of Maryland, USA*
Prof. José A. Sanchidrián	*Universidad Politecnica de Madrid, Spain*
Docent Agne Rustan	*Retired from Luleå University of Technology, Sweden*
Prof. Hans Peter Rossmanith	*Technical University, Vienna, Austria*
Prof. Sushil Bhandari	*Earth Resource Technology Consultants, India*
Dr. Cameron K. McKenzie	*Blastechnology, Australia*
Prof. Bibhu Mohanty	*University of Toronto, Canada*
Prof. Xuguang Wang	*Beijing General Research Institute of Mining & Metallurgy, China*
Mr. R. Frank Chiappetta	*Blasting Analysis International, USA*
Mr. Carlos P. Orlandi	*Enaex Servicios S.A., Chile*
Prof. Finn Ouchterlony	*Montanuniversitaet Leoben, Austria*
Prof. Kunihisa Katsuyama	*(Retired from) Ehime University, Japan*
Dr. William Robert Adamson	*Davey Bickford, Chile*
Prof. Panagiotis D. Katsabanis	*Queen's University, Canada*
Prof. Peter Moser	*Montanuniversitaet Leoben, Austria*
Dr. Ken Qian Liu	*Xstrata Nickel, Canada*
Dr. Ewan Sellers	*African Explosives, South Africa*
Dr. A.T. Spathis	*Orica, Australia*
Dr. Dale S. Preece	*Orica Mining Services, USA*

REVIEW COMMITTEE

Prof. W.L. Fourney	*University of Maryland, USA*
Prof. José A. Sanchidrián	*Universidad Politecnica de Madrid, Spain*
Docent Agne Rustan	*Retired from Luleå University of Technology, Sweden*
Prof. Sushil Bhandari	*Earth Resource Technology Consultants, India*

Dr. Cameron K. McKenzie	*Blastechnology, Australia*
Prof. Bibhu Mohanty	*University of Toronto, Canada*
Prof. Xuguang Wang	*Beijing General Research Institute of Mining & Metallurgy, China*
Mr. R. Frank Chiappetta	*Blasting Analysis International, USA*
Mr. Carlos P. Orlandi	*EnaexServicios S.A., Chile*
Prof. Finn Ouchterlony	*Montanuniversitaet Leoben, Austria*
Dr. William Robert Adamson	*Davey Bickford, Chile*
Prof. Panagiotis D. Katsabanis	*Queen's University, Canada*
Prof. Peter Moser	*Montanuniversitaet Leoben, Austria*
Dr. Ken Qian Liu	*Xstrata Nickel, Canada*
Dr. Ewan Sellers	*African Explosives, South Africa*
Dr. A.T. Spathis	*Orica, Australia*
Dr. Dale S. Preece	*Orica Mining Services, USA*
Dr. Pradeep K. Singh	*CSIR-Central Institute of Mining & Fuel Research, India*
Dr. Amalendu Sinha	*CSIR-Central Institute of Mining & Fuel Research, India*
Dr. Alastair Torrance	*Kilmorie Consulting, Australia*
Dr. Alexander Hennig	*RWTH Aachen University, Germany*
Prof. Ali Mortazavi	*Amirkabir University of Technology, Iran*
Prof. Ajoy K. Ghose	*Formerly, Indian School of Mines, India*
Mr. Akhilesh Joshi	*Hindustan Zinc Ltd, India*
Mr. Ashok Kumar Singh	*Central Mine Planning & Design Institute, India*
Dr. AymanTawadrous	*Orica Mining Services, USA*
Prof. C. Niemann-Delius	*RWTH Aachen University, Germany*
Prof. Carsten Drebenstedt	*Technical University, Freiberg, Germany*
Dr. Catherine T. Aimone-Martin	*New Mexico Tech, USA*
Prof. Charles H. Dowding	*Northwestern University, USA*
Prof. Claude Cunningham	*Blasting Investigations and Consultancy, South Africa*
Dr. Essaieb Hamdi	*Ecole Nationale D'Ingénieurs, Tunisia*
Dr. Geoff F. Brent	*Orica Research and Development, Australia*
Dr. Italo Andres Onederra	*CRC Mining – The University of Queensland, Australia*
Prof. John Kemeny	*University of Arizona, USA*
Dr. Lina M. López	*Universidad Politécnica de Madrid – E.T.S.I. Minas, Spain*
Dr. Michael Noy	*Orica, Australia*
Dr. Pablo Segarra	*Universidad Politécnica de Madrid – E.T.S.I. Minas, Spain*
Dr. Pijush Pal Roy	*CSIR-Central Institute of Mining & Fuel Research, India*
Prof. R.N. Gupta	*Consultant in Geotechnical/Rock Engineering, India*
Dr. Roger Holmberg	*Secretary General, EFEE, Malta*
Dr. Ruilin Yang	*Orica USA Inc, USA*
Prof. S.P. Singh	*School of Engineering, Laurentian University, Canada*
Prof. Stanley Vitton	*Michigan Technological University, USA*
Mr. Vinay Kumar Singh	*Northern Coalfields Limited, India*
Dr. William Birch	*Blastlog Ltd, United Kingdom*

Downloaded by [Visvesvaraya Technological University (VTU Consortium)] at 21:50 01 March 2016

Performance of Explosives and New Developments – Mohanty & Singh (Eds)
© 2013 Taylor & Francis Group, London, ISBN 978-0-415-62142-7

Sponsors

Downloaded by [Visvesvaraya Technological University (VTU Consortium)] at 21:50 01 March 2016

Diamond Sponsor

Coal India Limited

Platinum Sponsors

Solar Industries India Limited

Orica

Deepak Fertilisers & Petrochemicals Corporation Ltd.

Hindustan Zinc Limited
(Vedanta Group Company)

Tata Steel

Gold Sponsors

Singareni Collieries Company Limited

Jindal Steel & Power Limited

Silver Sponsors

NMDC Ltd.

Essel Mining & Industries Limited

National Aluminium Company Limited

Jaiprakash Industries Limited

Manganese Ore (India) Limited

Uranium Corporation of India Limited

EMTA Group of Companies

Sarda Mines Pvt. Ltd.

Downloaded by [Visvesvaraya Technological University (VTU Consortium)] at 21:50 01 March 2016

Bronze Sponsors

Gujarat Mineral
Development Corporation

IDL Explosives Limited

J.K. Cement

Hutti Gold Mines Limited

V.V. Mineral (VVM)

Navbharat Group of Companies

JSW Bengal Steel Ltd.

Neyveli Lignite Corporation Limited

Lunch Sponsor

Ganesh Explosive Pvt. Ltd.

Downloaded by [Visvesvaraya Technological University (VTU Consortium)] at 21:50 01 March 2016

Performance of Explosives and New Developments – Mohanty & Singh (Eds)
© 2013 Taylor & Francis Group, London, ISBN 978-0-415-62142-7

Ideal detonation reaction concepts for blasting engineers

M. Braithwaite
Laboratory for Scientific Computing, Cavendish Laboratory, Cambridge, UK

ABSTRACT: A review of ideal detonation theory, thermochemical computer codes for calculation of ideal detonation behavior and applications of these to blasting engineering is presented. This paper provides background for a first stage analysis of the ideal detonation process in an explosive composition and estimation of detonation parameters such as velocity of detonation and energy. Both these are critical parameters in design of blasts.

1 INTRODUCTION

This article, one of two, is concerned with the modeling of steady state detonations in the heterogeneous media that comprise the bulk of commercial explosives. These explosives are, from the point of view of detonation physics, complex in that they contain a number of reactive ingredients in different phases and the detonation process itself is influenced by the confining rock.

The aim of any detonation physics model for blasting applications is to provide details of available energy, detonation velocity and pressure decay history in order for the user to compare different explosives for different applications. These thermodynamic, and in the case of non-ideal detonation kinetic based, simulations give insight into the overall energetic of the detonating explosive but will not address issues such as damaged explosives (additional water, partial crystallization, pressure desensitization), effects of departures in formulations including density and also explosion fume characteristics. Only steady state detonations are considered here—the modelling on unsteady events, SDT, DDT etc is beyond the scope of these two articles.

The aim of understanding the energetics of detonation process is to provide information on the energy available to the blasting process, its rate and nature of delivery in terms of a pressure history at the detonation product-rock confiner interface. Inevitably only a fraction of the chemical energy released in the detonation process is available for rock fracture and heave because of losses (as heat), possible partial reaction and release of hot gas through rock mass and due to loss of stemming.

A host of different processes govern the overall detonation process e.g. mass, momentum and heat transfer, chemical reaction and phase changes. Treatises on detonation physics tend to be quite mathematical (some included at the end of this chapter—Fickett & Davis (1979), Zukas & Walters (1998), Persson, Holmberg & Lee (1994)). An attempt here is made to keep the mathematical derivations to a minimum and reference is made to comprehensive analyses of detonations published elsewhere. More details are given in Braithwaite, Sharpe & Chitombo (2009).

An analysis of explosive behaviour in a borehole provides the energy source for the fragmentation and movement of the rock mass. It begins (Fig. 1) with a shock wave travelling at a shock velocity D impacting an unreacted explosive and forming hot spots, mainly from the collapse of included voids. The high temperatures resulting from void collapse lead to an ensemble of reaction sites in the

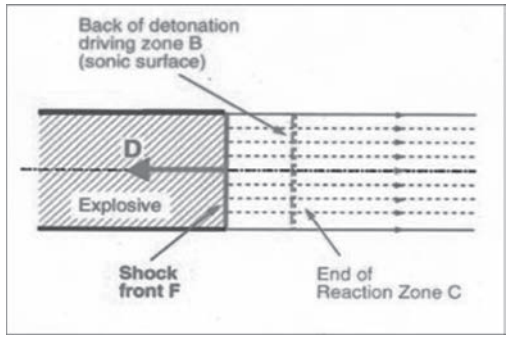

Figure 1. An overall picture of a steady 1-D detonation process in a cylinder with the shock wave moving from right to left at a velocity D. The DDZ zone is bounded by the shock front to the left and the CJ state (where local particle velocity and sound speed are equal) to the right. The starting state is a high pres-sure shock front and the end state of a ZND detonation is the standard CJ condition. The detonation zone is followed by a rarefaction wave where the products expand and the pressure falls rapidly.

Downloaded by [Visvesvaraya Technological University (VTU Consortium)] at 21:51 01 March 2016

condensed phase explosive and within the DDZ (Detonation Driving Zone) and energy liberated in these reaction centres contribute toward the detonation process. At the end of the detonation, the Chapman Jouguet detonate state, the explosion products formed are present as a dense high temperature fluid at equilibrium: much of the work performed on the rock takes place as the dense products expand to a much lower pressure. End pressures, those pressures below which the detonation products do no work on the confiner) are a matter of some debate but can be expected to be in the range 200 to 1000 bara.

In the simplest models of detonation (Fickett & Davis (1979)), only a one-dimensional (1-D) process is considered resulting in detonation products in a state of thermal, mechanical and chemical equilibrium. The first of these models from the turn of the 19th century, (Chapman Jouguet (CJ): Michelson) assumes an infinitely fast reaction rate i.e. the system consists of either fully reacted or (Zeldovich, von Neumann & Doering (ZND)): ZND theory remains a 1-D approach (Figures 1 & 2) starting with an impacting shock front (von Neumann spike) followed by reaction to a CJ state and a longitudinal rarefaction following this. It should be emphasized that in any 1-D analysis no work is done on the surrounding confiner.

The various loci and states of interest are shown in Figure 2. This 1-D solely thermodynamic approach provides a guide for maximum explosive performance, corresponding to large or very well-confined charges.

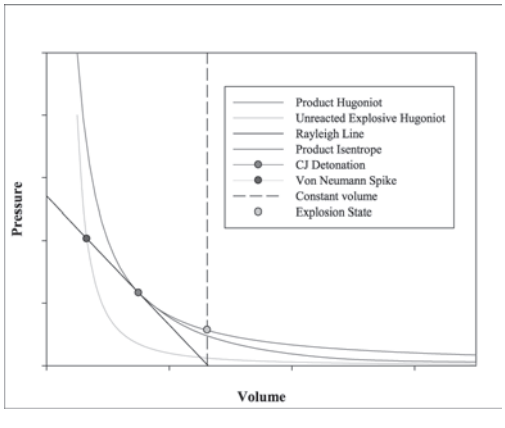

Figure 2. Overall Characteristics of Ideal Detonation Process. Illustrated are the Hugoniot curves for unreacted explosive and detonation products (governed by EOS), the Rayleigh line (mass, momentum conservation) for the CJ State, the product isentrope and the Explosion State (constant volume/energy explosion) on the Product Hugoniot.

A ZND detonation, followed by a rarefaction, is illustrated in Figure 3 for a typical ANFO Explosive. Figure 4 shows a typical set of detonation characteristics for a commercial explosive, albeit undergoing a ZND detonation. The following points are perhaps worth noting:

1. Shock (or Von Neumann spike) pressure (at the highest density) > CJ pressure > pressure along expansion adiabat at the same density as the original explosion.
2. The energy at the shock front > energy at CJ state > original explosive (the latter by a factor corresponding to the kinetic energy of the detonation products)
3. The time for the 99% of the explosive to react is ~50 microseconds

The CJ state, which is also the end detonation state for a ZND detonation, can be defined by that which the VOD is a minimum consistent with conservation of mass, momentum and energy in the

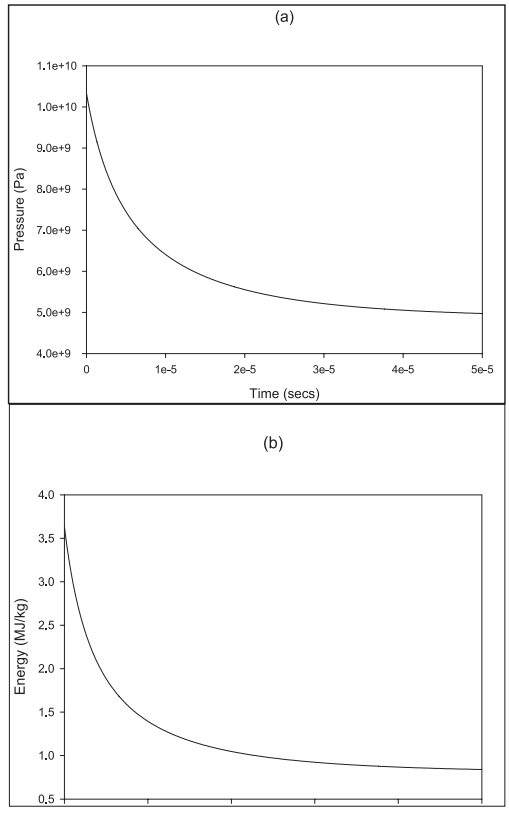

Figure 3. Pressure and Energy histories during a ZND detonation with an ANFO (800 kg/m^3) (a,b). Energies quoted are referenced to the initial energy of the explosive & the CJ state is indicated by a •.

Downloaded by [Visvesvaraya Technological University (VTU Consortium)] at 21:51 01 March 2016

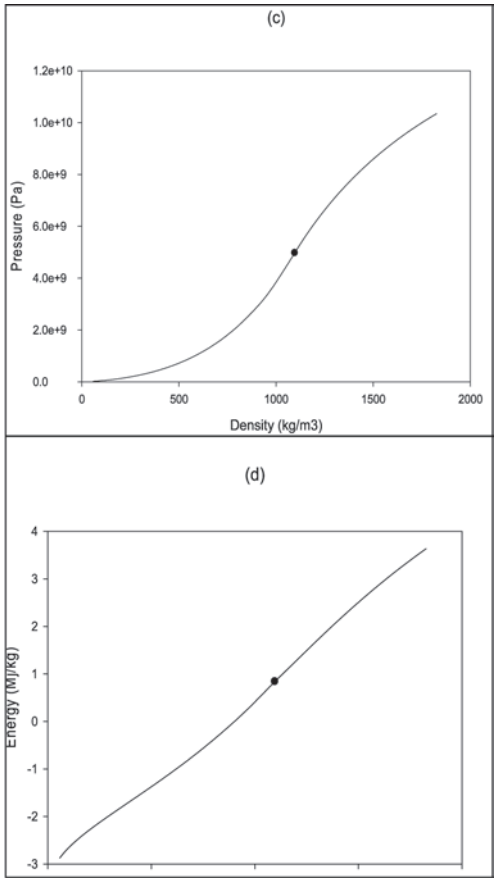

Figure 4. Pressure and Energy during detonation and expansion of detonation products (c,d). Energies quoted are referenced to the initial energy of the explosive & the CJ state is indicated by a •.

system. It can be determined given the following information about the explosive:

- its elemental formulation e.g. gram atoms of each element (C,H,N.O,Cl etc) per unit mass
- the initial density
- the heat of formation at its initial state (nominally 298 K and 1 bara)

The resultant ideal detonation characteristics are governed by the equations of state (EOS) of the fluid and solid detonation products. States may be calculated by empirically derived equations (Kamlet and Jacobs (1968), Rothstein and Petersen (1981)) or by assumptions regarding the detonation products produced.

The thermodynamic EOS of the detonation products, given the density and elevated temperature of this media, has to describe a multicomponent multiphase system. A variety of thermo-chemical computer programs have been written to determine the ideal detonation characteristics of explosive. They differ in prediction dependent on EOS selected though in recent years results have been in general accord when using statistical mechanics based EOS based on intermolecular potentials (Cheetah (Fried et al 1998-), Vixen (Braithwaite et al (2006)), IDeX (Braithwaite et al (1996)), IPX (BME), TDS (Victorov (2006)), Carte (Dubois et al (2010)) rather than semiempirical approaches (Tiger-JCZ3 (Cowperthwaite et al (1976)), TigerWin (Persson (2000))) or cruder approaches, almost entirely empirical and requiring re-parameterization (ex Fortran BKW (Mader (1979). These will be discussed in more detail later in this article.

2 EQUATION OF STATE IN THE DETONATION PROCESS

Ideal detonation (CJ), where the explosive attain mechanical, chemical and thermal equilibrium, requires equations of state to describe the behaviour of the detonation products over a wide range of temperatures and densities. Detonation products are generated typically in pressures and densities in excess of 1 GPa and 1000 kg/m^3: temperatures can be in the range 2000–5000 K. The products typically consist of CO_2, H_2O, N_2, CH_4, H_2, O_2, NO, CO, NH_3, C(s), Al, Al_2O_3, and NaCl etc. Note that commercial explosives tend to be reasonably oxygen balanced and the first three major fluid product species tend to dominate. NOx is sometimes observed in post-blast fumes: this is usually a product of either the reaction between NO and atmospheric O_2 or the breakdown of ammonium nitrate.

EOS can be considered in two categories depending on whether the chemical constituents of the products are explicit or implicit. Ideal detonation analysis involves the use of the former whereas non-ideal detonation simulations are almost entirely based on chemistry implicit EOS for computational efficiency.

3 EOS IN IDEAL DETONATION ANALYSIS

The principal calculation for the evaluation of ideal detonation characteristics is the determination of the chemical equilibrium between the detonation product species present in one or more phases (usually one fluid and possibly a number of solid phases). There are a plethora of texts on the calculation of chemical equilibria and the norm

Downloaded by [Visvesvaraya Technological University (VTU Consortium)] at 21:51 01 March 2016

in ideal detonation computer codes has been for a constrained global minimization of a Free Energy with respect to species concentrations. These calculations require a detailed knowledge of the chemical thermodynamics of each product constituent for the wide pressure-temperature-density domain of interest. Ideal detonations are largely governed by the behaviour of the fluid phase product and this chapter will focus on this. Solid products, such as graphite, alumina, or melts such as ionic halides are usually included by means of a simple solid phase EOS.

Ideal detonation (thermochemical) computer programs have been developed to determine chemical equilibrium conditions and thereby estimates of CJ detonation and explosion state properties and energy release during a subsequent isentropic expansion. They consist of a series of databases for detonation product thermodynamic parameters, a numerical algorithm for determining chemical equilibrium with different EOS and a series of energy balances for states of interest. Much of this software is either owned by individual companies (ex IDeX, IPX, Vixen) or organizations or subject to restrictions on availability because of defence applications (ex Tiger, Carte). Exceptions include the TDS code and the classical Fortran BKW.

An EOS for the fluid products of a detonation should satisfy the following:

1. give good agreement with shock Hugo-niot data (pressure and temperature (where available) for individual product species).
2. be thermodynamically consistent e.g. satisfy corresponding states criteria.
3. deal with polar contributions to energies where appropriate (H_2O, NH_3 etc).
4. not requiring any re-parameterisation i.e. be statistical mechanics based.
5. have realistic interspecies mixing rules.
6. allow calculation of chemical equilibria at modest computational cost.
7. give correct asymptotic behaviour (high and low pressure) and well behaved higher derivatives (adiabatic & Gruneisen Gammas etc).
8. give good agreement with measured ideal VODs (high explosives).

The first 40 years of ideal detonation computer codes were confined to empirical EOS for the dominant fluid phase product. These EOS lacked any detailed comparison with molecular and intermolecular properties and codes using EOS such as BKW (Becker-Wilson-Kistiakowsky) required parameterisation for different classes of explosive. They had the advantage of being computationally efficient and readily extendable. An early attempt to improve on the shortcomings of empirical EOS was made by the development of some semi-empirical EOS, notably (Jacobs, Cowperthwaite and Zwisler) JCZ3. This has been used with some success in Tiger and other codes.

In the 1980's full statistical mechanics based EOS, both hard sphere and variational (e.g. Weeks Chandler Anderson—WCA) based, were adopted and the substantial increase in processor time for detonation calculations largely resolved by the use of fitted EOS using Chebychev polynomials (Byers Brown (1987)). Codes based on this approach are now in common use (Cheetah, TDS, IDeX, Vixen, Carte, IPX and others) and their predictions satisfy all the previously mentioned criteria, in contrast to semi-empirical and empirical approaches. Detonation velocities determined with these more fundamentally based computer programs are

Table 1. Typical ideal detonation velocities compared with measured data.

Explosive	Initial density (kg/m^3)	Predicted detonation velocity (km/s)	Measured detonation velocity (km/s)
PETN	1770	8.25	8.29
NG	1600	7.65	7.70
ANFO	860	5.06	5.16
TNT	1640	6.90	6.95
NM	1130	6.36	6.29
HMN	1630	8.69	8.69
TETRYL	1710	7.74	7.85

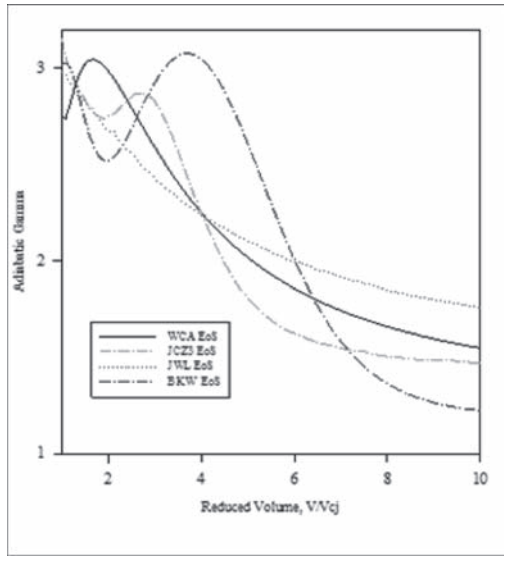

Figure 5. Comparison of adiabatic Gammas for different EOS.

compared with best available measurements for high (molecular) explosives (large diameter/confined cylinders) in Table 1.

The behaviour of the adiabatic Gamma, Γ,

$$\Gamma = -V/P\left(\partial P/\partial V\right)_S \quad (1)$$

where ∂P and ∂V its variation down an isentrope provides a means of discrimination between different EOS in common use. The empirical Jones Wilkins Lee representations as well as the JCZ3 and BKW EOS are at considerable variance with the more accurate WCA form (Fig. 5).

4 RAREFACTION WAVE—EXPANSION OF DETONATION PRODUCTS

As described elsewhere, a detonation process consists of a shock wave, a DDZ reaction zone between the shock front and the sonic locus, and this is followed by a rarefaction (or Taylor wave). In the Taylor wave, the high pressure products expand, (nomi-nally adiabatically) and the pressure and temperature of the products decrease. It is in this part of the detonation process that most of the work on the rock is done. The adiabatic assumption is usually valid as the time for heat transfer from the gas to the surrounds is small: the degree of reaction that might take place during expansion is also small due to the decreasing temperature and the expansion is normally regarded as isentropic.

The extent of the expansion is dependent on the confinement (both radial and lateral). At one extreme, in a closed incompressible system/fixed boundaries, the products can only initially expand to a state where the rarefaction particle velocity is zero and then to the original volume of the borehole. In practice there is lateral expansion of the borehole and loss of gas through rock and stemming. During the rapid expansion further reactions may take place and, due to rapid cooling, some species concentrations may become frozen and the chemical equilibrium condition lost. During the expansion condensation may take place e.g. formation of water.

Figure 6 illustrates the rapid decrease in pressure for an ANFO Taylor wave. It should be noted that high pressure compressibility's in the fluids can be ~10 compared with 1 for an ideal gas. The adiabatic Gamma, is also illustrated, demonstrating a monotonic gradient decrease with volume. A rule of thumb for rock and metal breakage suggests large Gammas preferred for dense, hard media and corresponding small Gammas for soft media.

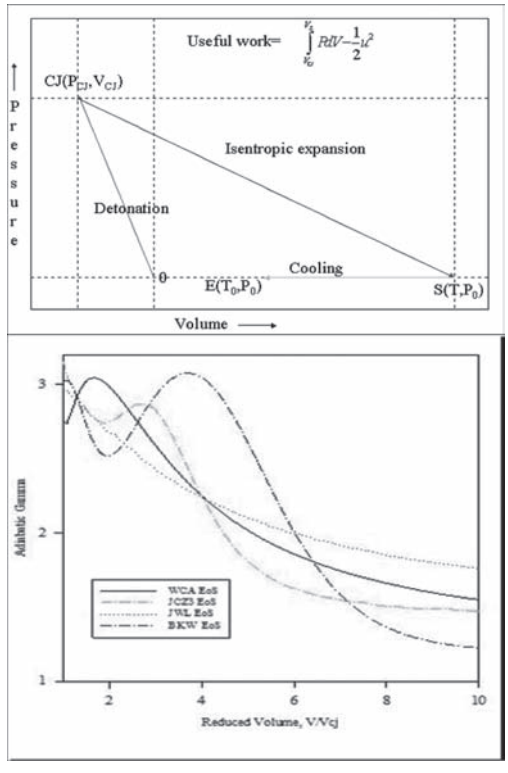

Figure 6. Overall Energetics of a idealised detonation cycle. Explosive is shocked and reacts to reach a CJ detonation state. This undergoes an isentropic expansion to atmospheric pressure (but not necessarily ambient temperature). Useful work is the energy release along isentrope—kinetic energy retained by system.

The useful or available energy from the explosive expansion has been given previously as in Figure 6.

$$E_A = \int_{V_{CJ}}^{V_{end}} PdV - u^2/2 \quad (2)$$

where P, V, and u and correspond to pressure, volume and the particle velocity at the CJ state: the integration is from the CJ state volume, V_{CJ} to the end volume, V_{END}.

The energy plotted in Figure 3 starts at a positive value corresponding to the kinetic energy at the CJ state in the above expression. There is no set end volume or end condition for this calculation. The cut-off pressure or volume where no more useful work on the rock can be done during the expansion will be application dependent. For some explosives the products will reach temperatures below the boiling point of water during the

Downloaded by [Visvesvaraya Technological University (VTU Consortium)] at 21:51 01 March 2016

Downloaded by [Visvesvaraya Technological University (VTU Consortium)] at 21:51 01 March 2016

expansion: however this will have only a marginal effect on the available energy—the latent heat of steam retaining a high temperature in the fluid and compensating for loss of gas volume.

Thermochemical codes cannot and should not be used to predict explosion fume (noxious or flammable by-products e.g. CO, NOx): this is governed by kinetic factors as well as quality issues with explosive and accessories.

5 SHOCK, DETONATION AND EXPLOSION: ROCK FRAGMENTATION AND HEAVE

An explosive in a borehole can either undergo a detonation, a deflagration or a thermal explosion—the last of these would normally be associated with accidental overheating in reactive ground. All these processes generate high pressure fluids that can lead to rock fragmentation and heave.

With reference to Figure 2 and (Sharpe and Braithwaite (2006)), the length of the DDZ zone is dependent on the nature of the explosive and the confinement—the contact zone between this and the confiner is less. It should also be noted that there is a substantial pressure drop between shock front and CJ state in rigid confinement. It may therefore be reasonably concluded than energy transfer out of the DDZ zone into the rock is small. The bulk of the energy transfer must take place during the expansion of the detonation products in the rarefaction wave.

The pressure decrease in the detonation products from the detonation state to an end pressure is a continuum. Simplistic analyses can be used to give an indication of the energy split between shock and heave.

Shock energy can be approximated along the CJ isentrope.

$$E_S = \int_{V_{CJ}}^{V_{bh}} PdV - u^2/2 \tag{3}$$

where V_{bh} is defined as the borehole equilibrium state (strain in rock equaling fluid product pressure) with the kinetic energy of the products (or the difference between CJ detonation state and original explosives internal energy) deducted.

Heave energy can be then estimated from the remaining energy e.g.

$$E_H = \int_{V_{bh}}^{V_{end}} PdV \tag{4}$$

For a deflagration or thermal explosion, the starting state becomes a constant volume, constant energy explosion and energy release is given by the integral between initial explosive volume and end state.

$$E_D = \int_{V_{initial}}^{V_{end}} PdV \tag{5}$$

which is derived from a different (explosion state) isentrope to the principal CJ detonation one referred to earlier.

6 CONCLUSIONS

Calculations based on ideal/1-D detonation (ZND/Chapman Jouguet) theories for the explosive performance of commercial heterogeneous explosives provide a good estimate of the performance of explosives in the large diameter/high confinement limit with the vast majority of useful work done on the confiner isentropically, starting at the detonation state.

A plethora of thermochemical computer codes have been used but only those based on full statistical mechanical equations of state can be considered reliable. There is some ambiguity in the explosives industry in the use of these codes due to differences in product equations of state, end pressures and whether condensation of the products can occur.

These ideal analyses can only be a starting point given that diameter/confiner effects the explosive performance. The gradient of the isentrope is a useful discriminator for determining which class of explosive should be used in different strength of rocks.

Analyses based on ideal detonation theories give no insight into non-ideal behavior (e.g. curved shock front, VOD less than ideal, failure diameter), unsteady processes (DDT, SDT), minimum initiation energy or explosion fume.

7 GLOSSARY

- Adiabat—locus of states with no heat loss
- BKW EOS—Becker Kistiakowsky Wilson EOS for fluids—empirical (ex Mader (1979))
- CJ Detonation—Chapman Jouguet Detonation—instantaneous reaction, mechanical, thermal & chemical equilibrium, detonation velocity a minimum
- DDT—deflagration to detonation transition
- DDZ—Detonation driving zone—reaction zone between shock front and sonic locus
- EOS—Equation of state
- Explosion State—state with same internal energy and volume after explosion

- Hugoniot, Rankine Hugoniot—locus of points satisfying conservation relations in shocked system
- Isentrope—as an adiabat but reversible
- JCZ3 EOS—Jacobs Cowperthwaite Zwisler 3 EOS—semi-empirical
- JWL EOS—Jones Wilkins Lee EOS for cylinder test fits
- Rarefaction—adiabatic expansion from explosion or detonation
- SDT—shock to detonation transition
- Taylor wave—see Rarefaction
- VOD—Detonation Velocity
- Von Neumann Spike—Shock front pressure (usually in context of ZND theory)
- Williamsburg EOS—empirical EOS—see Davis in Zukas and Walters (1998)
- ZND theory—Zeldovich, Von Neumann & Doering, 1-D detonation theory with finite reaction rate

REFERENCES

Braithwaite, M., Byers Brown, W. & Minchinton, A. 1996. The use of ideal detonation computer codes in blast modelling. *FRAGBLAST 5*. Rotterdam:Balkema.

Braithwaite, M., Cunningham, C., Parker, I. & Minchinton, A. 2006. Vixen Detonation Codes- Energy Input into HSBM, *FRAGBLAST 8*, Rotterdam:Balkema.

Braithwaite, M., Sharpe, G.J & Chitombo, G.P. 2009. Simulation of real detonations as an energy source term for the Hybrid Stress Blasting Model. *FRAGBLAST 9*. Rotterdam Balkema.

Byers Brown, W. 1987. Analytical representation of the excess thermodynamic equation of state for classical fluid mixtures of molecules interacting with α-exponential-six pair potentials up to high density. *Journal of Chemical Physics*: 87(1):568–577.

Byers Brown, W. & Amaee, A. 1992. Review of Equations of State of Fluids valid to High Density, *HSE Contract Research Report 39.*

Cowperthwaite, M. & Zwisler, W.K. 1976. The JCZ Equations of State for Detonation Products and Their Incorporation into the TIGER Code. *Sixth Symposium (International) on Detonation*, 162.

Dubois, V., Desbiens, N. & Auroux, E. 2010. New developments of the CARTE thermochemical code: Calculation of detonation properties of high explosives. *Chemical Physics Letters:* 494, 306–311.

Fickett, W. & Davis, W.C. 1979. Detonation Theory and Experiment, *University of California Press.*

Fried, L.E., Howard, W.M. & Souers, P.C. 1998. Cheetah v2.0.

Kamlet, M.J. & Jacobs, S.J. 1968. Chemistry of detonations. I A simple method for calculating detonation properties of CHNO explosives. *Journal of Chemical Physics*: 48, 23–35.

Mader, C.L. 1979. Numerical Modeling of Detonation *University of California Press.*

Persson P.A. 2000 TIGER WIN—a Windows PC Code for Computing Explosive Performance and Thermodynamic Properties, in: *Proceedings of 2000 High-tech Seminar, State-of-the Art Blasting Technology and Explosive Applications*, 541.

Persson, P.A., Holmberg, R. & Lee, J. 1994. *Rock Blasting and Explosives Engineering.* Boca, Florida: CRC Press (1994).

Rothstein, L.R. & Petersen, R. 1981. Predicting high explosives detonation velocities from their composition and structure. *Propellants, Explosives & Pyrotechnics*: 6, 91–93.

Victorov, S.B. & Gubin,S.A. 2006. A New Accurate Equation of State for Fluid Detonation Products Based on an Improved KLRR Perturbation Theory. *13th Int^{n}l Detonation Symposium*, Norfolk, Va.

Zukas, J.A. & Walters, W.P. ed, 1998. *Explosives Effects and Applications*. New York, Springer.

Downloaded by [Visvesvaraya Technological University (VTU Consortium)] at 21:51 01 March 2016

Performance of Explosives and New Developments – Mohanty & Singh (Eds)
© 2013 Taylor & Francis Group, London, ISBN 978-0-415-62142-7

Non-ideal detonation behavior in commercial explosives

M. Braithwaite
Laboratory for Scientific Computing, Cavendish Lab., University of Cambridge, Cambridge, UK

G.J. Sharpe
Department of Mechanical Engineering, University of Leeds, Leeds, UK

ABSTRACT: This paper comprises a review of non-ideal detonation theory for mining applications. This paper provides an outline of current research on accurate and efficient modeling real detonations using streamline techniques. Emphasis is placed on theory and modeling techniques rather than a wide range of applications.

1 INTRODUCTION

An earlier paper (Braithwaite (2012)) dealt with aspect of ideal detonations and thermo-hydrodynamic computer programs involving product equations of state to simulate them. Non-ideal detonations, in addition, require the following:

- a knowledge of the response of the confining media to shock and elevated pressures
- an EOS or constitutive relation that defines the behaviour of the unreacted explosive when exposed to shock
- a reduced (chemistry implicit) EOS that represents the behaviour of the detonation products
- mixing rules that describe the mixture behaviour for unreacted explosive and detonation products
- an overall burn or heat release rate expression and its parameters

This article attempts a brief review of this field, concentrating on sources of references rather than going into mathematical detail.

Unlike ideal detonations, non-ideal detonation behaviour cannot currently be predicted a priori. In addition to the ideal detonation analysis results, experimental data (shock behaviour and detonation characteristics in a well defined environment) are required in order to be able to extrapolate and allow predictions of explosive behaviour in different diameters and confinements.

It is known that in explosives, other than those with a single component typical of defence applications, the detonation process is not 1-Dimensional and, in contrast to CJ and ZND theories, these non-ideal explosives have the following properties:

- a curved shock front (confinement and charge diameter dependent)
- a critical detonation failure diameter (confinement dependent)
- partial or incomplete reaction at the sonic locus (or end of detonation driving zone)
- a dependence of detonation velocity on both charge diameter and confinement and a value less that the predicted CJ ideal value
- a pronounced reaction (DDZ) zone ~ cms
- a departure from the linear VOD vs. density rule of thumb for high explosives

Heterogeneous explosives exhibit these properties due to an overall slower reactivity e.g. reaction might require mass transfer, prill breakup, propagation from small hot spots, fuel and or oxidizer diffusion or disruption of a metal oxide layer.

Two significant areas of detonation physics are excluded from this chapter. The first, to do with low and high order detonations in nitroglycerine

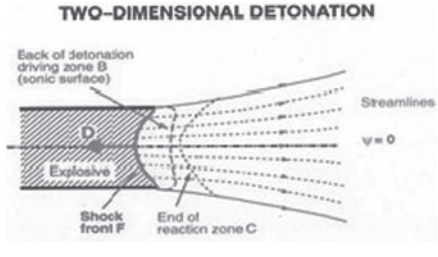

Figure 1. An overall picture of a steady 2-D detonation process in a cylinder with the shock wave moving from right to left at a velocity D. The DDZ zone is bounded by the shock front to the left and the sonic locus (where local particle velocity and sound speed are equal) to the right. This is followed by a supersonic expansion (rarefaction) to low pressure (Byers Brown (2002)).

Downloaded by [Visvesvaraya Technological University (VTU Consortium)] at 21:52 01 March 2016

based packaged products which are now of limited commercial interest. The second, where the detonation velocity of the explosive is less than the acoustic velocity of the perturbed confiner, is important in a number of applications: this is an area of current research.

In contrast to defence related applications of explosives, the whole issue of how accurate or precise detonation theory has to be to adequately describe the behaviour of a blasting explosive has never been adequately addressed in the sequence of simulations—ideal detonation ≥ non-ideal detonation ≥ rock fragmentation. Rock properties will never be known accurately because of the stochastic nature of this non-isotropic material.

There is a considerable number of papers and reviews on empirical non-ideal detonation theory (e.g. Bdzil & Stewart (2007), Clarke et al (1993), Fickett & Davis (1978), Sharpe & Braithwaite (2006), Watt et al (2011)) as well as the proceedings of the International Detonation Symposia.

2 NON-IDEAL DETONATION

Real heterogeneous explosives react at finite rates and undergo lateral energy and momentum losses along with radial expansion during the detonation process. The behaviour of a non-ideal explosive (i.e. that which exhibits non-ideal detonation behaviour) is strongly influenced by the nature of the confining media and the charge diameter.

Figure 2 shows the dependence of detonation velocity on inverse charge diameter for a generic ammonium nitrate solution—fuel oil emulsion in an unconfined charge. As the charge diameter is reduced the detonation velocity decreases until the detonation is no longer stable (corresponding to the critical detonation diameter). At diameters below the critical value, stable detonation is not possible.

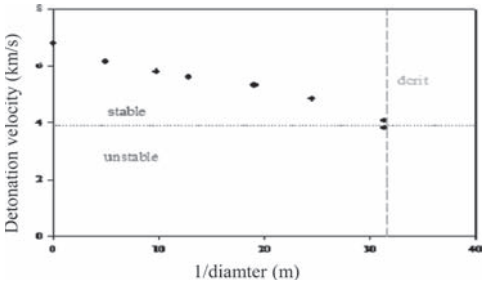

Figure 2. Typical VOD vs. charge diameter plot for a generic emulsion. Note that error bars are not included. The point at in-finite diameter is based on an ideal detonation code prediction.

Predictive capability for non-ideal detonation is in its infancy, even for steady state detonation in cylindrical geometry, due to the need to describe the reaction rate chemistry accurately as well as the influence of the confining media on the shock physics. There are usually only limited data to base any overall "rate law" to account for non-ideal behavior and heterogeneity. Existing approaches are largely based on characterizing unconfined or weakly confined charges and extrapolation to the realistic confined conditions.

Detonation models typically consist of approximate solutions of the Euler equations that describe the mass, momentum and energy conservation together with thermodynamic EOS and reaction rate terms for an adiabatic process involving inviscid fluids: approximate confinement dependent boundary conditions also require some constitutive rock properties. Heterogeneities in the explosive after being compressed by the shock wave are normally effectively "normalized" via the empirical EOS and rate law descriptions.

2.1 *Thermodynamic EOS & mixture rules—a brief outline*

Simulation of a non-ideal detonation requires constitutive relations or EOS for the unreacted explosives, detonation products and also the confining rock. These have to be expressions that do not involve excessive computation time. A previous publication in a Fragblast conference (Braithwaite, Sharpe & Chitombo (2009)) has discussed options for reduced expressions with implicit chemistry and these have also been reviewed elsewhere (ex Zukas & Walters (1998)) so these are not discussed in detail here. In this work, unreacted explosive and confiner are based around shock Hugoniot data (solids) and a well-established universal EOS for liquids (Woolfolk, Cowperthwaite & Shaw (1973)). The effects of porosity were included via a P-alpha model (Menikoff & Kober (1999)).

There are a number of options for describing detonation products on and off the critical CJ isentrope (Zukas & Walters (1998)). In our work we have favoured a Williamsburg EOS form to describe the CJ isentrope, given that it provides correct asymptotic behaviour and no anomalous behaviour in the Adiabatic and Gruneisen Gammas.

Typically the reacting material is considered to consist of a mixture of only two phases: reactants and products. The resulting mixture rules require energy and volume additivity. Closure conditions such as mechanical equilibrium are then also required. Either thermal equilibrium or thermal isolation between phases is also routinely assumed (ex Byers Brown et al (1995), Zukas & Walters (1995)).

Downloaded by [Visvesvaraya Technological University (VTU Consortium)] at 21:52 01 March 2016

2.2 *Rate laws*

A number of reviews (Peugeot (2003)) have been undertaken on rate laws for condensed phase detonation problems. The rate law is essentially an empirical expression that accounts for a myriad of processes—complex reaction, mass and heat transfer—and normally represents the heterogeneous explosive as a homogeneous fluid. Due to both the lack of homogeneity in the medium and uncertainty in temperatures, a formal rate temperature dependence (Arrhenius form) is not normally considered. Further-more it is well established that the rate law must have very weak state dependence in order to describe non-ideal behaviours.

For commercial explosives there will always be a constraint as to the available experimental data on which to base or fit a rate law. Such experimental data that can be obtained may be subject to a certain amount of statistical error due to fluctuations in density, composition and heterogeneity. For many emulsion and ANFO explosives it is not a trivial matter to make a representative sample for laboratory tests and invariably these tests are carried out at quite different confinement conditions to actual practice.

Taking account the nature and scarcity of experimental data for any given commercial explosive and also the statistical error associated with these data there seems little point in choosing an elaborate many parameter rate law for these media. Variants on Vieille's condensed phase combustion relation are in frequent use and a rate law of the form is recommended.

$$d\lambda/dt = \frac{(1-\lambda)^m}{\tau}\left(\bar{P}\right)^n \tag{1}$$

Where λ and $\bar{P}$ are extent of reaction and a scaled pressure, and τ,n and m are an inverse rate constant and two adjustable exponents. A more elaborate expression is used in the ICI/Orica code, CPeX (Kirby & Leiper (1986)) though there is little mathematical or experimental justification for the 10 or more adjustable parameters involved given the limited data and associated error analysis. High Explosives tend to be better characterised allowing the use of more complex rate laws e.g. 2 and 3 term ignition and growth models (Peugeot (2003)).

2.3 *Fluid mechanics*

The Reactive Euler equations can be solved approximately (slightly divergent flow or quasi 1-D analysis) for the central stream tube in the explosive: this is achieved by reducing the problem to a steady state set of equations in one spatial dimension. Detonation Shock Dynamics (DSD) has been used successfully for some explosives to describe the shock front in different environments for moderate non-ideality: here, a form for the detonation shock front curvature-detonation speed relation is assumed and Hugoniot matching (shock polar analysis matching pressure and deflection and the shock boundary with the confiner) is used. While under heavy confinement, DSD can be applied to commercial explosives (Sharpe & Braithwaite (2006)), it does not bridge the gap to weakly confined or unconfined very well. A further caveat is it is currently unknown how to modify the theory when VOD is in excess of local acoustic velocities in the confining rock. The use of higher order DSD theories to describe more non-ideal detonations appears promising but time con-suming.

Wood Kirkwood (slightly divergent flow), Q1D and DSD are discussed elsewhere (ex Fickett & Davis (1978), Sharpe & Braithwaite (2006), Bdzil & Stewart (2007)). They provide a means of extrapolating the detonation characteristics from one confinement/diameter condition to another and they require data (thermodynamic, detonic (for rate expression parameterization) as well as confinement characteristics). Codes simulating non-ideal detonations using Wood Kirkwood theory are in use (Kirby & Leiper (1985) but, as has been pointed out elsewhere, many of these suffer from a surfeit of parameters (Byers Brown (2002)): an extension of this approach to two dimensions (Chan & Kirby (2005), while addressing the rate parameter issue, has introduced additional empiricism to the overall analysis. Q1D (ex Sharpe & Braithwaite (2006)) has the benefit of not having to estimate a divergence term and the ease of its extension to a full DSD analysis.

A comprehensive (direct numerical simulation (DNS)) calculation which resolves the DDZ zone accurately requires finite element/finite volume computer programs with (shock capturing schemes) (ex Bdzil (2007), Sharpe & Braithwaite (2006)). Full DNS simulations of the detonation and ensuing expansion process are computationally expensive, even with simplified thermodynamics and rates: this is almost inevitable when having to simulate a discontinuity that is the shock front and the long rarefaction tail with the same computer program. The development of efficient adaptive mesh algorithms has made these calculations at least tractable for benchmark calculations. However, it is unlikely that this approach will be able to yield rapid enough results for practical work for some time to come.

In the blasting process nearly all the work is done on the rock after the passage of the shock wave and DDZ zone. If the DDZ can be predicted, full numerical simulation could be made more rea-

Downloaded by [Visvesvaraya Technological University (VTU Consortium)] at 21:52 01 March 2016

sonable by using Programmed Burn methods (ex Kapila (2006)) to separate out the two and use the result of the shock front DDZ analysis as the starting point in a more orthodox non-reactive fluid mechanics code. This approach has the added advantage of being potentially able to couple the products evolution with the elasticplastic behaviour of the neighbouring confining rock without a heavy computational penalty.

3 RECENT DEVELOPMENTS

A recent development (Watt et al. (2011)) offers a dramatic improvement in what can be achieved at very modest computational cost via a streamline flow based analysis. This has been compared with DNS calculations for highly non-ideal explosives and even with the assumption of straight streamlines shown to give excellent agreement with VODs and even critical detonation failure diameters in a matter of a few minutes computational time on a standard desktop machine. Agreement with shock shape results is good but can be further enhanced by use of a curved streamline/variational approach.

The advantages of this approach over existing simplified analyses (DSD, Wood Kirkwood etc) are:

- much improved agreement with full "exact" DNS calculations
- all calculations done within one analysis and efficiently
- ability to routinely auto-fit to experimental data in order to determine rate parameters

A typical application is illustrated below.

3.1 *Burn rate calibration*

The Leeds model (Watt et al (2011)) can generate of the order of 60 data sets per minute, this enables rapid auto-calibration of the burn rate to any available VOD measurement data (unconfined or confined). This example shows burn rate model calibration to ANFO data at initial densities of 880 and 800 kg/m^3 with the ideal (infinite diameter) VODs determined from a thermochemical model. The thermodynamic EOS (equation of state) models for ANFO take into account the porosity (density) dependence of the shock response as referred to earlier in this article.

3.2 *Prediction example: ANFO 0.8 g/cc confined in different limestones*

Once the burn rate has been calibrated, the model can then be used to predict diameter effects in other confinements. The incorporation of the rock confinement effect requires some constitutive information about the rock: Hugoniot (shock response) data in particular.

The example, illustrated in Figure 5, shows the prediction of the diameter effects in two different limestones using the ANFO 800 kg/m^3 model as calibrated above. Limestone Hugoniot data (Ahrens (1995)) has been used. Also shown are VOD measurements data from the literature (115 mm data (Indian Ministry of Coal (2001)) and 165 mm data (Sellers et al. (2007)).

It should be noted that no critical diameter is predicted for the higher density Limestone. This could be due to an assumption that the available Hugoniot data can be extrapolated linearly. For porous rocks porosity effects on the Hugoniot at lower shock speeds/pressures need to be included.

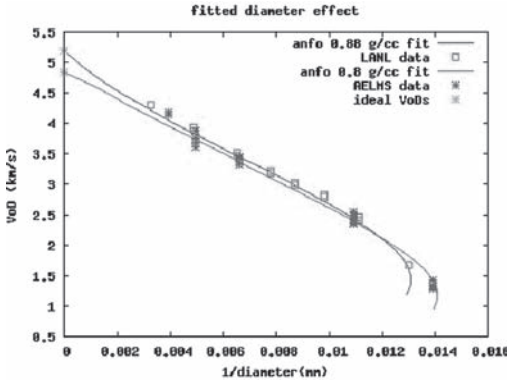

Figure 3. Experimental data (Detonation velocity vs inverse charge diameter) and theoretical fit for ANFO explosives at two different initial densities. Infinite diameter values are obtained with an ideal detonation code.

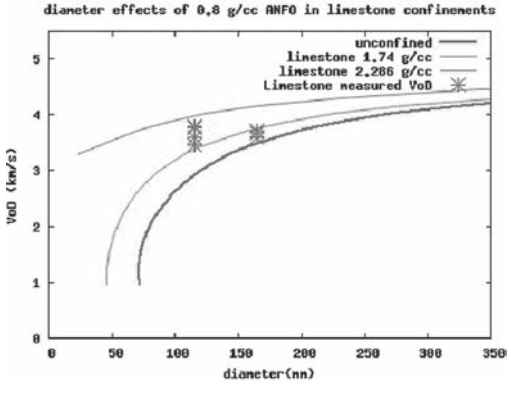

Figure 4. For a typical ANFO charge the shock front is shown moving up the page followed by the sonic locus. The limited divergence/confiner movement is also shown at the boundary of the detonation zone.

Downloaded by [Visvesvaraya Technological University (VTU Consortium)] at 21:52 01 March 2016

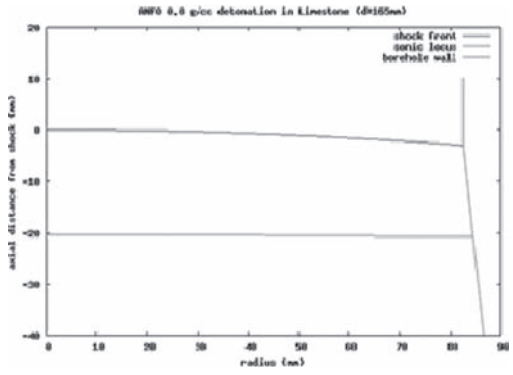

Figure 5. Predictions of the effect of confiner density on detonation velocity in different diameter boreholes. Experimental data taken in a limestone rock of unknown density is also included.

However, in general, for a given sufficiently strong confinement, there will be a critical VOD, below which the Hugoniot alone does not determine directly the confinement effect.

3.3 *Extrapolation to different rock types*

Alternatively, given some field VOD measurements, the calibrated model can also be used in reverse to provide some information about the rock and its confining effects. In particular when the Hugoniot data for the rock being blasted is sparse or not available, fitting to confined VOD data can be used to determine information about the shock response of the rock.

There have been considerable advances in the modelling of steady state condensed phase detonations since the early work on slightly divergent flow in the 1950s (Fickett & Davis (1978)). With more powerful computers and the use of adaptive mesh refining "exact" DNS calculations are possible but very time consuming and these provide invaluable benchmarks with which to compare more approximate, but much more rapid, calculation. Since the 1980's DSD (Bdzil & Stewart (2007)) has offered an approach that has proved satisfactory for moderately non-ideal explosives, particularly when confined. More recent work using a streamline based approach has bridged the gap to include highly non-ideal detonation and the unconfined scenario on which laboratory based data is typically based. This approach has been shown to give results sufficiently good as compared to the computationally intensive DNS simulations, negating the need for the latter. Indeed, due to the solution requiring virtually no computational cost, we can now readily accommodate automated regression analyses, e.g. to determine rate data from experimental measurements and then predict commercial explosive behaviour in different rock confinements, or conversely to determine rock constitutive properties given field VOD data.

4 GLOSSARY

- Adiabat—locus of states with no heat loss
- DDZ—Detonation driving zone—reaction zone between shock front and sonic locus
- DNS—Direct Numerical simulation
- DSD—Detonation Shock Dynamics (after J B Bdzil)
- EOS—Equation of state
- Mie Gruneisen equation—relationship between changes in internal energy and pressure from a known reference state
- Reactive Euler equations—standard conservation relations for mass, momentum and energy for adiabatic conditions with chemical reaction but no viscous losses, turbulence etc
- Q1D—1-D analogue of DSD
- Taylor wave—see Rarefaction
- VOD—Detonation Velocity
- Wood Kirkwood, slightly divergent flow—see Fickett and Davis (1979)
- ZND theory—Zeldovich, Von Neumann & Doering, 1-D detonation theory with finite reaction rate

REFERENCES

Ahrens, T.J., (Ed.), 1995. Rock Physics & Phase Relations: A Handbook of Physical Constants, *AGU Ref. Shelf*, vol. 3, 236 pp., AGU, Washington, D.C.

Bdzil, J.B. & Stewart, D.S. 2007. The Dynamics of Detonation in Explosive Systems, *Annual Reviews of Fluid Mechanics*, 39, 263–292.

Braithwaite, M., Cunningham, C.V.B, & Sharpe, G.J. 2006. Modelling and Numerical Simulation of Steady State Detonations in Highly non-Ideal Explosives, *13th Intnl Symposium on Detonation*, Norfolk Va.

Braithwaite, M., Sharpe, G.J. & Chitombo, G.P. 2009. Simulation of real detonations as an energy source term for the Hybrid Stress Blasting Model, *FRAGBLAST 9*. Rotterdam:Balkema.

Byers Brown, W. & Braithwaite, M. 1993. Development of the Williamsburg equation of state to model non-ideal detonation, *10th International Symposium on Detonation*, 377, Williamsburg USA.

Byers Brown, W, Zhao Feng, Z. & Braithwaite, M. 1995. Williamsburg Equation of State for Modelling Non-Ideal Detonation, *Journal de Physique IV, Colloquum* C4–209,

Chan, S.K. & Kirby, I.J. 2005. Analysis of VOD-diameter data using an analytical two-dimensional non-ideal detonation model,*14th APS Conference on Shock Compressed of Condensed Matter, Baltimore*,

Cooper, P.W. 1996 A text book of Explosives Engineering, New York, Wiley.
Fickett W. & Davis W.C. 1979. *Detonation Theory and Experiment*. University of California Press.
Kapila, A.K., Bdzil, J.B. & Stewart.D.S. 2006. On the structure and accuracy of programmed burn, *Combustion Theory and Modeling*, 10, 289–321.
Kirby, I.J. & Leiper, G.A. 1985. A small divergent flow detonation theory for intermolecular explosives, *8th Intnl Detonation Symposium*, Albuquerque, 917–922.
Menikoff, R. & E Kober, E. 1999. Equation of State and Hugoniot Locus for Porous Materials: P-α Model Revisite. *American Physical Society. Conference on Shock Compression of Condensed Matter,* Albuquerque (1999).
Indian Ministry of Coal. 2001. http://arblast.osmre.gov/downloads/International/India%20papers/VODST-final.pdf
Persson P.A., Holmberg, R. & Lee, J. 1994. *Rock Blasting and Explosives Engineering.* Boca, Florida: CRC Press.
Peugeot, F. & Sharp, M. 2003. NIMIC nations collaborative efforts in shock modelling - Reactive models for hydrocode: past, present and future, *Proc 5th Intnl Symposium on High Dynamic Pressures*, Vol 1, Paris.
Sellers, E.J., T Thomas, T. & Cunningham, C. 2007. Velocity of detonation of Non-Ideal explosives: investigating the influence of confinement, ISEE, Nashville.
Sharpe, G.J. & Braithwaite, M. 2006. Steady non-ideal detonations in cylindrical sticks of explosives. *Journal of Engineering Mathematics*, 54(3), 39–58.
Watt, S., Sharpe, G.J., Falle, S.A.E.G. 2012. A Streamline approach to two dimensional steady non-ideal detonation: the straight streamline approximation. *Journal of Engineering Mathematics*, 75(1)1–14.
Woolfolk, R.W., Cowperthwaite, M. & Shaw, R. 1973. A Universal Hugoniot for Liquids. *Thermochimica Acta*, 5: 409.
Zukas, J.A. & Walters, W.P. Ed. 1998. *Explosives Effects and Applications*. New York, Springer.

Downloaded by [Visvesvaraya Technological University (VTU Consortium)] at 21:52 01 March 2016

Performance of Explosives and New Developments – Mohanty & Singh (Eds)
© 2013 Taylor & Francis Group, London, ISBN 978-0-415-62142-7

Comparisons of explosive performance measures in theory and practice

E.J. Sellers
AEL Mining Services, Johannesburg, South Africa

ABSTRACT: A number of explosive performance measures have been investigated to provide assistance in understanding the correct application of the various types of commercial explosive. Conventional ideal delivered energy do not relate to physical effects and underestimate the shock energy and overestimate the gas energy by considering only rock stiffness. It is shown that the pond or underwater test also does not partition the energy as the water confinement does not respond as rock does. Non-ideal detonation codes are now able to reproduce the changes in velocity of detonation with confinement though the results are dependent on the particular form of rate law and confinement model. The Gurney test exhibits a lot of scatter and is quite insensitive to variations in formulation and diameter due to the very strong copper confinement and is measuring a mixture of shock and gas energy. Cavity expansion and gas flow models include the rock strength and stiffness. These become complex and cannot provide a single "energy parameter" for direct comparison between formulations. As a final offering it is suggested that the simple schematic of energy partitioning should be superseded by a consideration of both the strength and the stiffness indicating that the shock energy due to crushing expends a much larger component of the total energy delivered than previously accepted. More work is required to upgrade our knowledge to identify the correct strength model and finally produce a suitable test to engineer the choice of explosive for a particular result.

1 INTRODUCTION

The blasting community has developed a number of ways of measuring explosive performance. Some are energy based and relate to the chemical energy produced from the reactions of the component chemical within the product. Most explosive companies have ideal detonation codes that factor in the energy lost to the kinetic energy of the shock wave transmission and provide measures of the possible energy available for delivery to the rock. These measures depend on the type of equation of state used and the lower bound pressure cut-off considered. However, in practice, detonations are non-ideal and depend significantly on the type of confinement, the borehole diameter and the way that the constituent chemicals react after the detonation driving zone. Another measure of performance is to invoke the velocity of detonation and to relate this either to ideal detonation code predictions or to unconfined pipe tests experiments. This is often done as a result of the theoretical relationship between velocity of detonation and pressure, surmising that pressure relates to performance. Pressure can now be actually measured in the borehole. Often there is a desire to separate the shock and heave energy components and the pond and Gurney tests have been proposed for this, knowing that the confinement is dissimilar to the eventual rock where the product will be applied. More recent work on cavity expansion theories suggest that the explosive performance is tightly linked to the rock mass behaviour. The paper will review the multitude of different performance measures; ask how they relate to the actual field performance required in terms of fragmentation and heave, and compare theoretical relationships to the outputs of ideal and non-ideal codes. Data from range and field measurements are used to apply as many of these measures as possible to a consistent set of explosives to identify the variations in performance measures in relation to variations in blasting parameters. This will provide assistance in understanding the correct application of the various types of commercial explosive.

2 IDEAL DETONATION

Much has been said about ideal detonation and the energy measures associated with attempts to characterise the usefulness of particular explosives in a given rock mass (Cunningham 2002, Sarahan et al. 2006). The theory assumes that the detonation is travelling in one dimension with

Downloaded by [Visvesvaraya Technological University (VTU Consortium)] at 21:52 01 March 2016

effectively infinite confinement strength and stiffness and that the reactions are in mechanical, thermal and chemical equilibrium (Byers-Brown and Braithwaite 1993, Braithwaite et al. 1996). Early attempts considered a range of equations of state for the detonation products (Braithwaite et al. 1996) and current versions of the Vixen2009 code use the Williamsburg equation (Braithwaite et al. 2010).Cunningham (2002) has compared a number of explosive adiabats and the pressure volume adiabat for ANFO is shown in Figure 1 for reference.

The pressure drops rapidly to a fifth of the CJ pressure within an expansion of twice the original volume. By the time it has expanded size of seven times the pressure has dropped to almost nothing. As the pressure drops behind the detonation driving zone, the delivered energy increases rapidly (Cunningham 2006) until it reaches an asymptote. Conventionally, the delivered energy is curtailed at a selected cut-off pressure that is typically 100 MPa or 20 MPa. The energy delivered down to the cut-off pressure divided by the equivalent value for ANFO is termed the Relative Effective Energy (REE or RWS). Once scaled by the explosive density divided by the reference explosive density it is termed the Relative Bulk Strength (RBS). Much has been discussed about the application of these two numbers (e.g. Cunningham 2002, Rustan 2009). Cunningham (2005) uses the REE to scale the energy of fragmentation in the Kuz-Ram fragmentation model. Sheahan and Beattie (1990) found that the square of the heave velocity at constant burden with the RBS for a range of low density ANFO based products.

The drive to define the action of the explosive on the rock led to the shock and gas partition model (e.g. Lownds 1986). As shown in Figure 2 the rock stiffness is used to partition the shock energy that is required to reach the adiabat in an elastic manner from the subsequent energy, which acts in fragmentation and heave. The shock—gas energy partitioning has been calculated for a surface emulsion and two doped products using 20% and 35% prill in 60GPa stiffness rock, typical of a hard rock (Yumlu and Ozbay 1995) as shown in Figure 3. The large gas energy component, ranging between 68% and 80% of the delivered energy, and low shock component leads to a deficit in energy between the apparently available energy and the measure output energies such as seismics, fragmentation and heave (e.g. Spathis 1999, Ouchterlony et al. 2003).

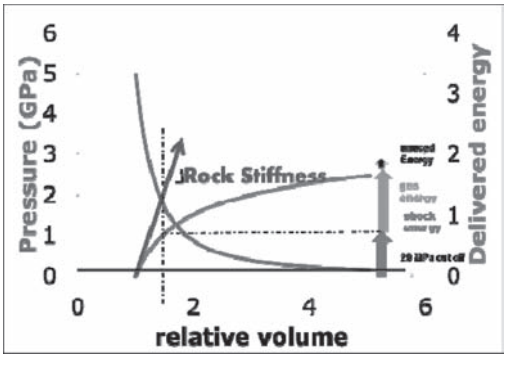

Figure 1. Schematic of conventional calculation of gas and shock energy components.

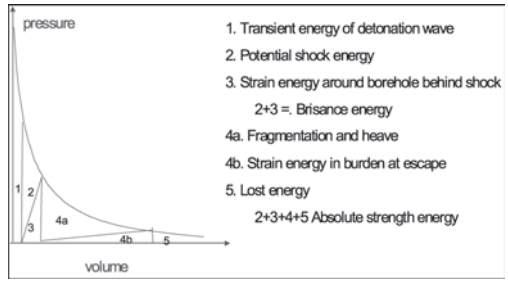

Figure 2. Energy partitioning (after Lownds 1986).

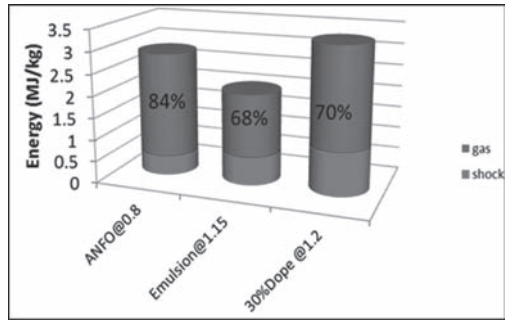

Figure 3. Comparison of shock and gas components for three explosives with a rock stiffness of 60GPa.

3 POND OR UNDERWATER TEST

The pond test has been explained in detail in a number of papers by Hagfors (2007) and will not be expounded here. Simply, the charge is fired in a specially designed pond or open body of water. The shock energy at the point of detonation is extrapolated from the measured pressure of the first pulse and the bubble energy is calculated from the time between the two subsequent bubble formations.

Downloaded by [Visvesvaraya Technological University (VTU Consortium)] at 21:52 01 March 2016

Results from tests on two emulsions done at the AEL test range are shown in Figure 4. The Figure shows that the shock energy requires a significant correction of the same order of magnitude of the original measurement. Once corrected, the values of energy appear to be independent of density, which is unexpected. The larger icons relate to tests with the transducer at 5 m. If moved to 6.3 m the energy drops, but is in line with the delivered energy reported in Figure 4. The energy results from emulsion E2 are very similar to the values for E1 at 6.3 m and suggest that the pond test is insensitive to formulation and density.

It is interesting to note the data from Hagfors (2007) in Figure 5 that shows how the total energy is sensitive to the mass of explosive used in the test and it is estimated that a mass of at least 7 kg is required for consistent results. This makes it difficult to test consistently in smaller ponds. The shock energy requires a much larger minimum mass for stable results. Looking at the ratio of the shock and gas energies to the total energy, it can be seen that there is a much lower shock component at lower masses. Thus, as the charge becomes less ideal at smaller sizes, the energy partition transforms from shock to gas. Figure 6 shows how the shock energy is highest (35%) for the emulsion and lower and equal at (21%) for the doped products. The ANFO product (94%prill) is from Hagfors (2007) and the difference may represent sample size variations.

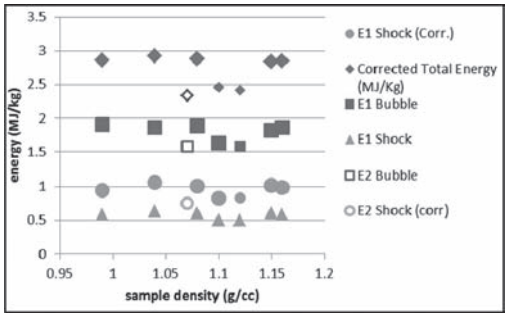

Figure 4. Effect of density on pond results of two emulsions.

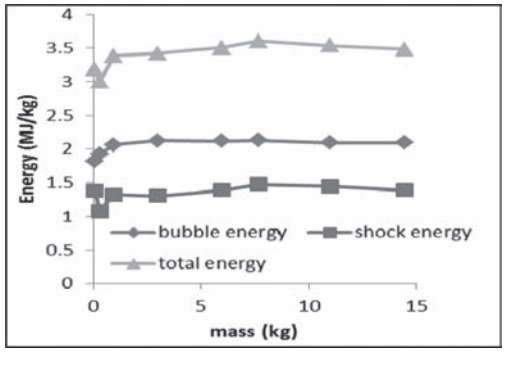

Figure 5. Effect of sample mass on pond energy results (after Hagfors, 2007).

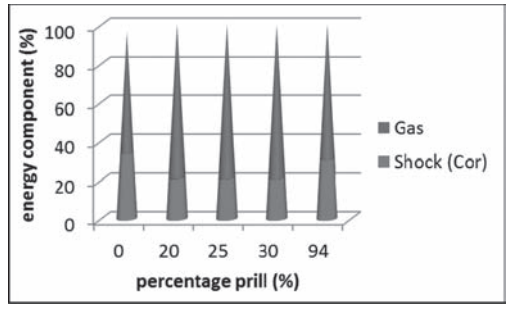

Figure 6. Relative percentages of bubble and shock energy for a range of prill contents.

4 CAVITY EXPANSION

For any given target material, there is a constant ratio between the energy input and the cavity volume created by a hypervelocity penetrator (Cunningham et al. 2007). The kilojoules of energy required to create a unit cubic centimeter of volume is about four times the unconfined compressive strength, expressed in GPa. Cunningham et al (2007) converted this theory to apply to detonation by realizing that the axial penetrator can be considered to be equivalent to the radially expanding detonation product fluids, whose densities typically fall from above 1.5 to below 0.1 g/cm^3 as the expansion progresses. This implies that more energy is required when the density of the penetrating medium (explosive fluid) decreases and so the efficiency with which explosive gases drive permanent expansion of the blasthole wall will decrease as expansion causes density to reduce. The rock strength, expressed as energy required to create a given cavity volume and the explosive density will play an important role in the energy required for chambering and how much remains for heave. The shock energy is considered to be the internal energy less the kinetic energy of the explosive gasses delivered until the stage where the relative volume is such that the parameter is attained at the intersection with the curve of the adiabat divided by the rock uniaxial compression strength.

$$\Psi_c = \sqrt{\frac{\rho_R}{\rho_e}} + 2 + \sqrt{\frac{\rho_e}{\rho_R}} \quad (1)$$

Downloaded by [Visvesvaraya Technological University (VTU Consortium)] at 21:52 01 March 2016

The rock density is ρ_R and ρ_e is the varying explosive density. Thus, the shock—heave partition is very different to that from the ideal detonation elastic rock model and the pond model. The cavity expansion approach is the first that associates more energy to the crushing and fracturing (shock component) in line with the understanding from mineral processing that crushing uses much more energy than tensile fracturing. The model provides a simple approach in the absence of numerical models.

5 NON IDEAL DETONATION

The ideal detonation theory implies that the confinement of the rock is perfectly rigid. This enables the solution of the one dimensional ZND equations (Braithwaite et al 1996, Sheahan and Minchinton 1988). However, rock provides a compliant or plastic confinement that deforms under the action of the shock wave. The deformation occurs prior to the reaction reaching completion and extracts energy from the detonation reaction. This results in a lower internal energy for propagation of the detonation front that leads to a drop in the velocity of detonation. The non-ideal codes seek to predict the effect of specific confinement on the detonation energy and velocity of detonation. The first solution approach is a quasi-one-dimensional approximation where a divergence term is introduced in the equations to divert energy from the central streamline Braithwaite et al. (2010).Themanner in which the energy is diverted required assumptions about the properties of the explosives and the confinement. Codes such as CPeX (e.g. Sheahan and Minchinton, 1988) and Vixen_n (Cunningham et al. 2006) require many input parameters that are attributed to physical properties of the solid, liquid and hot spot phases. In order to simplify the input requirements, Sharpe and Braithwaite (2006) extended this to atwo dimensional analysis using the Detonation Shock Dynamics theory and the shock polar analysis to evaluate the effect of the confinement. The confiner is described by its shock hugoniot i.e. the relationships expressing the particle velocity in the rock for any given shock speed wave speed (Braithwaite et al. 2010). This is now included in the Vixen 2009 code (Braithwaite et al. 2010) as part of the HSBM model (Furtney et al. 2009, Sellers et al. 2012).

The second approach is the Dynamic Numerical Simulation (DNS) of shock waves for example (Sharpe & Braithwaite 2006), in which an adaptive-grid scheme is used to model detonation in a cylindrical explosive surrounded by an inert medium. In this case, the confining material was assumed to obey the same gas law as the explosive, without the addition of thermal energy, but with increased density to represent approximately a solid material such as rock. The fine grid required to solve this complex problem was very computationally expensive. Cundall and Detournay (2008) developed a coarse grid approximation using the general-purpose finite difference code FLAC (Itasca 2011) to provide good results for shock and detonation simulations within a reasonable solution time.

The DNS solver used here applies a constant gamma equation of state, which has serious limitations (Braithwaite et al 1996) and has been subsequently adapted to use the Williamsburg Equation of State as described Braithwaite et al. 1996, 2010). This DNS model uses a solid confining material that obeys an elastic/plastic Mohr Coulomb constitutive model, which is a better representation of rock than the "heavy fluid" of Sharpe & Braithwaite (2006). Figure 8 shows pressure contours using the modelfor a small diameter test emulsion that indicate how the shock front is curved in the unconfined case and how the addi-

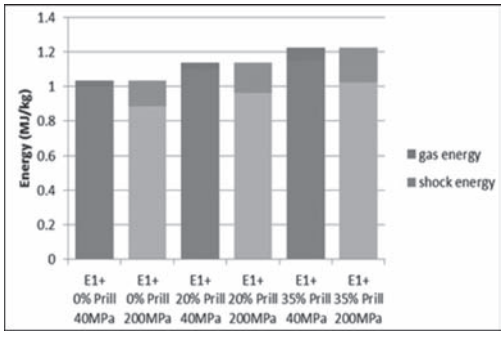

Figure 7. Shock and gas energies for a doped emulsion calculated from cavity expansion theory for two rock types and different prill contents.

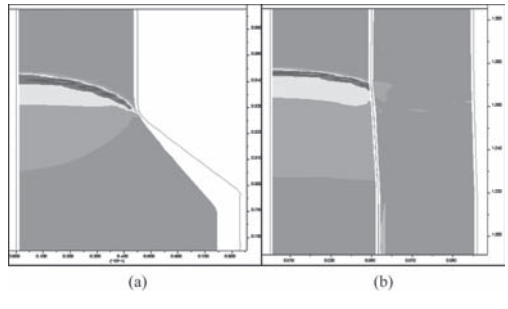

Figure 8. Pressure contours for small diameter emulsion E2: a) unconfined and b) confined by quartzite at 100 mm diameter using the DNS developed by Cundall and Detournay (2008).

Downloaded by [Visvesvaraya Technological University (VTU Consortium)] at 21:52 01 March 2016

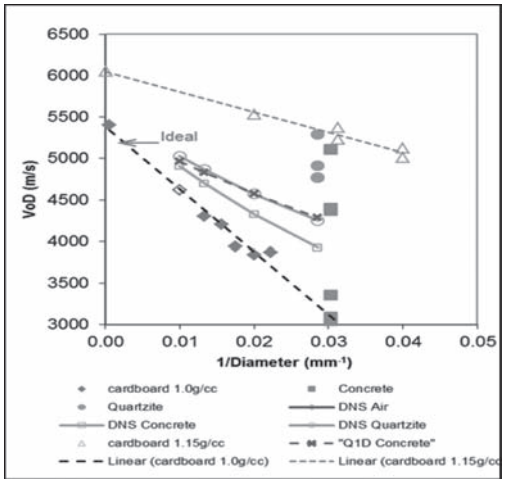

Figure 9. Velocity of detonation results for small diameter emulsion and modelling predictions using DNS and Q1D.

Table 1. Confinement properties.

Property	Concrete	Quartzite	Copper
Young's modulus (GPa)	23	78	115
Poisson ratio	0.2	0.2	0.318
UCS (MPa)	45	175	175
friction angle (°)	47	65	65
cohesion (MPa)	8.86	19.40	19.40
bulk modulus (GPa)	12.8	43.3	105.3
shear modulus (GPa)	9.6	32.5	43.6
tensile strength (MPa)	3	10	300
density (kg/m^3)	2500	2700	7450

tion of confinement acts to reduce the shock front curvature and decrease the expansion of the borehole wall. The model is perhaps too coarse for the unconfined tests and more work is needed to improve stability.

The comparison of experimental results with the model is performed using data for the small diameter emulsion E2 (Sellers et al. 2007). Two sets of unconfined data are presented in Figure 9, the lower set being for a density of 1.0 g/cc and the upper set having a density of 1.15 g/cc. Both the DNS and the Vixen2009 quasi-1D models were fitted to the lower set of data and then used to predict the effect of confinement. Two sets of confined data are shown. The first is derived from concrete block testing (Sellers et al., 2010) and the second from underground testing in a quartzite rock.

Sellers et al (2007) suggest that since the VOD can be reported on any portion of the column length and can also tend to vary along the length it is important to quantify the degree to which the measured VOD is representative of the entire column. The VOD uniformity index was proposed.

$$I_U = \frac{L_D \times 100}{L_{tot}} \tag{2}$$

Where L_D = length over which the VOD is measured; and L_{tot} = length of the explosive column. For the concrete, the VODs were variable due to the problems encountered in charging and so each I_u ranges from 30% to 57%. For the quartzite the I_u values were 90% and 95%. The rock properties used in the DNS analysis are given in Table 1. The hugoniots for the rock used in the Q1d analysis were obtained from Braithwaite (2009), assuming that the Quartzite was similar to the quartz/feldspathic gneiss.

The DNS and the Q1D models show an increase in VOD for the concrete above the unconfined values. The Q1D model cannot provide a value for the quartzite as the wave speed is faster than the VOD. The variation in the results is most likely due to insitu variations in density as it is difficult to exactly charge such small holes and to ensure consistent measurements. However, the models are able to give reasonable predictions of an increase in VOD with confinement.

6 ULTRA-HIGH SPEED PHOTOGRAPHY

The application of modern ultra-high speed photography perhaps provides a method for validation of the results. Preliminary tests have been made by filming emulsion E2 in cardboard pipes with 36 mm inner diameter. The results (Fig. 10) indicate that the frame rate of 75000 frames per

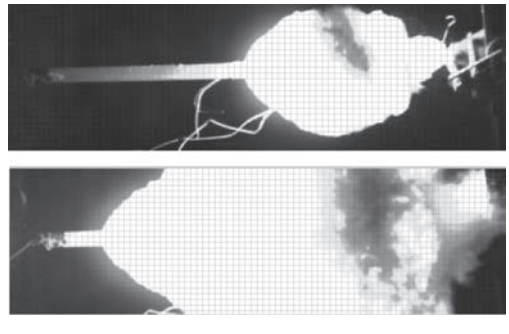

Figure 10. Detonation of emulsion in pipe (note pipe was actually vertical).

Downloaded by [Visvesvaraya Technological University (VTU Consortium)] at 21:52 01 March 2016

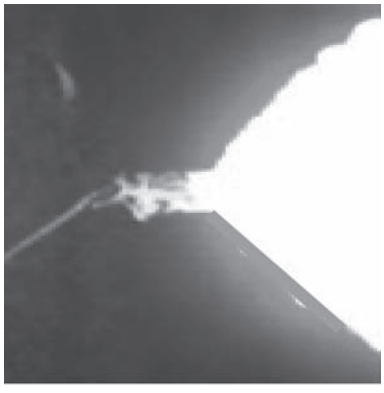

Figure 11. Expansion of detonation products of emulsion in pipe (note pipe was actually vertical).

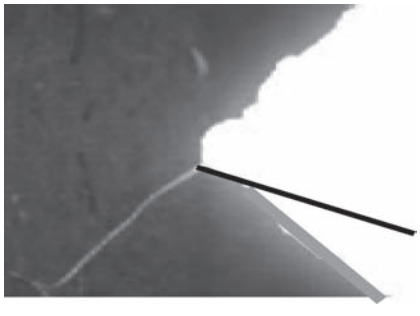

Figure 12. Detonation of emulsion in pipe at final stage with tape confinement steepening expansion angle.

second was barely sufficient to capture the full tests sequence. The VOD calculated between frames was 2368 m/s and is very dependent on the scaling of the test sample, the selection of the frames and the selection of the actual shock front position. The expansion of the detonation products with distance can be seen in Figure 11 and can be compared with Figure 8a. With sufficient resolution this could provide confirmation of the equation of state. Incidentally, the strong effect of confinement is illustrated in Figure 12 where the duct tape sealing the end of the pipe provides enhanced confinement and hence a reduced expansion of the detonation products.

7 GURNEY TESTS

The Gurney expansion test is described extensively elsewhere (Cooper 1996, Nyberg et al. 2003, Sanchidrian & López 2006, Esen et al. 2005). A large cylinder of explosives is confined by a copper tube of 5 mm to 10 mm thickness. The expansion of the tube after detonation is monitored by a series of shorting pins and the expansion energy is calculated as the energy required to propelling the mass of copper at the measured velocity. The DNS model uses the copper properties shown in Table 1 and the hugoniotfor copper for the Q1D model was obtained from Cooper (1996) with c = 5041 m/s and s = 1.42 m/s. The Q1D model predicted that the sound speed in the copper was faster than the ideal VOD of the ANFO and could not calculate a shock polar (Case 2 of Braithwaite et al. 2010) so does not predict a VOD. A snapshot of the shock front predicted by the DNS model is given in Figure 13 and shows that the stiff, dense copper provides a very high confinement, even though it is just a narrow tube leading to a very flat shock front with a high pressure. The DNS model results are shown in Figure 14 along with other ANFO test data from Sellers et al (2007). This is

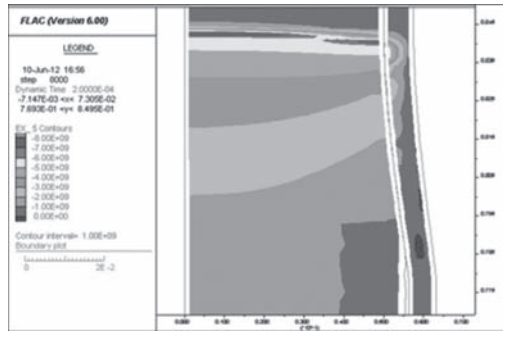

Figure 13. DNS model of 100 mm diameter Gurney test on ANFO with 10 mm copper tube.

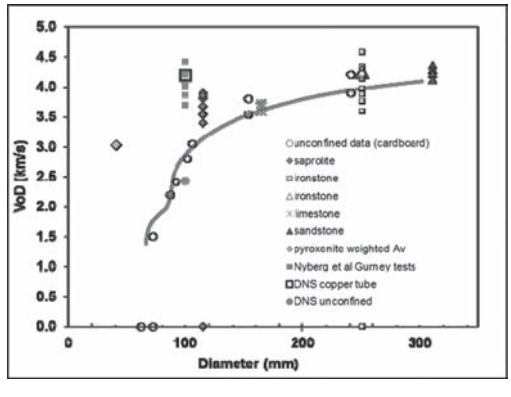

Figure 14. VOD data for ANFO with DNS results for unconfined and copper tube models compared with Gurney test data.

Downloaded by [Visvesvaraya Technological University (VTU Consortium)] at 21:52 01 March 2016

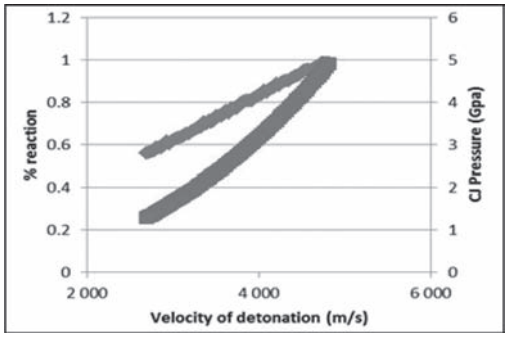

Figure 15. Relationship between VOD, pressure and reaction extent for ANFO using Q1D (Braithwaite et al. 2010).

effectively a numerical Gurney test though, like the analytical equivalent (Sanchidriánand López 2006) the results will be sensitive to the choice of equation of state.

The Gurney test exhibits a lot of scatter due to sample variation and preparation inconsistencies and is quite insensitive to variations in formulation, diameter and is slightly sensitive to explosive density. The Gurney energy obtained in the tests ranges from 1.4 MJ/kg to 2.0 MJ/kg for various ANFOs. This is much lower than the total heat of reaction Q (3.8 MJ/kg from Vixen 2009 and 3.88 MJ/kg from W-DETCOM), or even the 100 MPa delivered energy (2.26 MJ/kg from Vixen 2009 and 2.54 MJ/kg from W-DETCOM). Sanchidriánand López, (2006) equate the delivered energy to results from W-DETCOM by matching the percentage reaction completion to VOD outputs. The relationship between VOD, percentage reaction and detonation pressure calculated using VIXEN 2009 based on the Q1D approach (Sharpe and Braithwaite 2006) is given in Figure 15. The curves will depend on the detonation code and the selected equation of state. The test appears to be measuring a mixture of shock and gas energy. The use of the test to predict the non-ideal reaction extent must be done cautiously as the copper provides a much higher confining effect than normal rocks.

8 PRESSURE MEASUREMENT

Modern technology allows the measurement of the pressure using carbon gauges and high speed data acquisition devices (e.g. Mencacci & Chavez 2005, Canavough & Onederra 2011, Cavanough et al. 2011). The results of the DNS simulations need to be compared to measurements in order to ascertain their veracity. Mencacci and Chavez (2005) present data for ANFO in 95 mm and 110 mm boreholes that suggests that the detonation pressure increases from 7.4 GPa to 8.3 GPa with the increase in diameter. They do not specify the rock so the DNS was run with the generic quartzite properties. The detonation velocity predicted is 3700 m/s, which is close to their measurement of 3800 m/s. The predicted detonation pressure is shown in Figure 16 and is much lower than their measurements. This raises the issue of interpretation of the experimental results for the determination of the detonation pressure (P_d), which can be estimated from:

$$P_d = \rho D^2 / (\gamma + 1) \tag{3}$$

Where D = detonation velocity; ρ = density; and γ is the ratio of specific heats of detonation products (Cooper, 1996) and is assumed to be equal to 3.0 here. For the given velocity of detonation of 3800 m/s, this gives a CJ pressure of 2.89 GPa. The peak pressure is approximately twice the CJ pressure (Cooper, 1996) and hence is no more than 5.78 GPa. The approach of Sharpe and Braithwaite (2006) produces a CJ pressure of 3.26 GPa at a detonation velocity of 3800 m/s (Fig. 15). This suggests that the measurements are affected by other influences such as possible shock reflections as they were positioned at the boundary of the explosives and stemming. The measurements from Cavanaugh et al. (2011) in a plastic pipe indicate a maximum pressure of 3.8GPa, which is more in line with the models. Thus, there are measurements to validate the models and yet other measurements suggest that in some situation the pressure gauges may not be reading what the experimentalists anticipated.

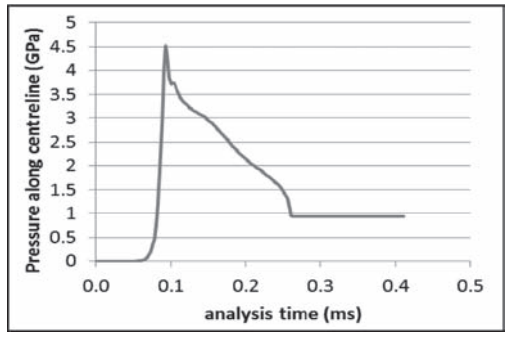

Figure 16. Centreline pressure trace with time for DNS model of ANFO confined in quartzite.

9 GAS FLOW MODEL

Of interest to note in Figure 16 is the constant pressure of just under 1 GPa when the explosive gasses become in equilibrium with the confining rock pressure. This is observed in the results of Mencacci and Chavez (2005) though their pressure is twice that of the model. A similar effect is shown in Cavanough and Onederra (2011) for heavy ANFO on a coal mine in Australia.

This equilibrium pressure plays a great role in the simple gas model of Furtney et al. (2012) where we realized that the rock properties define the magnitude of the equilibrium pressure and yet it is this pressure that drives the heave behavior of the rock mass as it acts on the borehole wall and projects the, now broken, burden forward if the burden is sufficiently small. In the example given by Furtney et al. (2012), the ANFO uses 40% of the energy for crushing in a 100 MPa rock and only 34% in a 200 MPa rock. The emulsion uses 58% and 55% for the 100 MPa and 200 MPa rock strengths, respectively, highlighting that this is a measure that does actually represent the emulsion as acting with much high shock properties than the ANFO as would be expected in practice. Thus, the explosive performance in a given situation is defined by the rock properties as much as the explosive properties. The disadvantage is that there is now no single number that represents the "strength" of any particular explosive. Additionally, the shape of the low pressure part of the adiabat or isentrope (e.g. below 100 MPa) that was previously discarded becomes of vital importance.

10 DISCUSSION AND CONCLUSIONS

A number of explosive performance measures have been investigated to provide assistance in understanding the correct application of the various types of commercial explosive. Each has their advantages and disadvantages. The ideal delivered energy and the expression relative to ANFO is simple to comprehend, but requires an ideal detonation code and does not necessarily relate to physical effects. Enhancements to include the partition between shock and gas energy consider only the rock stiffness and hence underestimate the shock energy and over-estimate the gas energy. The pond test naturally partitions into shock and gas energy and provides total energies that are very similar to the total ideal delivered energy if the sample size if big enough. However, the partitioning is also incorrect due to the low confinement of the water. The pond test appears insensitive to the product density.

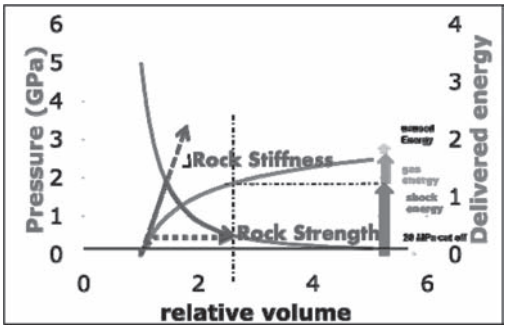

Figure 17. New schematic of shock and gas energy delivery.

Non-ideal detonation codes have become more readily available, though limited to certain organizations. The results are able to reproduce the changes in velocity of detonation with confinement though the results are dependent on the particular form of rate law and confinement model. Some of these codes have impossibly large parameter requirements.

The Gurney test appears at first glance to be a reasonable test with a physical basis, but exhibits a lot of scatter and is quite insensitive to variations in formulation and diameter due to the very strong copper confinement. The test appears to be measuring a mixture of shock and gas energy.

The cavity expansion and gas flow models include the rock strength and stiffness. These become complex and cannot provide a single "energy parameter" for direct comparison between formulations. As a final offering we suggest that the simple schematics of Figures 1–2 that only differentiate between shock and gas energy due to rock stiffness should be superseded by a consideration of both the strength and the stiffness as shown in Figure 17 indicating that the shock energy is a much larger component of the total energy delivered than previously accepted, but the exact partitioning depends on the rock type and the model selected.This may confound purchasing departments trying to compare the price per delivered energy and yet provides an excellent method for engineering the choice of explosive for a particular result.

ACKNOWLEDGEMENTS

I would like to thank my colleagues at AEL for assistance with experiments and data; Claude

Downloaded by [Visvesvaraya Technological University (VTU Consortium)] at 21:52 01 March 2016

Cunningham, Jason Furtney and Italo Onederra for many interesting discussions; Martin Braithwaite and Gary Sharpe for programming the Q1D model and Peter Cundall for developing the DNS code.

REFERENCES

Braithwaite, C. 2009. High Strain Rate Properties of Geological Materials. *University of Cambridge.* Thesis submitted for the degree of Doctor of Philosophy.

Braithwaite, M., Byers Brown, W. & Minchinton, A. 1996. The use of ideal detonation computer codes in blast modelling. *Proc. 5th Int. Symp.on Rock Fragmentation by Blasting: FRAGBLAST 5*, 37–44. In B. Mohanty (ed.), Rotterdam: Balkema.

Braithwaite, M. Sharpe, G.J. & Chitombo, G.P. 2010. Simulation of real detonations as an energy source term for the Hybrid Stress Blasting Model. *In J.A. Sanchidrian (ed.), Proc. 9th Int. Symp. On Rock Fragmentation (Fragblast 9),*327–333.Grenada, Spain, 13–17 September.

Byers Brown, W. & Braithwaite, M. 1993. Development of the Williamsburg equation of state to model non-ideal detonation. *Proc. 10th Int. Symp. Detonation: pp.* 377–385, Williamsburg, USA, ONR.

Cavanough, G., Onederra, I. & Torrance, A. 2011. Prototype gauges for measuring detonation temperature and pressure of commercial explosives. *Proceedings of the thirty-seventh annual conference on explosives and blasting techniques.International Society of Explosives Engineers*. San Diego.

Cavanough, G. & Onederra, I. 2011. Development of pressure and temperature gauges to monitor in-situ performance of commercial explosives. *IMM Journal*. In press.

Cooper, P.W. 1996. A textbook of Explosives Engineering. *Edition October 1996, ISBN 978-0-471-18636-6,* John Wiley & Sons. 460p.

Cundall, P.A. & C. Detournay. 2008. Modelling Shock and Detonation Waves with FLAC in Continuum and Distinct Element Numerical Modelling in Geo-Engineering. Proceedings, *1st International FLAC/DEM Symposium, Minneapolis, August 2008),* Paper No.10–06. R. Hart et al., Eds. Minneapolis: Itasca Consulting Group, Inc., 2008

Cunningham, C., Braithwaite, M. & Parker, I. 2006. Vixen detonation codes: Energy input for the HSBM. *Proceedings of the 8th International symposium on rock fragmentation by blasting (Fragblast 8),* pp. 169–174. Santiago, Chile.

Cunningham, C., Sellers, E.J. & Szendrei, T. 2007. Cavity expansion energy applied to rock blasting, *EFEE conference* Vienna.

Cunningham, C.V.B. 2002. The energy of detonation: a fresh look at pressure in the borehole. *FRAGBLAST*, *Int J. Blasting and Fragmentation.* Vol. 6. pp. 137–150.

Cunningham, C.V.B., 2005. The Kuz-Ram fragmentation model-20 years on. Brighton Conference Proceedings, R. Holmberg et al. 2005 European Federation of Explosives Engineers. 201–210.

Cunningham, C. 2006. Concepts of blast hole pressure applied to blast design. FRAGBLAST. *Int J. Blasting and Fragmentation.* 10. 1. pp. 33–46.

Esen, S., Nyberg, U., Hyroyuki, A. & Ouchterlony, F. 2005. Determination of the energetic characteristics of commercial explosives using the cylinder expansion test technique. Swebrec report.

Furtney, J.K. Cundall, P.A., & Chitombo, G.D. 2009. Developments in numerical modeling of blast induced rock fragmentation:Updates from the HSBM project. *In J.A. Sanchidrián (ed.), Proc. 9th Int. Symp.on Rock Fragmentation by Blasting—FRAGBLAST 9, pp.* 335–342. Granada, Spain, 13–17 September 2009. Rotterdam: Balkema.

Furtney, J., Sellers, E. & Onederra, I. 2012. Simple models for gas flow and burden movement during blasting. *International Society Explosive Engineers.*Nashville.

Hagfors, M. 2007. Underwater explosions part 5: Minimum weight of an explosive charge for the reliable energy mesurements. *Proceedings 33rd conference on explosives and blasting techniques*. Nashville, USA. ISEE.

Itasca Consulting Group, Inc., 2011, "FLAC (Fast Lagrangian Analysis of Continua)", Version 7.0. Minneapolis: Itasca.

Kirby, I.J. & Leiper, G.A. 1985. A small divergent detonation theory for Intermolecular Explosives. *Proc. 8th Int. Symp. Detonation*, Albuquerque, NM, USA, ONR.

Lownds, CM. The strength of explosives. In: *The Planning and Operation of Open-Pit and Strip Mines.* Deetlefs, JP, (editor), SAIMM, Johannesburg, 1986:1,51–159.

Mencacci, S. & Chavez, R. 2005. The measurement and analysis of detonation pressure during blasting. *Proceedings of the European Federation of Explosives Engineers*, Brighton, UK, 231–236.

Nyberg, U, Arvanitidis, I., Olsson, M., & Ouchterlony, F. 2003. Large scale cylinder expansion tests on ANFO and gassed bulk emulsion explosives. *Proc. Explosives and Blasting Techniques.*R. Holmberg (ed). EFEE, pp. 181–191.

Ouchterlony, F., Nyberg, U., Olsson, M., Bergqvist, I., Granlamd, L. & Grind, H. 2003. The energy balance of production blasts at Nordkalk's Klinthagen quarry. *EFEE 2003*, pp. 193–203.

Rustan, P.A. 2009. A new principal formula for the determination of explosive strength in combination with the rock mass strength. *In J.A. Sanchidrián (ed.), Proc. 9th Int. Symp.on Rock Fragmentation by Blasting—FRAGBLAST 9*, Granada, Spain, 13–17 September 2009, pp. 155–164. Rotterdam: Balkema.

Sanchidrián J.A. & López, L.M. 2006. Calculation of the energy of explosives with a partial Reaction model, comparison with cylinder test data. *Propellants, Explosives, Pyrotechnics.* 31, 1, pp. 25–32.

Sarahan, M.R., Mitri, H.S. & Jethwa, J.L. 2006. Rock fracturing by explosive energy: review state of the art. *FRAGBLAST. Int J. Blasting and Fragmentation.* 10. 1. pp. 33–46.

Sellers, E.J., Thomas, T. & Cunningham C., 2007. Velocity of detonation of Non-Ideal explosives:investigating the influence of confinement. *Proceedings 33rd confer-*

Downloaded by [Visvesvaraya Technological University (VTU Consortium)] at 21:52 01 March 2016

ence on explosives and blasting techniques. Nashville, USA. ISEE.

Sellers, E.J., Furtney J. & Onederra, I. 2012. Field-scale modelling of blasting in kimberlite using the hybrid stress blasting Model. *Proceedings International Society Explosive Engineers.* Nashville.

Sellers, E., Kotze, M., Dipenaar, L. & Ruest, M. 2010. Large scale concrete cube blasts for the HSBM model. *In J.A. Sanchidrian (ed.), Proc. 9th Int. Symp. On Rock Fragmentation (Fragblast 9)*, Grenada, Spain, 13–17 September.

Sharpe, G.J. & Braithwaite, M. 2006. Steady non-ideal detonation in cylindrical sticks of explosives. *J Eng Math,* 54(3), pp. 39–58.

Sharpe, G.J. & Braithwaite, M. 2005. Steady Non-Ideal Detonations in cylindrical sticks of explosives. *J. Engr. Math. 53(1):* 39–58.

Sheahan, R.M. and Minchinton, A. 1988.Non-Ideal Explosive Performance prediction using the CPEX Model.*Explosives in Mining Workshop.* AUSIMM.17–21.

Sheahan & Beattie, T. 1990. Effect of explosive type on fines generation during blasting. *FRAGBLAST'90*. pp. 413–416.

Spathis, A.T. 1999. On the energy efficiency of blasting. *FRAGBLAST–6*. Johannesburg, pp. 81–90. SAIMM.

Yumlu, M. & Ozbay, M.U, 1995. A study of the behavior of brittle rocks under plane strain and triaxial loading conditions. *Int. J. Rock Mech. Min. Sci*. 32. 7, pp. 725–733.

Downloaded by [Visvesvaraya Technological University (VTU Consortium)] at 21:52 01 March 2016

Performance of Explosives and New Developments – Mohanty & Singh (Eds)
© 2013 Taylor & Francis Group, London, ISBN 978-0-415-62142-7

Energetics and performance of modern commercial explosives

B. Mohanty
Department of Civil Engineering and Lassonde Institute of Mining, University of Toronto, Toronto, Canada

ABSTRACT: The blasting performance of a commercial explosive depends on a variety of factors aside from the blast design or rock type. These include variability of detonation characteristics of the explosives system such as total energy, energy partitioning between shock and gas, mode of initiation of the explosive in the borehole, and both intra-hole and inter-hole sympathetic pressure effects. These issues and their interaction are discussed in detail in the light of specified performance in a blast, which can range from instantaneous detonation irrespective of the delay time used to total failure.

1 INTRODUCTION

Significant progress in explosives manufacturing and technology in recent decades has made the commercial explosives and initiators more reliable, cheaper, as well as safer. This has however brought in some additional performance constraints, as these explosives such as emulsion, slurry and ANFO (and their many variations) and in combination with the various initiators, have a more restricted range over which their performance remains invariant than the old NG-based or TNT-based products. In other words, their blasting performance is liable to be dictated by both 'intra-hole' conditions (e.g. density, VOD, diameter, etc.) as well as 'inter-hole' conditions (e.g. sympathetic pressures, timing, etc.). In addition, modern blasting practice requires a much higher level of predictability of blast results due both to economic pressures and scale of blasting than was the practice before. Although considerable progress is being made in accurately defining and controlling the detonation characteristics of both explosives and initiators, it is important to consider the key parameters and the prevailing field conditions to obtain the desired results in blasting operations.

2 DETONATION CHARACTERISTICS

The key parameters in this regard are the i) velocity of detonation (VOD), ii) energy content in the explosive, iii) nature and degree of sensitization of the explosive product in use, and iv) initiation mode employed to detonate the explosive in the borehole. All these, by themselves and in combination with blast design, play a vital role in the overall performance of the explosive. It should also be noted that even under ideal detonation assumptions, the process of estimating the energy yield from a commercial explosive is far from being a straightforward exercise (Braithwaite, 2012).

2.1 *Velocity of detonation*

The variation of VOD as a function of a borehole diameter is well known. Figure 1 shows its variation with diameter for three common explosives under unconfined conditions. VOD is shown as a ratio of the measured value against ideally calculated value. As expected, ANFO exhibits the largest variation, and even at 200 mm diameter, it has not reached its terminal value. In contrast, emulsion explosive reaches its terminal value at around 150 mm diameter. The data for 'doped' emulsion is a variant of Heavy-ANFO, where 10% (by weight) of AN prills.

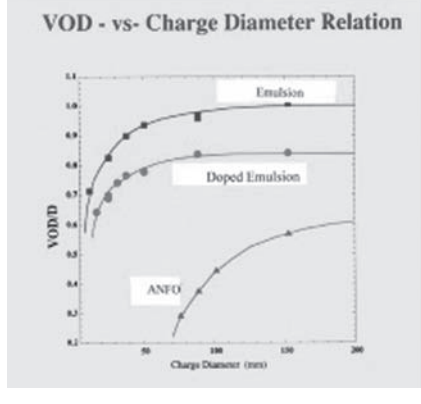

Figure 1. Change of velocity of detonation with diameter for some typical explosives.

is added to the emulsion. It shows an intermediate behavior between ANFO and emulsion. It should be noted however that the terminal velocity for this product is significantly lower than that of pure emulsion. Despite these proven variations, except for advanced blast modeling, these variations in VOD are taken to be more a measure of quality and consistency of the product rather than as a direct aid in regular blast design.

2.2 *Energy*

The energy value quoted for commercial explosives is the 'ideal' energy content for a specific composition. In this case, the amount of heat released can be taken to be the equivalent of the energy content in an explosive. The heat released in a detonation reaction is the difference between the heat of formation of the original reactants and those of its reaction products. By convention, the heat of formation of all elements in the standard state (25°C and 1 atmosphere) is taken to be zero. Thus the known heat of formation of compounds can be used to predict the heat of detonation, which can be obtained from standard tables (Cooper, 1996). A certain reaction hierarchy is assumed in these calculations, e.g. all carbon becomes carbon dioxide, all hydrogen becomes water (steam), all nitrogen becomes nitrogen gas, all aluminum to aluminum oxides, etc. The detonation of Nitroglycerin (NG) can then be described as,.

$$\Delta Hp(\text{explosion}) = \Delta Hp(\text{products}) - \Delta Hp(\text{explosive})$$

Thus,

$$4[C_3H_5(NO_3)_3] \rightarrow 12CO_2 + 10H_2O_g + 6N_2 + O_2$$

$$-\Delta Hp = 12(94) + 10(58) - 4(83) = 367 \text{ kcal/ – mole}$$

at 0 deg.C or 1620 cal/g.

Similarly, the energy content in ANFO for various oil fractions can be calculated as follows:

$$\text{ANFO (94.5\% AN + 5.5\% Fuel oil)} \rightarrow CO_2 + 3N_2 + 7H_2O \rightarrow 930 \text{ cal/g}$$

$$\text{ANFO (96.6\% AN + 3.4 Fuel oil)} \rightarrow CO_2 + 4N_2 + 2NO + 11H_2O \rightarrow 600 \text{ cal/g}$$

The above calculations are only first-order estimates of the energy content. What is actually released during detonation of the product will depend on the reaction parameters, such as pressure, temperature, the equilibrium of various gas phases and their respective Equation of State (EOS), degree of confinement, etc. The 'strength' values (weight strength and bulk strength) of the explosives supplied by the great majority of manufacturers closely resemble these 'ideal' energy estimates, whereas in actuality they could be very different depending on the in-hole conditions. In addition, even if the energy release in the borehole for specific loading conditions could be accurately estimated, the actual energy available to fragment rock would also depend on the venting pressure, i.e. the pressure at which explosion gases vent out into the atmosphere and thus ceasing any further work on the surrounding rock mass The pressure-volume relationship used in calculation of the energy content would depend on the exact composition, and the energy rating of various products falls off differentially with venting pressure (Mohanty, 1981).

2.3 *Measurement of energy*

There is no direct means of measuring explosive energy release from a borehole in an actual blast. However, specific tests have been developed to estimate energy release under specific confining conditions in the laboratory. The Cylinder Expansion Test developed by Los Alamos National Laboratory is one such test (Nyberg et al, 2003). It measures the kinetic energy during the first few hundred microseconds after initiation of the explosive charge by measuring the expansion rate of the confining copper cylinder. Because of the nature of the test and the need to keep the walls of the copper cylinder intact during its expansion, only relatively small charges can be studied and only for limited time duration. In contrast, the explosive action in expanding the borehole wall and causing fracture and fragmentation even for a single hole blast may last for several milliseconds.

An alternate method of measuring energy release from an explosive has been studied extensively by the Underwater Test (Bjarnholt and Holmberg, 1976; Roth, 1983; Sanchidrian, 1998; Mohanty, 2000; Hagfors, 2009). A typical experimental arrangement for this test is shown in Figure 2. The explosive in question is detonated at a specified depth, and the resulting shock wave in water and subsequent expansion of the explosion gas bubble is measured by means of suitable transducers. The corresponding shock energy and the associated gas energy can be calculated from the shock pressure time history and by either the bubble diameter or the time period of oscillation of the gas bubble. This yields the 'shock energy' and the 'bubble energy' directly for the explosive. There are of course strict experimental conditions and calculation techniques which must be adhered to in order to obtain the true energy release from the explosive in this test.

The total energy yield then is the sum of the measured shock energy (after correction for the

Downloaded by [Visvesvaraya Technological University (VTU Consortium)] at 21:52 01 March 2016

Downloaded by [Visvesvaraya Technological University (VTU Consortium)] at 21:52 01 March 2016

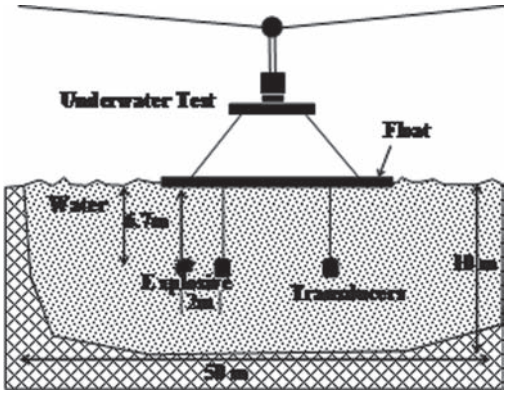

Figure 2. Underwater Test arrangement for measurement of shock and bubble energy.

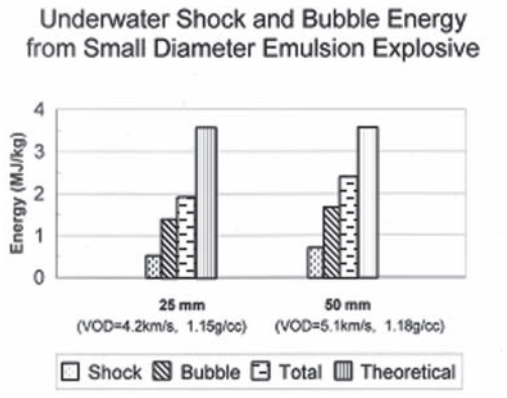

Figure 3. Measured energy in detonator sensitive emulsion explosive for two diameters in Underwater Test.

losses due to heating of the water and other non-linear losses incurred in the immediate vicinity of the detonating explosive) and the bubble energy.

Typical results of both shock and bubble energy along with corresponding VOD are shown in Figure 3 for an emulsion explosive in 25 mm and 50 mm diameter charges. The shock energy values shown are as measured and not corrected for shock energy loss factor. The total theoretical energy (i.e. 3.5 MJ/kg) for the composition is also shown for comparison. It should be noted that it only depends on the composition and therefore independent of the charge diameter. The actual measurements show that not only VOD increases with diameter as expected, but the energy partitioning between shock and gas changes with charge diameter. More importantly, the total measured energy falls far short of the calculated theoretical energy, even after incorporating the shock energy loss factor. Although both shock and bubble energy increase with charge diameter, the energy efficiency (i.e. ratio of measured total energy to theoretical energy) of this nearly ideal explosive not only varies with charge diameter, but remains less than 85% for the larger diameter charge. For less ideal explosives like ANFO or Heavy-ANFO, this ratio is found to be even lower.

The main advantage of this test lies in the ease of conducting this test, ability to test relatively large charge sizes (up to 20 kg, depending on the size of the test pond), studying the effect of various initiators and initiation modes for detonating the explosive, and the high reproducibility of the results. The main drawback of the test relates to the bubble energy measurement, as in the final expansion stage the bubble diameter is considerably larger and the temperature lower than what happens to the expanding explosion gases in the borehole. Therefore, the energy measured cannot be directly equated to that utilized in fragmentation of rock and its throw in blasting. However, for measurement of energy release efficiency, diameter effect, compositional variations, and study of non-ideality, the Underwater Test represents a very powerful as well as uniquely diagnostic tool.

3 NATURE OF SENSITIZATION

The performance of a commercial explosive also depends on the nature of sensitization employed to make the product reactive. There is overwhelming emphasis on eliminating explosives sensitizer in formulating explosive compositions. These include NG, TNT, RDX, MAN, NM, Perchlorates, etc. The physical sensitizers replacing them are simply voids, confined either by plastic or glass microballoons or just air bubbles. Just like grits in a reactive composition, these voids when compressed serve essentially as 'hot spots'. The sensitizing effect of trapped voids has been known and studied for a long time. For the simplest case, the rise in temperature inside a void under adiabatic compression is governed by the compression ratio,

$$T_2 = T_1(P_2/P_1)^{(\gamma-1)/\gamma}$$

where T_2 and T_1 are final and initial temperatures (absolute) inside the void, P_2 and P_1 are the final and initial pressure, and γ is the ratio of the specific heats (e.g. γ for air being 1.4).

It has been shown that a volume compression ratio of 20:1 can raise the temperature inside the

Downloaded by [Visvesvaraya Technological University (VTU Consortium)] at 21:52 01 March 2016

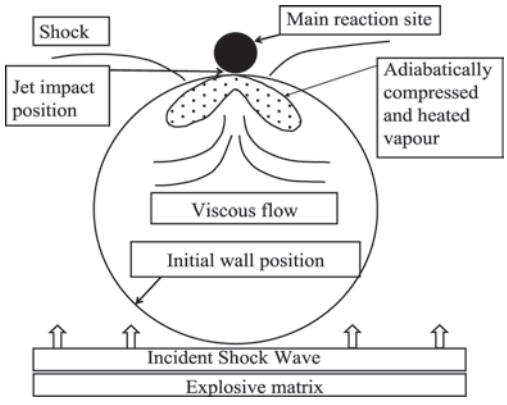

Figure 4. Nature of bubble collapse due to incident shock wave in a reactive explosive matrix.

void to ~450 deg. C, sufficient to initiate reaction around the void in a reactive composition like nitroglycerine (Bowden and Yoffe, 1952). Such a compression ratio can be easily achieved either through ordinary impact or passage of a weak shock wave through the medium. The nature of deformation of an air bubble due to an incident shock is shown schematically in Figure 4. The spherical bubble in the medium is increasingly compressed from one side, whereby the spherical void becomes increasingly elliptical. At its terminal stage, the maximum temperature rise occurs at the top end of the flattened elliptical void, as evidenced by emission of light (Bourne and Field, 1999). This would be more typical of what happens within an explosive matrix containing the bubbles. The onset and propagation of a detonation reaction would thus depend not only on the size of the voids and their distribution within the reactive medium, but also on the nature of shock wave impacting on the explosive matrix (Hanasaki and Terada, 1981; Hattori et al, 1982).

Replacement of a chemical sensitizer in the current slurries and emulsion explosives by voids thus makes their performance highly dependent on external pressures. The latter are characteristic of all multi-hole or deck blasting operations. A variety of void types are in current use, from air bubbles from gassing to plastic and glass micro-balloons. The exact choice is determined on the basis of cost and specific blasting performance considerations. Inclusion of voids has no contributions to the energy content of the explosive however. And in case of plastic or glass micro-balloons they can be viewed simply as diluents. The importance of this aspect on the performance of these explosives will be dealt with in a subsequent section.

4 INITIATION PRACTICE AND PERFORMANCE OF EXPLOSIVES

A variety of initiation modes in explosive columns are in common practice today. This ranges from simple bottom initiation of an explosive column by a detonator or a booster to any combination of detonating cord plus booster, and even by detonating cord alone, along with use of multiple explosive decks. This is done on the assumption that irrespective of the initiation mode employed, the energy released and its partitioning between shock and gas energy remains invariant. The underwater energy release and its partitioning between shock and bubble for a gassed booster-sensitive emulsion cartridge (90 mm × 400 mm) is shown in Table 1 for various initiation modes.

The four initiation modes employed are, 20 g Pentolite booster only, 1.4 g/m detonating cord plus the same booster, 1.9 g/m detonating cord plus booster, detonator with any delay period was used in this case. The highest energy yield for both shock and bubble corresponded to booster-only initiation, whereas, the explosive yielded no appreciable energy (except that due the booster only) for the 4.5 g/m cord case. As the data show, there is steady decline in energy release with side initiation by cord, with the shock energy being more seriously degraded than the bubble energy. With a 4.9 g/m cord only, the explosive essentially deflagrates.

The variation of bubble energy efficiency (i.e. ratio of bubble energy to theoretical total energy) in crushed ANFO is shown in Figure 5 for five different initiation modes (i.e. 20 g Pentolite booster alone, booster + 10 g/m detonating cord taped on side inside steel cylinder, booster +1 g/m cord, 10 g/m by itself, and 1 g/m cord by itself).

As expected, for bottom initiation by booster, the bubble energy efficiency increases with charge diameter, and with 1 g/m cord only the explosive deflagrates. Also, there appears to be no measur-

Table 1. Underwater energy release in booster-sensitive emulsion (90 mm × 400 mm cartridge) for different initiation modes (shock energy as measured and uncorrected for shock energy loss factor).

Detonation cord strength (g/m)(1)	Shock energy (MJ/Kg)(2)	Bubble energy (MJ/Kg)
0	0.68	1.79
1.4	0.43	1.63
1.9	0.30	1.54
4.5	Fail	Fail

(1) Cord taped tp side of test explosive and connected to a 20 g Pentolite booster at end of sample.

(2) Shock energy measured at 2 m from charge.

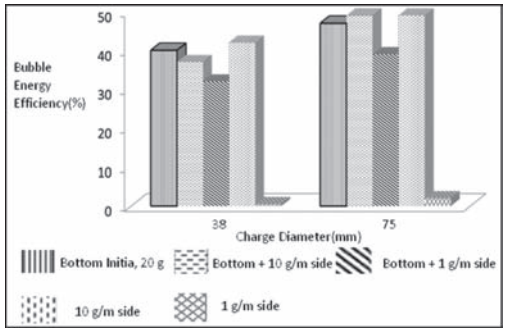

Figure 5. Bubble energy efficiency (ratio of bubble energy to theoretical energy) as a function of diameter and initiation mode in crushed ANFO (steel confinement, density: 0.93 g/cm^3).

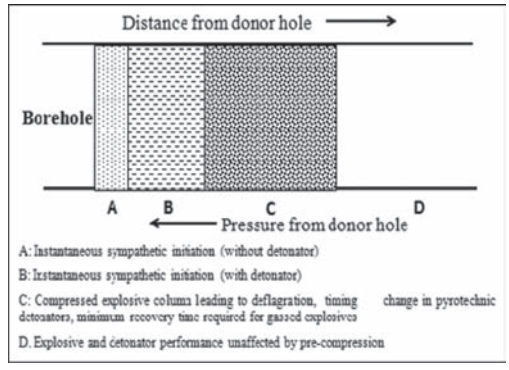

Figure 6. Effect of pressure on the performance of an explosive-detonator system.

able difference between initiation by 10 g/m cord side initiation or booster, because of detonator sensitive nature of crushed ANFO. However, a combination of 1 g/m cord side initiation and booster there is significant degradation of energy yield, as the cord must initiate deflagration across the bore hole diameter before the detonation front arrives from bottom initiation with booster. These observations apply only to the bubble energy, as already shown in Table 1, the corresponding shock energy is degraded very significantly because of side initiation by detonating cord (Mohanty and Joyce, 1994). As in the case of VOD in borehole, the issue of side initiation by detonating cord and its deleterious effect on total energy yield, and more specifically, on energy partitioning is rarely taken into account in actual blast design.

5 SYMPATHETIC EFFECTS

It essentially deals with all aspects of pressure-induced malfunction in a blast. The net effect could be confined to a single blast hole (e.g. channel effect and propagation of pressure from one explosive deck to the next explosive deck), or between two blast holes. This manifests in either a failed explosive column or out of sequence, or even instantaneous detonation of the receptor explosive column. In case of detonators, this can lead to out of sequence or even instantaneous firing.

The general case of pressure-induced malfunction in an explosive system is shown schematically in Figure 6. Close to a detonating borehole (i.e. zone A), the high pressure from the explosion will be sufficient to initiate a nearby explosive column nearly instantaneously even without a detonator, whereas, some distance away from this borehole (i.e. zone B), the shock pressure would not be sufficient to initiate the explosive column by itself, but be of sufficient magnitude to initiate the detonator within the explosive column. Further away in zone C, the pressure may still be of sufficient amplitude to either desensitize the explosive column by compression of or damage to the voids, or alter the firing time of the detonator, or both. Far away from the blasthole (i.e. zone D), the neighboring explosive column will remain unaffected, and should detonate at its designed delay time. Besides explosives, sympathetic pressures can also change the firing time of the detonators (Mohanty, 2009).

The best way to examine the effect of sympathetic pressure on an explosive-detonator system is to study the behavior of a receptor element (i.e. explosive, detonator, or any combination of the two) is to study the minimum shock pressure required to detonate the explosive. This has been studied systematically for slurry and emulsion in small diameters (Mohanty and Deshaies, 1992; Mohanty, 1994; Nie, 1997). The effect of sympathetic pressure on the detonation behavior of a detonator, slurry explosive and an emulsion explosive cartridge in 50 mm diameter is given in Table 2. The results show that it requires a minimum of 75 MPa (or 46 cm from a 220 g Pentolite donor) to sympathetically initiate a standard detonator by itself in water.

For sympathetic initiation of a 50 mm diameter detonator sensitive slurry cartridge and emulsion cartridge with glass micro-balloons without a detonator, the minimum respective pressures are 308 MPa and 738 MPa with the same Pentolite donor. However, when the same cartridges enclose a detonator, the minimum incident shock pressure required to sympathetically initiate the charges drops to 14 MPa and 40 MPa respectively. That means, although the incident pressures are too low to initiate the explosives, there is obvious amplification of the shock pressure within the respective

Downloaded by [Visvesvaraya Technological University (VTU Consortium)] at 21:52 01 March 2016

Downloaded by [Visvesvaraya Technological University (VTU Consortium)] at 21:52 01 March 2016

Table 2. Minimum distance and shock pressure in water for detonation of a standard pyrotechnic detonator, and 50 mm diameter slurry and emulsion explosive cartridge from a 220 g Pentolite donor.

Product	Distance from donor	Pressure
# 10 LP Detonator	46 cm	75 MPa
Water-gel slurry (ρ = 1.20 g/cc) (without detonator)	13 cm	308 MPa
Water-gel Slurry (with # 10 LP Detonator)	200 cm	14 MPa
Emulsion (ρ = 1.20 g/cc) (without detonator)	6 cm	738 MPa
Emulsion (ρ = 1.20 g/cc) (with # 10 LP Detonator)	80 cm	40 MPa

cartridges to at least 75 MPa for the detonators within the former to have detonated. In other words, the explosive matrix with air bubbles or glass micro-balloons amplify the transmitted shock pressures very differently (Mohanty, 1994; Sumiya et al, 2001), and therefore, the resistance against sympathetic detonation of void-sensitized products would depend on the type of voids employed, and not just the void fraction.

A similar scenario could occur within the same borehole containing multiple explosive decks separated by stemming decks (Lee et al, 2000; Mohanty, 2009). The measured VOD involving two explosive decks separated by a stemming deck and instrumented with a continuous probe throughout the hole is shown in Figure 7. The VOD in each explosive deck is steady at 4.3 km/s. However, since the probe was continuous, one could examine the propagation of the detonation reaction products in the stemming deck as well. This is observed as a decaying 'pseudo-VOD' in the stemming deck. It means that there is sufficient energy propagating through the stemming to cause collapse of the VOD probe and yield a VOD-like reading, and possibly damage the upper explosive deck. However, in this case the stemming was of sufficient length (i.e. 18xborehole diameter for the 162 mm diameter borehole) to prevent sympathetic initiation or degradation of the upper deck of TNT-slurry and its detonation at the specified 25 ms delay. However, when the inter-deck stemming is reduced to 2.3 m (i.e. 15xborehole diameter), the upper explosive deck deflagrates, as shown in Figure 8. The minimum inter-deck stemming length required to prevent malfunction of the succeeding explosive deck would depend on the type of explosives (ANFO, slurry, emulsion, etc.) and the nature of sensitizer employed.

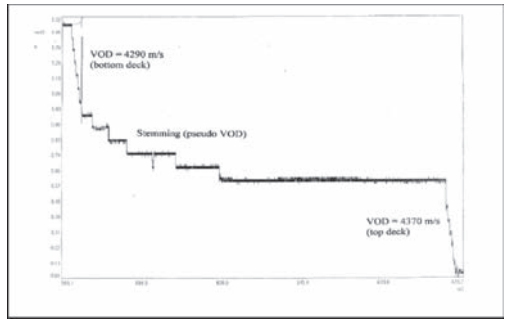

Figure 7. Measured VOD in a borehole with two explosive decks separated by a 3.5 m stemming column with a continuous probe (note the steady VOD of 4.3 km/s in the bottom deck at the beginning at left and the top deck at the end on the right).

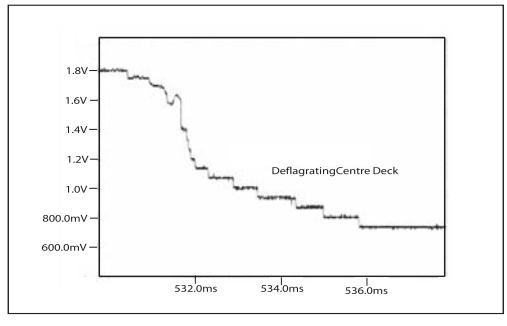

Figure 8. Deflagration of the middle deck of a 3-deck blast with 2.3 m inter-deck stemming (i.e. 15 × borehole diameter).

6 CONCLUSIONS

In order to obtain expected blasting performance from a typical commercial explosive, it is essential that one recognizes the complex and often the non-ideal nature of the detonation reaction in the explosive composition. The varying field conditions contribute very significantly to this uncertainty. The use of void sensitization as replacement of earlier chemical sensitizers adds greatly to the uncertainty in the performance of modern commercial explosives, Even if one were to know the actual detonation parameters of the explosive employed, there is little chance that it would yield the expected blasting performance independent of the prevailing field conditions, from one site to another even if the blast design remains unchanged. As the study has shown, in-hole and intra-hole sympathetic pressures can affect both the sensitivity of the explosive as well the firing time of the detonators, and therefore their performance. There is a need for in-hole measurement of detonation

parameters on a regular basis in order to check on the quality and the consistency of the explosive product used. Ultimately, the performance of an explosive depends as much on the actual in-use field conditions prevailing at the site as its theoretically calculated detonation properties. The response of the target rock in question and proper characterization of its dynamic strength and in situ properties is an equally important but separate element in designing a blast.

ACKNOWLEDGEMENTS

The author acknowledges the financial support provided by Research Canada and the Centre of Excellence in Mining Innovation (CEMI.).

REFERENCES

Bjarnholt, G. & Holmberg, R. 1978. Explosives expansion work in underwater detonations. *Proc. 6th Int. Symp. on Detonation*: 540–550. US Govt. Printing Office.

Bourne, N.K. & Field, J.E. 1999. Shock-induced collapse and luminescence by cavities; *Phil. Trans. R. Soc. Lond. A*,357, 295–311.

Bowden, F.P. & Yoffe, A.D. 1952. *Initiation and Growth of Explosions in Liquids and Solids*, Cambridge Univ. Press., 1–104.

Braithwaite, M. 2012. Ideal detonation concepts for blasting engineers, *Proc. Workshop on Performance of Explosives (FRAGBLAST 10),* Francis & Taylor, (in press).

Hagfors, M. 2009. Underwater Explosions—Particle size effect of AL powder to the energy content of PBX. *Proc. 35th Ann. Conf. on Explosives & Blasting Tech.*: 207–216. ISEE.

Hanasaki, K. & Terada, M. 1981. Studies on slurry explosives: Temperature change due to thermal conductivity around the air bubble repeatedly subjected to impact compression and expansion, 1981. *J. Ind. Explosives Soc. Japan*, vol. 42.,161–168.

Hattori, K., Fukatsu, Y. & Sakai, H.1982. Effect of the size of glass microballoons on the detonation velocity of emulsion explosives, *J. Ind. Explosives Soc. Japan*, vol. 43, 298–309.

Lee, R.A., Rodgers, J.A. & Whitaker, K.C. 2000. Explosives malfunctions in decked blasts, *Proc. 26th Ann. Conf. on Explosives and Blasting Tech.*: 25–34. ISEE.

Mohanty, B. 1981. Energy, strength and performance, and their implications in rating commercial explosives, *Proc. 7th Ann. Conf. on Explosives and Blasting Tech.*, 293–306, ISEE.

Mohanty, B. & Deshaies, R. 1989. Pressure effects on density of small diameter explosives. *Proc. 5th Symp. on Explosives and Blasting Res.*: 91–108. ISEE.

Mohanty, B. & Deshaies, R. 1992. Conditions for sympathetic initiation of explosives in small diameters. *Proc. 8th. Symp. on Explosives and Blasting Res.*: 1–17. ISEE.

Mohanty, B. 1994. Characteristics of shock wave transmission in porous visco-elastic explosive matrix', *Proc. 15th Symp. on Explosives and Pyrotechnics, Franklin Appld. Phys.*

Mohanty, B. & Joyce, D.K. 1994. Explosive initiation practice and its effect on energy release in commercial explosives—Part II, *Proc. 10th Symp. on Explosives and Blasting Res.*: 149–161. ISEE.

Mohanty, B. 2000. The Underwater Test as a tool for rating explosives, *Proc. 26th Ann. Conf. on Explosives and Blasting Tech.*, Int. Soc. Explo. Engrs., Anaheim, 9–24.

Mohanty, B. 2007. Dynamic blast conditions and explosives system performance. In Wang, X. (ed.) *Proc. 1st Asian-Pacific Blasting Conf.—New Developments on Engineering Blasting*: 16–22. Metallurgy Industry press, Beijing.

Mohanty, B. 2009. Intra-hole and inter-hole effects in typical blast designs and their implications on explosive energy release and detonator delay time—A critical review, *Proc. 9th Int. Symp. on Rock Fragmentation by Blasting (FRAGBLAST 9)*, Sanchidrian (ed), Taylor & Francis, 23–31.

Nie, S. 1997. Pressure desensitization of a gassed emulsion explosive in comparison with micro-balloon sensitized emulsion explosives. *Proc. 12th Symp. on Explosives and Blasting Res.*: 151–172. ISEE.

Nyberg, U., Arvanitidis, I., Ouchterlony, F. & Olsson, M. 2003. Large size Cylinder Expansion Tests on ANFO and gassed bulk emulsion explosives. *Proc. 2nd World Conf. on Explosives and Blasting; Prague*: 181–191.

Roth, J. 1983. Underwater Explosions. Encyclopedia of Explosives and Related Items, vol. 10, UARDC, Dover: U38-U81.

Sanchidrian, J.A. 1998. Numerical modeling evaluation of underwater energies. *Propellants, Explosives and Pyrotechnics 23*: 301–308.

Sumiya, F., Hirosaki, Y., Kato, Y., Ogata, M., Seto, M., & Katsuyama, K. 2001. Characteristics of pressure wave propagation in emulsion explosives. *Proc. 27th Ann. Conf. on Explosives and Blasting Tech.*, ISEE, 1–12.

Downloaded by [Visvesvaraya Technological University (VTU Consortium)] at 21:52 01 March 2016

Performance of Explosives and New Developments – Mohanty & Singh (Eds)
© 2013 Taylor & Francis Group, London, ISBN 978-0-415-62142-7

The effect of booster size on vibration and airblast and on VODs

M. Addy & T. Thomas
AEL Mining Services, Ghana

F. Korankye
Golden Star, Bogoso Mine, Ghana

ABSTRACT: Bogoso Mine operates in very close proximity to some of its neighboring communities, and complaints related to blasting vibration and airblast were becoming alarming. Several modifications to the blast parameters have proved successful in reducing vibration and airblast below threshold levels. This paper investigates one of the techniques used, which was to stop using 400 g boosters in favor of 250 g and 150 g boosters. Most explosive suppliers recommend the use of 400 g boosters in hole diameters greater than 102 mm. Any potential correlation was therefore thought to be related to a run-up in Velocity of Detonation (VOD) and that steady state VOD is not reached due to the very short bench height and explosive column length. The investigation found that there was no correlation between the different booster sizes and vibration and airblast levels and VOD's generated. The successful reduction of these levels is therefore only attributable to the other blast parameters that were modified.

1 INTRODUCTION

Golden Star owns and operates the Bogoso/Prestea Mine, which is located in the Western Region of Ghana, approximately 300 kilometers west of the capital, Accra. The mine operates in very close proximity to some of its neighboring communities, and complaints related to blast generated ground vibration and airblast were becoming alarming. AEL Mining Services is the explosives supplier to the mine, and works closely with the mine in efforts to minimize these complaints.

Before going into the specific details of this project, it is useful to provide some background information. Ghanaian mining legislation has set vibration and airblast limits at 2 mm/s and 117dB respectively, and this is closely monitored by the local Environmental Protection Agency (EPA). These limits are much lower than those set in other parts of the world, primarily because of the types of structures involved. Buildings in the mining community of Bogoso Township come in a variety of structural types and they can be classified as wattle and daub houses, mud houses, landcrete houses and sandcrete houses (Agbeno, 2006). Figure 1 shows an example of a house constructed with mud and sticks. It is not the objective of this paper to discuss the validity of these limits in relation to these types of structures, and this information is only provided to appreciate some of the local conditions.

Figure 1. Example of typical house.

The standard blast design at Bogoso Mine, where blasting activities are not constrained by proximity to local communities, uses a bench height of 8 m, hole diameters of 115 mm and 140 mm, and a shocktube initiation system. Figure 2 shows the relative locations of the Bogo-North Pit and the community.

The closest distance from the mine and the community is approximately 450 m at the southern side of the Bogo-North Pit. The vibration and airblast limits are exceeded if the standard blast design is used here, even if the number of holes per blast is limited. Mine management has discounted the use of electronic delay detonators as an option because of their comparatively high cost and because it is a relatively small area affected. Alternative hook-ups with

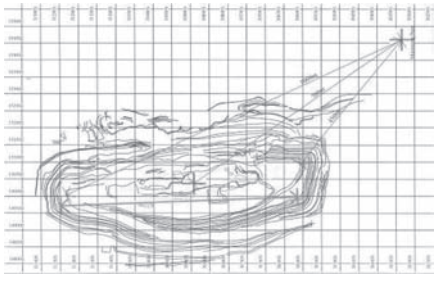

Figure 2. Proximity of Bogo-North Pit to community.

shocktube have however been tried in an attempt to increase the probability of single hole firing. Drilling smaller diameter holes was also not a viable option to reduce the mass of explosives per hole, so the mine decided to reduce the bench height from 8.0 m to 4.0 m. Finally, they also decided to stop using 400 g Pentolite boosters in favor of 150 g boosters or 250 g boosters, depending on availability.

These modifications have been largely successful in reducing the vibration and airblast levels to acceptable levels. While it is logical that the reduction in the bench height reduces the mass of explosive per hole and therefore reduces vibration and airblast, the belief that reducing the booster size also has a similar effect is not well documented. The objective of this paper was therefore to conduct a technical investigation to investigate the validity of this perception.

2 HYPOTHESIS

Explosive suppliers generally recommend the use of a 400 g Pentolite booster for reliable initiation of bulk explosives in hole diameters greater than 102 mm. Based on this, the hypothesis for the claims made at Bogoso Mine is that there may be a significant run-up in VOD and that steady state final VOD is not reached because the explosive column length is very short (±1.2 m, typically 22 kg). Although vibration, airblast and VOD data gathered from other mines have previously not shown any discernable correlation to booster size, this could be attributed to the longer explosive column lengths and the diminishing influence of run-up on the overall performance of the explosive.

3 METHODOLOGY

The investigation incorporated the following methodology.

– Collation of vibration and airblast data that had been previously recorded by the mine.
– Measurement of new vibration and airblast data from close and far range monitoring. A general analysis of the waveforms was conducted, rather than purely relying on the summary report.
– Measurement of VOD to identify any run-up, whether steady state VOD is reached and if there is significant difference in the final VOD.

The instrumentation used included two Nomis Mini Supergraph seismographs for vibration and airblast monitoring, and a MicroTrap VOD instrument, using high resistance (10.8 ohm/m) probe-cable.

4 RESULTS

4.1 *Vibration and airblast*

Peak Particle Velocity (PPV) was plotted against the square-root Scaled Distance ($D/\sqrt{E}$), as shown in Figure 3; and Airblast was plotted against the cube-root Scale Distance ($D/\sqrt[3]{E}$), as shown in Figure 4; where D is the distance between the blast and the monitoring point and E is the

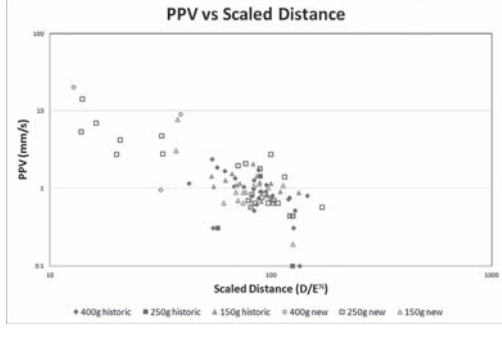

Figure 3. PPV vs. Scaled Distance.

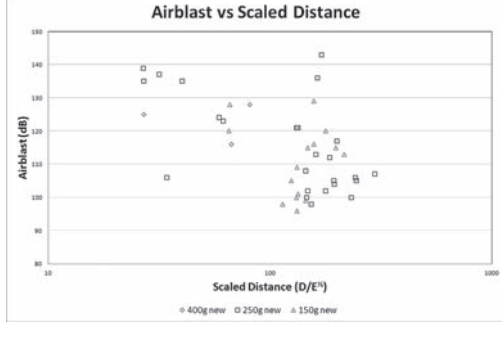

Figure 4. Airblast vs. Scaled distance.

Downloaded by [Visvesvaraya Technological University (VTU Consortium)] at 21:53 01 March 2016

Downloaded by [Visvesvaraya Technological University (VTU Consortium)] at 21:53 01 March 2016

mass of explosive per delay. Airblast is commonly scaled by the cube root of charge mass, which is justifiable for concentrated heaps of unconfined explosives but may be quite different for confined or much dispersed explosives. This is because, particle wave spreads out in full in the hemisphere and the energy in the blast which ideally fits into the full hemisphere has its volume proportional to the radius cubed. So for geometrical attenuation of a wave, dividing the radius by the cube root seems to be suitable whiles ppv in the ground which is at equivalent closer distance attenuates rapidly has the square root rule used. Due to the effect of timing scatter with shocktube systems, for the purpose of consistency and simplicity E was assumed to be the average mass of explosive per hole.

Analysis of the PPV and Airblast vs. Scaled Distance graphs does not show a correlation with the booster size as had been initially claimed.

4.2 *Velocity of Detonation*

Although the analysis of the vibration and airblast data did not seem to show the perceived correlation to booster size, it was nevertheless decided to complete the investigation with the planned VOD measurements. Nine holes were monitored and the results are summarized in Table 1. The hole diameter was 140 mm and the hole depths ranged from 3 m to 5 m. All the holes were wet and were loaded with emulsion explosive at a cup density of 1.15 g/cc.

Examples of the VOD traces using different booster sizes are shown in Figures 5–7, indicating that there was no significant difference in run-up to steady state VOD.

The VOD measurements do not show any distinct difference in explosive performance with the different boosters. The lower than expected VOD recorded in the 9th hole may be a result of contamination of the emulsion explosive with water/

Table 1. VOD results.

Hole	Booster size	VOD (m/s)*
1	400 g	4190
2	250 g	5000
3	150 g	4620
4	400 g	No VOD
5	250 g	4210
6	150 g	4500
7	400 g	3820
8	250 g	4380
9	150 g	2870

* VOD's rounded to nearest 10 m/s.

Table 2. Blast parameters.

Parameter	Units
Burden	5 m
Spacing	6 m
Hole Dia.	140 mm
Bench height	5 m
Sub-drill	0.5 m
Explosives	S110
Density	1.15 g/cc
Number of holes	66
Avg. mass per	40 kg

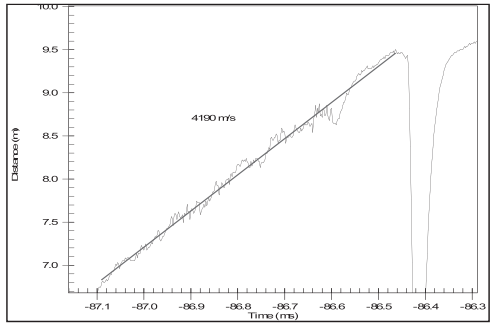

Figure 5. Hole 1–400 g booster.

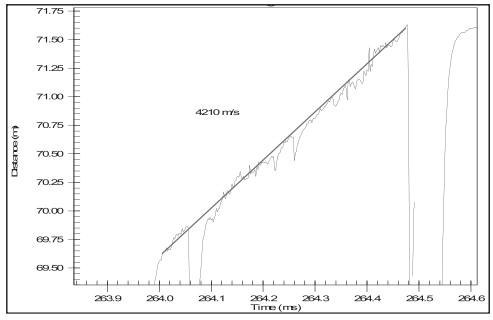

Figure 6. Hole 5–250 g booster.

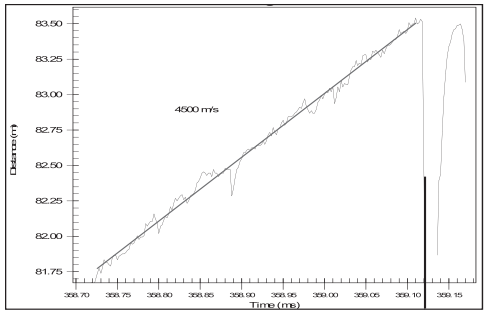

Figure 7. Hole 6–150 g booster.

Downloaded by [Visvesvaraya Technological University (VTU Consortium)] at 21:53 01 March 2016

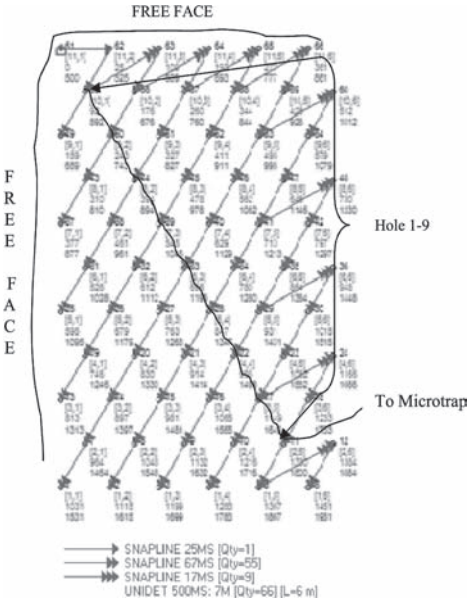

Figure 8. Modified blast design.

mud from the bottom of the hole or from dynamic desensitization, and reinforces recommendation for the use of a 400 g booster for better reliability of initiation.

For the smaller 150 g and 250 g boosters to produce a lower PPV and airblast than 400 g boosters, it would require the explosive in all or most of the blastholes to undergo sub-normal performance. Even if a small number of blastholes using the smaller boosters are initiated to give a similar performance as with a 400 g booster, they would result in a similar PPV and airblast. Therefore, although this was a very small sample of VOD measurements, it is adequate to substantiate the lack of correlation between the booster size and the vibration and airblast results.

5 CONCLUSION

The modified blast designs (Fig. 8) at the southern side of the Bogo-North pit have been successful in keeping vibration and airblast below threshold limits, but this investigation found no correlation to the booster size used. These successes can therefore be attributed entirely to the lower mass of explosive per hole as a result of the shorter bench height, the reduction in the number of holes fired per blast and the modified timing designs employed.

REFERENCES

Agbeno, S.K. & Affam, M. 1996. Impacts of blasting on buildings near Prestea Plant North Pit, Prestea. *Report for Golden Star (Bogoso/Prestea) Limited:* 17–34.

AEL'S Explosive Engineers course, surface & underground, Module 6-Airblast & Blasting Vibrations: pp. 1–89.

Richards, A.B. & Moore, A. Environmental Blast Simulation. *Terrock Consulting Engineers:* pp. 1–8.

Siskind, D.E., Stagg, M.S., Kopp, J.W. & Dowding, C.H. 1980. Structure Response and Damage Produced by Ground vibration from Surface Mine Blasting, *U.S. Bureau of Mines, R.I. 8507*, 74 p.

Performance of Explosives and New Developments – Mohanty & Singh (Eds)
© 2013 Taylor & Francis Group, London, ISBN 978-0-415-62142-7

A technique for highly precise and safe delay detonator without primary explosive

Du Jian-guo, Ma Hong-hao & Shen Zhao-wu
Modern Mechanics Department, University of Science and Technology of China, Hefei, Anhui, China

ABSTRACT: Aiming at solving the problems caused by use of primary explosives in detonators, a new kind of non-primary explosive detonator based on the principle of slapper plate detonator is devised, in which the excitation setting is the key component. A new delaying method named linear delay element is introduced in this paper. Combining these two techniques together, a highly precise and safe delay detonator without primary explosive is introduced. Correlative experiments show that, the new detonator is more reliable, safe and precise than the traditional ones. Because of its excellent performance for resisting high temperature, water ingress and impact, it has very significant commercial potential.

1 INTRODUCTION

At present, a detonator is mainly initiated by primary explosive. Delay time is decided by the length of lead delay element and the formula of delay composition. However, the design has obvious drawbacks in terms of safety and consistency.

1.1 *Ignition technique*

Nowadays, DDNP (diazodinitrophenol) is the most widely used primary explosive. Compared with lead azide and mercury fulminate, DDNP is less sensitive to impact and friction, more reliable to initiate TNT. While DDNP is weak in resisting laser, so it doesn't fit the requirement that detonator must be coded by laser in China (GA441, 2003). When 1 kg of DDNP is produced, 200–300 kg of waste water comes into being, and likely to pollute the environment, but difficult to be treated. DDNP is also more likely to cause an accident because of its high sensitivity. Other primary explosives have similar safety problems.

The non-primary explosive detonator technique can overcome the inherent disadvantages of a primary explosive. This new technique is based on the slapper plate detonator. The slapper plate detonator (McCormick, 1984) works in this way. Firstly, when a current of thousands of ampere goes through certain metals, the metals would be immediately vaporized, producing a plasma with high temperature and high pressure. Then, the plasma drives the plate to high velocity to impact and initiate the explosive. Although the slapper plate detonator is safe, it has proven impractical for civil use because of the size of (Stroud, 1988). Many new detonator techniques are derived from the slapper plate detonator, such as patents simple flyer non-primary explosive detonator (Shen, 1989) and impacting flyer non-primary explosive detonator (Shen, 1990).

This paper deals with a new non-primary explosive detonator based on slapper plate detonator principle. It will be shown that he technique is safe, reliable and adaptable to current detonator manufacturing technology. It has also been used by some enterprises in China.

1.2 *Delay technique*

At present the traditional delay element is drawn from the lead tube which contains the delay-composition. Firstly, one has to make sure that after several drawing processes the lead tube filled with delay-composition can be put into detonator shell. Usually the internal diameter of detonator shell is about 7 mm. Then, the drawn lead tube is cut into segments with proper length. The segment is called delay element. Finally, fix the delay element is inserted into the detonator shell. Figure 1 shows the traditional delay element mentioned above. In order to be bayoneted with the detonator firmly, the diameter of the traditional delay element couldn't be too small. So it's impossible to reduce the element's diameter any further.

Ordinarily, delay time is classified into 60 segments according to the time length. Delay time periods are sorted into several teams and each of them has a corresponding delay-composition formula. Consequentially various kinds of delay-composition formulas are needed which makes it inconvenient for production and difficult to ensure

Downloaded by [Visvesvaraya Technological University (VTU Consortium)] at 21:54 01 March 2016

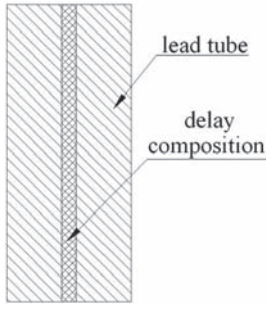

Figure 1. Sketch map of traditional delay element.

accuracy of each kind. In cases that require long delay time, delay element with a longer size should be used, which leads to long detonator shell and increased cost. In addition the lead sheath constitutes a serious environmental hazard.

Extensive research has been carried out in the past on the burning velocity of the delay tube. According to experimental results, the ignition ability and stability of the composition, which is designed for long delay time use, are both fallible, as ignition cut-off variation in delay times do occur.

In this paper an innovative linear delay technique is described, with the promise of decreased use of lead, reduced cost and enhanced delay precision.

2 HIGHLY PRECISE AND SAFE DELAY DETONATOR (HPSDD)

The combined non-primary explosive technique and the linear delay technique are known as HPSDD. Figure 2 is the typical sketch map of HPSDD. The main components are linear delay element, excitation setting and bottom explosive. When the detonation tube has been initiated by an external electric signal, the detonation wave arriving at the linear delay element would fire the delay-composition. After a period of time, the burning front reaches the open end of the bayonet plug and ignites excitation explosive. Under the high pressure made by the combustion of excitation explosive in the cap, the bottom part of the cap would be separated. This part is called flyer. The flyer with high velocity would impact and explode the bottom explosive, which finally realizes the detonation of HPSDD. The key technique of HPSDD is as follows.

2.1 *Excitation setting*

The function of excitation setting is to produce flyer with high velocity.

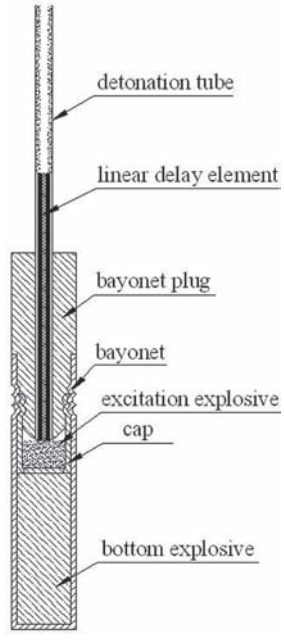

Figure 2. Sketch of HPSDD.

2.1.1 *Structure*

The components of the excitation setting are cap and initiating explosive (Fig. 3). The cap is fixed in the detonator shell by bayonet. The density of the initiating explosive is 0.5–2.5 g/cm^3, and the height is 0.5–2 times the external diameter of the cap.

1. Cap: The cap is made of Fe, Al or other materials. Caps in the experiments described were all made of Al. Its surface was smooth, without rip or pinhole porosity. The outside diameter is about 6.8 mm and the shell is 0.5 mm thick. Its height is often determined by the requirement of the production process, usually not less than 18 mm. To make it easier to form flyer, the cap's bottom is produced with rift circle or thinning treatment.
2. Initiating explosive: The initiating explosive can produce high pressure in the cap to separate its bottom and drive the flyer while it is burning rapidly. The explosive is made from pure substance or a mixture of RDX, HMX, TNT, PETN, etc. Comparatively the granulated RDX is found to be a better initiating explosive.

2.1.2 *Initiating explosive selection (Ou, 2006)*

Excitation setting is the key component of HPSDD, and the excitation explosive is the most important part of the setting. So far it has been shown that RDX and PETN are suitable for the excitation

Downloaded by [Visvesvaraya Technological University (VTU Consortium)] at 21:54 01 March 2016

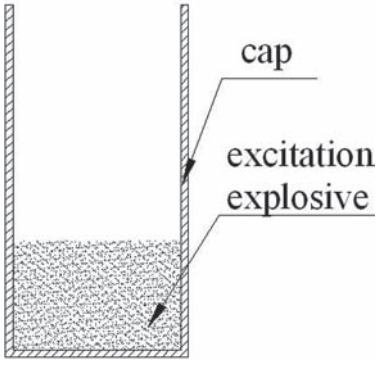

Figure 3. Sketch of initiation setting.

explosive. But the properties are different. The thermal stability of pure RDX is better than that of PETN (Zheng, 1990 & Chen, 2002). The critical thermal initiation temperature of PETN in 1.74 g/cm^3 is 197°C, for RDX at 1.72 g/cm^3 it is 214°C. Experiments show that under identical conditions PETN is more sensitive to shock wave than RDX (Zhang, 1990). Because the principle of igniting initiating explosive in electric detonator is different from that in non-electric detonator, PETN and RDX used as excitation explosive act dissimilarly. It has been shown that granulated RDX is more stable and reliable than PETN (Ma, 2008). Unless otherwise specifically stated, granulated RDX is used as the initiating explosive in this investigation.

2.2 *Linear delay element*

2.2.1 *Action principle*

The delay line can be obtained by drawing the traditional delay element to a small diameter (usually 1.4 mm). The delay line is cut into proper length to be inserted into the space in the detonation tube, resulting in the linear delay element (Fig. 4). The length of the linear delay element is determined by the delay time required.

The HPSDD including linear delay element is shown in Fig. 2. The production process is as follows. Firstly, the linear delay element is inserted into the vacuum of the bayonet plug, and the ends are on the same plane, making sure that the end of the plug touches the excitation explosive. Then it is fixed with the detonator shell by bayonet. When the detonation tube has been initiated, the delay-composition would be initiated by the shock wave arriving at the linear delay element. After the designed delay time, the initiating explosive in the cap starts to conflagrate (Li, 2006). Under the high pressure in the cap produced by the excitation explosive, a 'flyer' is produced to impact and initiate the bottom explosive.

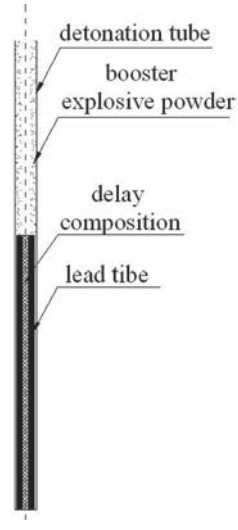

Figure 4. Linear delay element.

2.2.2 *Advantages*

The difference between traditional delay element and linear delay element isn't just the dimension but the idea. Obviously the traditional delay element is in the detonator, while the linear delay element is in the detonation tube which is outside the detonator. The advantages are as follows.

1. Lower cost: Compared with a traditional delay element, delay line has a smaller diameter, which means that with equivalent lead the linear delay element can realize longer delay time than traditional delay element. For example, the diameter of the delay line is usually 1.4 mm (d_1); the diameter of the traditional delay element is 6.2 mm (d_2). According to the volume relationship:

$$\pi d_1^2 l_1 / 4 = \pi d_2^2 l_2 / 4 \quad (1)$$

That means $l_1 = 19.6 l_2$.

As the delay time is controlled by the length of the delay element, to realize the required delay time with same delay-composition, linear delay element uses approximately 1/20 the amount of traditional delay element. It's obvious that the linear delay element technique can lower the cost significantly.

2. Precision: According to experimental data (Part 3), in the long time periods the linear delay element is more precise than the traditional delay element.
3. Independence: For there is no primary or sensitive explosive, the processes of production, preservation and transportation are safe. So delay

Downloaded by [Visvesvaraya Technological University (VTU Consortium)] at 21:54 01 March 2016

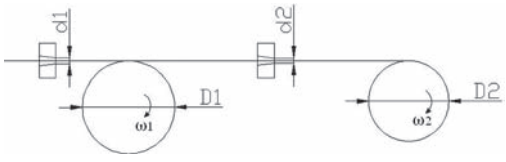

Figure 5. Sketch of the delay line drawing technique.

line can be produced separately which results in increased efficiency and reduced cost.

4. Safety: Because the delay line is in the detonation tube, its length is not limited by detonator shell. It is possible to realize all the delay time requirements with only several kinds of delay-composition. It can increase security and be convenient for management during the production process.

2.2.3 *Production technique*

Utilizing the mature wire production technique, the lead tube filled with delay-composition and drawn continuously through molds to produce the delay line. The rotating speed of rollers should be controlled. The diameter of rollers and that of molds should be matched.

Suppose there are 2 rollers. If the diameter of the rollers and the delay line, rotating speed are D_1, d_1, ω_1 and D_2, d_2, ω_2 respectively, these parameters need to meet the following equation:

$$\pi d_1^2 \omega_1 D_1 / 8 = \pi d_2^2 \omega_2 D_2 / 8 \tag{2}$$

Simplified as:

$$\omega_1 D_1 d_1^2 = \omega_2 D_2 d_2^2 \tag{3}$$

Equation (3) is the basic formula to guide the delay line drawing technique.

The production line of the delay line consists of many rollers and molds with different diameters. The sequence and diameter of molds are decided by the delay-composition, lead quality and machinery equipment level. For example, to get Φ1.4 mm from Φ4.0, the diameters and the sequence of the molds should be: 4.0 mm, 3.8 mm, 3.6 mm, 3.4 mm, 3.2 mm, 3.0 mm, 2.8 mm, 2.6 mm, 2.4 mm, 2.2 mm, 2.0 mm, 1.9 mm, 1.8 mm, 1.7 mm, 1.6 mm, 1.5 mm, 1.4 mm.

3 TEST

A certain amount of HPSDD is made. The capabilities are tested such as delay time accuracy, reaction rate, resistance to high temperature, water resistance and impact.

Table 1. The test data (2#).

Delay element length/mm	10	10	10	10	10
delay time/ms	65.0	66.1	65.4	67.23	60.0
delay linearity ms/mm	6.5	6.6	6.5	6.7	6.0
delay element length/mm	14	15	19	19	23
delay time/ms	93.2	103.0	121.4	127.6	159.6
delay linearity ms/mm	6.6	6.8	6.4	6.7	6.9
delay element length/mm	30	32	35	36	35
delay time/ms	182.2	202.7	214.8	233.0	213.0
delay linearity ms/mm	6.1	6.3	6.1	6.4	6.1
delay element length/mm	40	40	15	22	36
delay time/ms	247.9	262.4	107.1	144.5	219.4
delay linearity ms/mm	6.2	6.5	7.1	6.6	6.3

* original testing data of 2# delay-composition.

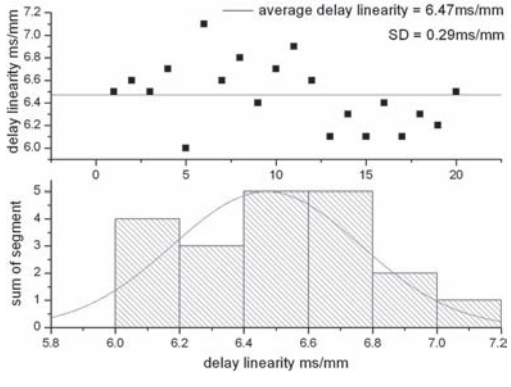

Figure 6. Figure of data (2#).

3.1 *Delay time accuracy*

Three kinds of delay-composition (2#, 5# and 10#) from one manufacturing facility are used in the following experiments. The delay line is Φ1.4 mm. Linear delay elements with different length are made to produce HPSDD. Detonating velocity measuring instrument (ZBS9601 made by Nanjing University of Science and Technology) is used to record delay time. The original data and figures are shown as follows.

Downloaded by [Visvesvaraya Technological University (VTU Consortium)] at 21:54 01 March 2016

Table 2. The test data (5#).

Delay length/ mm	50	49	46	43	44	41
delay time/ms	512.6	502.9	466.6	436.3	454.5	418.9
linearity ms/mm	10.3	10.3	10.1	10.1	10.3	10.2
delay length/mm	29	27	24	25	20	17
delay time/ms	297.0	277.6	237.4	249.9	203.0	167.3
linearity ms/mm	10.2	10.3	10.0	10.0	10.1	9.9
delay length/mm	14.5	12	10	10		
Delay time/ms	146.0	125.2	95.5	103.7		
linearity ms/mm	10.1	10.4	9.6	10.3		

*original testing data of 5# delay-composition.

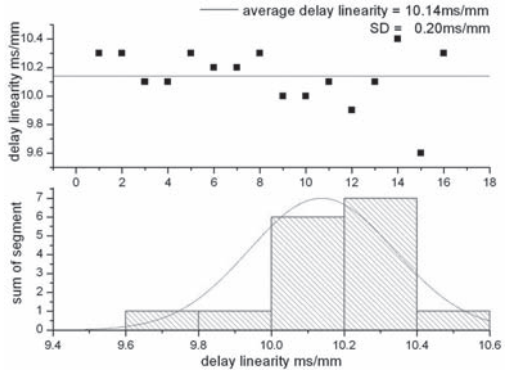

Figure 7. Figure of data (5#).

Table 3. The test data (10#).

Delay length/mm	50	50	62	63	63	93
delay time/ms	1.675	1.566	1.953	2.039	2.024	2.991
linearity ms/mm	33.5	31.3	31.5	32.1	32.1	32.1
delay length/mm	125	155	156	16	15	
delay time/ms	4.064	4.822	5.071	0.542	0.518	
linearity ms/mm	32.5	31.1	32.5	33.8	34.5	

* original testing data of 10# delay-composition.

According to the datum and figures above, it is known that the datum of 2#, 5# and 10# are distributed uniformly with standard deviation (SD) less than 1.0. The experiment shows that HPSDD with linear delay element has good accuracy and excellent reproducibility.

3.2 *Explosion reliability*

The same batch of HPSDD (i.e. #2, #5 and #10) is used to test the explosion reliability. The result is shown in Table 4.

Data in Table 4 shows that HPSDD could be exploded reliably. It also proves the feasibility of the ininitiation arrangement.

3.3 *Test for resisting impact*

The test device is a block of wood with 5 suitable holes (Fig. 9). The one in the middle is 1.3 cm distant from surrounding holes. HPSDDs are inserted in holes. After the center one is initiated, the others were found to have been seriously deformed but not detonated (Fig. 10). These 4 detonators could be exploded yet. This test shows that HPSDD can resist strong impact.

3.4 *Test for resisting high temperature*

Ten non-primary explosive detonators with excitation setting were kept in the oven at 100°C for

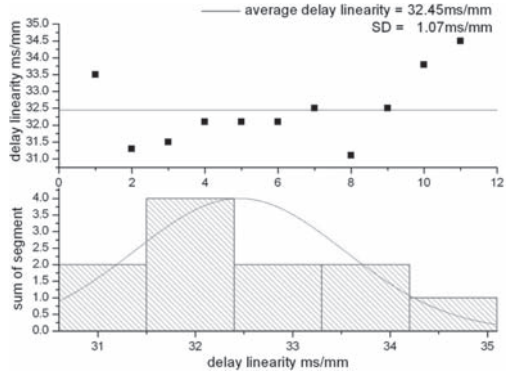

Figure 8. Figure of data (10#).

Table 4. Test data of exploding rate.

Number	Detonator quantity	Explosion rate/%
2#	100	100
5#	100	100
10#	100	100

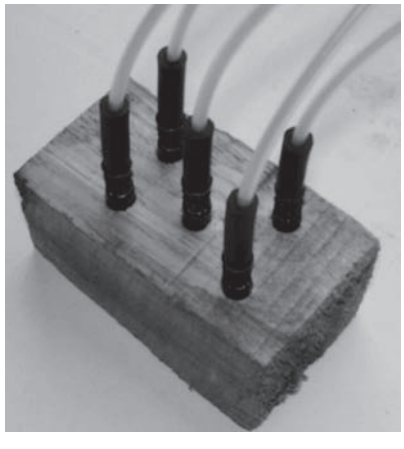

Figure 9. Device for impact resisting test.

Downloaded by [Visvesvaraya Technological University (VTU Consortium)] at 21:54 01 March 2016

Figure 10. Distorted detonators.

8 hours. They could all be initiated reliably afterwards (GB, 2005).

3.5 *Test for water resistance*

Ten non-electric and ten electric non-primary explosive detonators with excitation setting were kept at a pressure of 0.2 MPa underwater (equal to 20 m deep water) for 24 hours, There was 100% initiation afterwards (GB, 2003, 2005).

3.6 *Application in harsh environment (Ma, 2006 & 2008)*

The electric non-primary explosive detonators with excitation setting are used in dealing with drill jammed accident in some large mine. The detonator is settled in bangalore torpedo, and the bangalore torpedo is placed 640 m underneath the ground in the well, which is filled with slurry and crushed stone. The working environment is harsh. But the detonators could still be detonated successfully.

4 LASER INITIATING TECHNIQUE

In some special circumstances, such as high temperature, strong radiation, strong magnetic field, high pressure conditions, the traditional initiation technique cannot work well. The detonation tube cannot resist high pressure and high temperature; the electric initiating circuit is sensitive to strong magnetic field, strong radiation, stray current and thunder. Therefore, the laser initiation technique is proposed to adapt to the complex environment mentioned above.

A more safe and reliable detonator can be obtained by replacing the detonation tube with fiber. Figure 11 shows the combination of non-primary detonator with the laser initiating system.

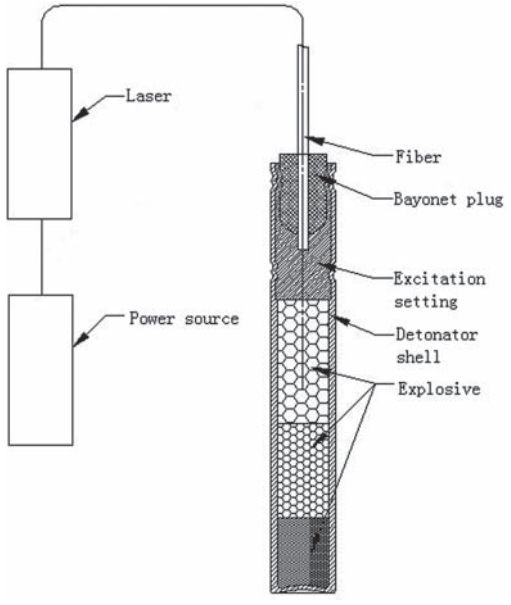

Figure 11. Laser initiating technique.

The excitation setting makes it possible for low power laser to initiate the detonator, thus reducing volume and cost. For the reasons that fiber works well in resisting high pressure and high temperature, and the laser owns the ability of anti-interference, the laser initiating technique to our non-primary explosive detonator has good potential.

5 CONCLUSION

The non-primary explosive detonator with excitation setting is based on the slapper plate technology. The initiation setting produces a high speed flyer to initiate the explosive at the bottom of the detonator. Experiments have shown that the detonator with excitation setting has excellent performance of resisting impact, high temperature and water.

The linear delay element technique is evolved from the traditional delay technique. Although its diameter is only 1.4 mm, it can burn steadily and initiate the excitation explosive reliably. What's more, the precision of delay time has improved considerably.

The two techniques above are combined to form HPSDD. HPSDD exhibits the advantages of non-primary explosive detonator and linear delay element. Experiments have shown that the HPSDD is safe, steady, reliable precise and low-cost.

REFERENCES

Chen, Rong-yi. 2002. The detonation performance of granulated PETN and RDX. *Changsha Mining and Metallurgical Research Institute.*

GA441. 2003. General industrial detonators coding. *The Ministry of Public Security of the People's Republic of China*.

GB19417. 2003. Tube detonator. *National Standard of the People's Republic of China*.

GB8031. 2005. Industry electric detonator. *National Standard of the People's Republic of China*.

Li, Ji. 2006. Research on improving the delay time precision. *Nanjing University of Science and Technology*.

Ma, Hong-hao & Shen, Zhao-wu. 2006. The research on application of blasting gasification energy in water. *7th national academic conference*: 110–115.

Ma, Hong-hao & Shen, Zhao-wu & Chen, Wen-chuang. 2008. Research on the performance of PETN and RDX as the excitation powder. *Chinese Journal of Energetic Materials* (3): 285–289.

Ma, Hong-hao, Shen, Zhao-wu & Sun, Yu-xin. 2008. Solution to drill jam with multiple underwater blasting in excavation of large diameter deep tunnel. *Engineering Blasting* (1): 38–40.

McCormick, R.N. & Melissa, D. 1984. Boyd. Bidirectional slapper detonator. *US4471697.*

Ou Yu-xiang. 2006. Explosive. Beijing Institute of Press.

Shen, Zhao-wu. 1989. Simple flyer non-primary explosive detonator. *CN87106394.8.4.*

Shen, Zhao-wu. 1990. Impacting flyer non-primary explosive detonator. *CN89218986. X,8.*

Stroud, J.R. 1988. Flying-plate detonator using a high-density high explosive. *US4788913.*

Zhang, Guan-ren & Chen, Da-nian. 1990. Detonation dynamics of condensed explosive. *Beijing: National Defense Industry Press.*

Zheng, Meng-ju. 1990. The capability and test technique of explosive. *Beijing: Weapon Industry Press*.

Downloaded by [Visvesvaraya Technological University (VTU Consortium)] at 21:54 01 March 2016

Performance of Explosives and New Developments – Mohanty & Singh (Eds)
© 2013 Taylor & Francis Group, London, ISBN 978-0-415-62142-7

Explosives initiation mode and blast performance

M.P. Roy & P.K. Singh
CSIR—Central Institute of Mining & Fuel Research, Dhanbad, India

A.K. Jha & D. Basu
Central Mine Planning & Design Institute Limited, Ranchi, India

ABSTRACT: The theoretical treatments of detonation process under both ideal and non-ideal conditions are noteworthy, but they are still based on somewhat hypothetical situations. The actual variables that are essential parts of normal blasting practice have not yet been taken into account in such treatments. These include the various initiation practices employed to detonate a column of explosive, from single point initiation to multi-point initiation in blast holes, and the effect on detonation characteristics of both detonators and explosives under multi-deck and multi-hole blasting conditions. The in-the-hole VOD of an industrial explosive is dependent on explosive's charge diameter and borehole diameter.

The in-hole VOD of some standard commercial explosives was measured at four experimental sites for different borehole diameters i.e. 150 mm to 311 mm, withthe explosive parameters (i.e. composition, density, particle size, viscosity and confinement) being kept constant.The results of the studies demonstrated that there is definite relationship in in-the-hole VOD of the explosive and the diameter of the blast hole. The study also confirmed that the explosives initiated with concentrated boosters yielded higher VOD in comparison to those explosives that were initiated with multi-point priming. However, this result is clearly anomalous, and additional tests have to be performed to study this effect further. The measured increase in VOD of explosives for increasing diameter of holes was up to 24%. The rate of change in in-the-hole VOD of explosives increases with increasing borehole diameter. It can be further stated that the in-the-hole VOD of the explosive reaches a fairly constant value after reaching a limiting/threshold diameter of 311 mm.

1 INTRODUCTION

Although explosives have been used for rock blasting for a very long time; plausible scientific theories on rock fragmentation by blasting have emerged only during the last few decades. However, the rock breakage process is still difficult to quantify and control to the level now demanded by blasting customers. Computer modelling as an engineering tool has been extended to blasting to carry out extensive blast simulations. Nevertheless, the validity of these models is dependent on knowledge of the explosive and rock interaction process (Mohanty, 1981, Leiper & DuPlessis, 2001, Cundall et al. 2001 & Cunningham, 2001). Therefore, the prediction of explosive performance is crucial to understanding the explosive-rock interaction process and rock breakage.

There is now a very wide range of commercial explosive products available to the mining industry. Their performance is dependent upon their detonation properties in addition to the rock type and blasthole diameter. The selection of a suitable explosive for a given geotechnical environment in order to produce the desired blasting results has become more important and vital to the economics of mining operations. This means that the ability to understand explosive behaviour has become even more important than it has been before.

The methods available for determining explosive performance range from simple calculations to field tests. The essential objective in the use of explosives for rock breakage consists in having a chemically concentrated energy source, properly placed and in sufficient quantity so that when it is liberatedin a controlled manner, in time and space, it can achieve the desired fragmentation of the rock material. Chemical explosives, depending upon the conditions to which they are exposed, can offer different behaviour than would be expected from their explosive matrix. To determine the suitability of an explosive substance for a particular use, its physical-properties must be known first. The decomposition processes of an explosive compound can range from combustion, accelerated reaction, and lastly to detonation. The nature of the compound itself as well as the initiation system and the external conditions govern the reaction process. Detonation reaction

Downloaded by [Visvesvaraya Technological University (VTU Consortium)] at 21:55 01 March 2016

is characterised by its high speed and the formation of large quantities of gaseous products at an elevated pressure and temperature. Once initiated, the reaction is self-sustaining, with the resulting shock propagating into the unreacted medium. The reaction rate in detonation is too fast for the heat to dissipate through conduction in the surrounding rock in any appreciable manner.The immense pressure in the borehole results in transmission of a shock wave into the surrounding rock, followed by expansion of the explosion gases in the borehole and then into surrounding rock mass (Konya & Walter, 1990). With sub-optimum initiation of the explosive column, the unreacted explosive mass may never fully react, resulting in deflagration or total failure of the explosive column.

The in-hole VOD of explosives is one of the most important parameters that affect the blast results. The detonation wave starts at the point of initiation in the explosive column and travels at supersonic speed, in relation to the sonic velocity of the explosive material itself. This velocity remains fairly constant for a given explosive matrix but varies from one explosive matrix to another depending primarily on the composition, particle size, density, charge diameter and degree of confinement. Detonators or cast boosters are used as priming systems to initiate or activate the detonation of the explosive column in the blast hole so as to minimize any run-up to full VOD. In order to understand the role of concentrated or distributed cast boosters in the blast hole loading configuration on energy release and release rate characteristics, several field experiments were carried out at opencast mines (Kusmunda, SonepurBazari, Jayant and Umrer).

2 GEOLOGICAL DETAILS OF EXPERIMENTAL SITES

2.1 *SonepurBazari opencast mine*

Sonepur Bazari opencast mine of Eastern Coalfields Limited is located in the Eastern part of Raniganj Coalfields. Four coal seams viz. R-IV, R-V, R-VI and R-VII are mainly exposed in the mine. Presently, seams R-V and R-VI are being extracted by opencast method of mining. The total reserve of the project is 188.26 Mt.

2.2 *Kusmunda opencast mine*

Kusmunda opencast mine is located on the western bank of Hasdeo River in the central part of Korba Coalfields. The upper Kusmunda seam in-crops below a cover of 6–31 m in an elliptical fashion and overlies lower Kusmunda seam after sandstone parting of 65 to 75 m. The area constitutes a doubly plunging anticlinal trend. The lower Kusmunda seam is composite in the western part of the property but the same splits into two section viz. lower Kusmunda (top split) and lower Kusmunda (bottom split) eastwards. One oblique set of faults strike across the anticlinal axis, while the other set of faults appear to strike parallel to the anticlinal axis. The seam generally has a dip ranging from 5° to 10° (1 in 5.6 to 1 in 11.5) and the overall grade of coal is Grade 'F'.

Figure 1. The overview of the Jayant opencast mine.

2.3 *Jayant opencast mine*

Jayant opencast mine of Northern Coalfields Limited is located in the Singrauli Coalfields. The area geographically lies between Latitudes 24°6′45″ to 24°11′15″ and Longitudes 82°36′40″ to 82°41′15″. The project is situated on a high plateau ranging from 300 m to 500 m above M.S.L. The rocks are of Lower Gondwana formation. There are three coal seams namely Turra, Purewa Bottom and Purewa Top. The thicknesses of the coal seams are 13–19 m, 9–12 m and 5–9 m respectively. The direction of strike is towards E–W with broad swings. The dip of the coal seam is 1°–3° in northerly direction (Figure 1). The total leasehold area is 2,464 hectares. The average stripping ratio is 2.6 m^3 of overburden per tonne of coal.

2.4 *Umrer opencast mine*

Umrer project of Western Coalfields Limited is located in the Umrer Coalfields. Three coal seams viz. seam IV, seam III and seam II are mainly exposed in the mine. Presently, production is going on in all three seams. The average stripping ratio of the mine is 2.7 m^3 per tonne coal produced. The dip of the mine is 1 in 10.

3 EXPERIMENTAL DETAILS

Industrial chemical explosives are classified in two large groups, according to their shock wave

Downloaded by [Visvesvaraya Technological University (VTU Consortium)] at 21:55 01 March 2016

velocity, primary and secondary, depending upon their applications. The primary ones have high detonation velocity and sensitivity and are used as initiators for the secondary explosives. Among the former are compounds used in detonators and cast primers (mercury fulminate, PETN, Pentolite, etc.). The secondary explosivesdo more useful work and constituethe mainstay of blasting operations (Du Pont, 1980; Mohanty, 1981). The most common industrial explosives for civilian use are ANFO, ALANFO, Slurries or Watergel, and Emulsion-ANFO combinations. It is well recognised that commercial explosives exhibit non-ideal detonation behaviour since their performance is influenced by blasthole diameter and confinement. Although the basic physico-chemical nature of non-ideal detonation and the law governing it in mathematical form have been known for decades, there is still a lot of work to be done (Byers Brown, 2002). However, a number of mathematical codes are available to solve the problem with some degree of accuracy.

The energy calculations are based on single point initiation and steady state detonation of the explosive column in the blast hole, the former is rarely employed in actual practice in deep hole coal mining because the length of explosives column is sometimes 35–40 m. A common practice is to employ two boosters located at two locations in the blasthole, which may or may not have the same delays. The explosive column may also be traced with detonating cords of specific strengths and connected to these boosters (Mohanty, 2009). Pentolitecast boosters andboth Emulsion and AN-doped Emulsion (10–20% AN)explosive were used in the experimental studies. An attempt was made to maintain the prill size of AN as identical in the study because the prill size of AN has influence upon the density of the explosives. The cup density ranged between 1,04 and 1.06 g/cc.

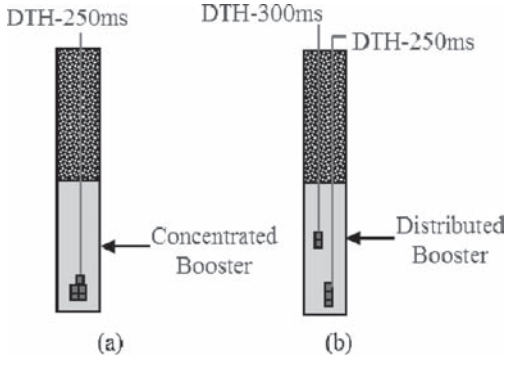

Figure 2. Cast booster distribution in the blast hole.

3.1 *Details of blast performed at SonepurBazari opencast mine*

Field experiments with varying initiation practice were conducted at Sonepur Bazari opencast mine. In each experiment, one blasthole with concentrated boosters and another blasthole on the same bench with distributed boosters as shown in Figure 2 were employed. The in-hole VOD of both the holes were recorded while keeping the drilling pattern, blast design parameters and explosives matrix and loading practice identical. The blasthole loading configuration and the recorded in-the-hole VOD of explosives at Sonepur Bazariopencast mine are given in Table 1.

The recorded in-hole VOD of explosives at SonepurBazari opencast mine due to variation in theplacement of boosters locations (concentrated and distributed) is shown in Figure 3. The other blast design parameters viz. length of explosive column, density,borehole diameter, percentage of cast booster etc. in each experiment (two holes) were kept identical in both cases.

3.2 *Details of blast performed at Kusmunda opencast mine*

The field experiments with varying initiation practice were conducted at Kusmunda opencast mine.

Table 1. Blast loading configuration and recorded in-the-hole VOD of explosives at Sonepur Bazari opencast mine.

Sl. no.	Hole depth (m)/ Hole dia. (mm)	Bottom charge/ Top charge (kg)	Boosters per hole (g)	VOD of explosives (m/s)	Boosters loading configuration	% change in VOD
SBP- 1	12.5/270	300/0	750	4729	Concentrated	3.20
	12.5/270	300/0	750	4582	Distributed	
SBP- 2	26/270	275/0	750	4938	Concentrated	10.40
	26/270	320/0	750	4473	Distributed	

Downloaded by [Visvesvaraya Technological University (VTU Consortium)] at 21:55 01 March 2016

In each experiment i.e. one blasthole with concentrated boosters and another blasthole on the same bench with distributed boosters as shown in Figure 2 were detonated. VOD in both holes were recorded while keeping the drilling pattern, blast design parameters and explosives matrix and loading practice identical. The blast hole loading configuration and the recorded VOD of explosives at Kusmundaopencast mine are given in Table 2.

The recorded in-the-hole VOD of explosives at Kusmundaminefor various booster placement locations (concentrated and distributed) is shown in Figure 4. The recorded VOD traces for concentrated and distributed booster placements are shown in Figures 5 & 6.

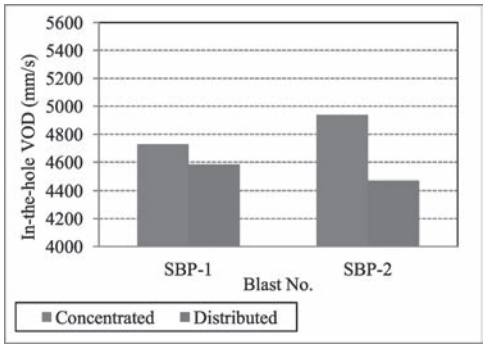

Figure 3. A comparison of the measured in-hole VOD of explosives with varying placement of boosters in the blastholes at SonepurBazari opencast mine.

3.3 *Details of blast performed at Jayant opencast mine*

Field experiments with varying initiation practice were conducted at Jayant opencast mine. In each experiment i.e. one blasthole with concentrated

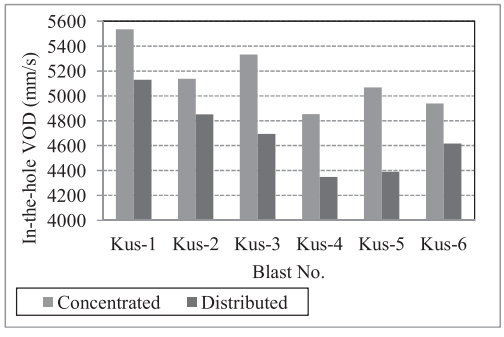

Figure 4. Measured in-the-hole VOD for various booster placements atKusmunda opencast mine.

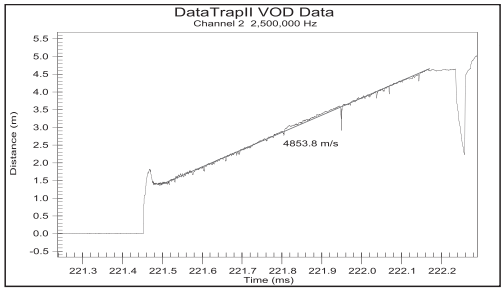

Figure 5. In-the-hole VOD trace where boosters are at one location at Kusmunda opencast mine.

Table 2. Blast loading configuration and recorded in-the-hole VOD of explosives at Kusmunda opencast mine.

Sl. no.	Hole depth (m)/ Hole dia. (mm)	Bottom charge/ Top charge (kg)	Boossters per hole (gm)	VOD of explosives (m/s)	Boosters loading configuration	% change in VOD
KUS-1	15/260	350/0	750	5535	Concentrated	7.87
	15/260	350/0	750	5131	Distributed	
KUS-2	14/260	275/0	600	5168	Concentrated	6.51
	14/260	320/0	750	4852	Distributed	
KUS-3	15/160	175/0	400	5334	Concentrated	13.63
	15/160	175/0	400	4694	Distributed	
KUS-4	15/260	250/180	500+300	4853	Concentrated	10.47
	15/260	250/180	500+300	4393	Distributed	
KUS-5	15/260	380/0	750	5069	Concentrated	15.44
	15/260	380/0	750	4391	Distributed	
KUS-6	15/260	175/0	500	4939	Concentrated	6.95
	15/260	190/0	500	4618	Distributed	

Downloaded by [Visvesvaraya Technological University (VTU Consortium)] at 21:55 01 March 2016

boosters and another blasthole on the same bench with distributed boosters as shown in Figure 2 were detonated.VOD in both holes were measured while keeping all the other parameters constant. The blast hole loading configuration and the recorded VOD of explosives at Jayantopencast mine is presented in Table 3. The recorded VODat Jayant opencast minefor various booster placement locations (concentrated and distributed) is shown in Figure 7.

3.4 *Details of blast performed at Umrer opencast mine*

Field experiments with varying initiation practice were conducted at Umrer opencast mine. In each experiment i.e. one blasthole with concentrated boosters and another blasthole on the same bench with distributed boosters as shown in Figure 2 were detonated. VOD in both blastholes were recorded while keeping the drilling pattern, blast design parameters and explosives matrix and loading practice identical. The blast hole loading configuration and the recorded in-the-hole VOD is presented in Table 4.

The recorded VOD of explosives at Umrer opencast minefor various booster placement locations (concentrated and distributed) is shown in Figure 8. The VOD traces for concentrated and distributed booster placements are presented in Figure 9 & 10.

3 DISCUSSION

The recorded in-the-hole VOD at different drill hole diameters were compared for concentrated and distributed booster combinations and are reproduced in Figure 11. Similarly, the recorded VOD for different depth of holes were compared for concentrated and distributed booster combinations and is presented in Figure 12.

The recorded VOD of explosives of 26 blast holes for different diameter and depth of holes are presented in Figures 11 & 12 respectively. Ina number of instances the recorded VOD in bottom deck was higher than the recorded VOD on top deck (Figs. 13, 14 & 15).VOD of explosives in various boreholediameterswere recorded at Umrer and Kusmunda projects for a number of experimental set-ups. The recorded data are given in Tables 5 & 6 respectively.

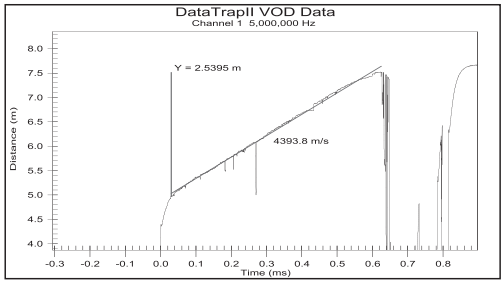

Figure 6. VOD trace where boosters are at two locations at Kusmunda opencast mine.

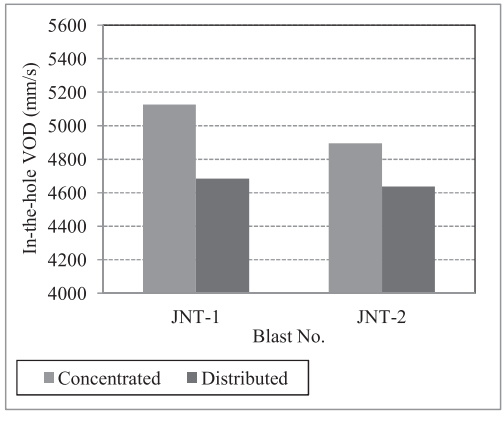

Figure 7. Measured VOD for various booster placements at Jayant opencast mine.

Table 3. Blast loading configuration and recorded in-the-hole VOD at Jayant opencast mine.

Sl. no.	Hole depth (m)/ Hole dia. (mm)	Bottom charge/ Top charge (kg)	Boosters per hole (gm)	In-the-hole VOD of explosives (m/s)	Boosters loading configuration	% change in VOD
JNT-1	13/160	210/0	250	5125	Concentrated	9.41
	13/160	210/0	250	4684	Distributed	
JNT-2	22/270	630/420	1200+800	4895	Concentrated	5.56
	22/270	630/420	1200+800	4637	Distributed	

Downloaded by [Visvesvaraya Technological University (VTU Consortium)] at 21:55 01 March 2016

Table 4. Blast loading configuration and recorded in-the-hole VOD at Umrer opencast mine.

Sl. no.	Hole depth (m)/ Hole dia. (mm)	Bottom charge/ Top charge (kg)	Boosters per hole (gm)	VOD of explosives (m/s)	Boosters loading configuration	% change in VOD
UMR-1	7.5/270	250/0	500	4911	Concentrated	10.63
	7.5/270	250/0	500	4439	Distributed	
UMR-2	7.5/160	90/0	200	4547	Concentrated	1.49
	7.5/160	90/0	200	4480	Distributed	
UMR-3	7.5/270	200/0	400	5539	Concentrated	18.48
	7.5/270	200/0	400	4675	Distributed	

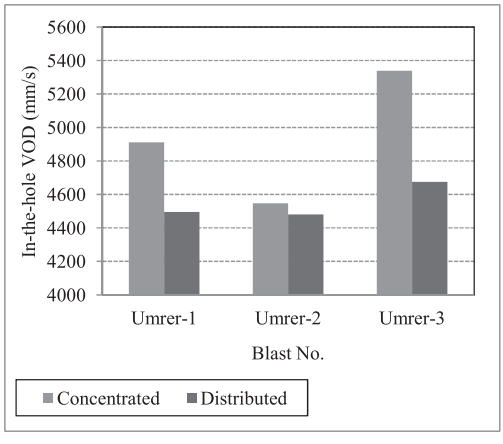

Figure 8. Measured in-the-hole VOD of explosives for various booster placements at Umreropencast mine.

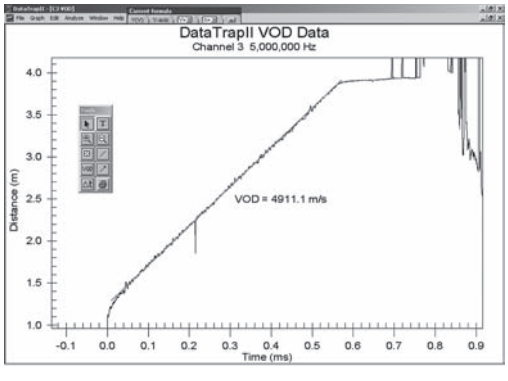

Figure 9. In-the-hole VOD trace when boosters are at one location at Umrer opencast mine.

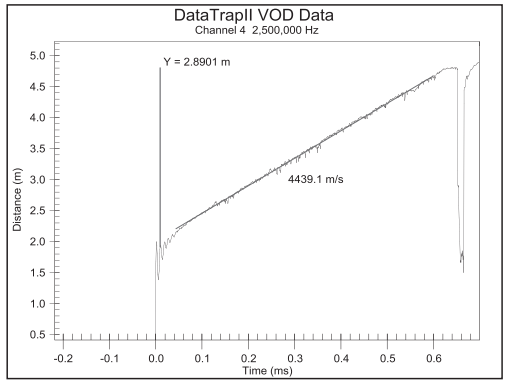

Figure 10. In-the-hole VOD trace when boosters are at two locations at Umrer opencast mine.

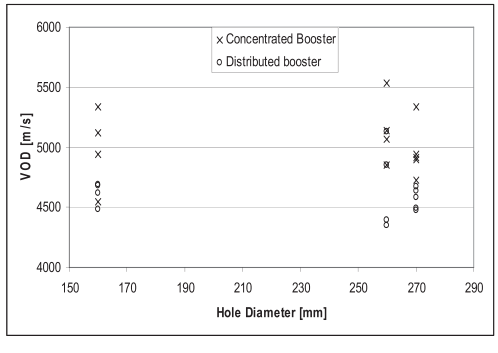

Figure 11. Plot of recorded VODs against hole diameters for concentrated and distributed booster locations.

4 RESULTS AND CONCLUSIONS

The recorded in-the-hole VOD of explosives data from 26 holes i.e. 13 sets of experiments with varying hole depths and drill hole diameters shows that when the boosters are placed at one location (concentrated) e.g. at sub-grade levels, higher VODs were recorded in all the mines. There was drop in the VOD when the boosters were distributed at two locations (distributed). Concentrated boosters in a blasthole always yielded higher VOD when compared to the distributed booster charging configuration.

Downloaded by [Visvesvaraya Technological University (VTU Consortium)] at 21:55 01 March 2016

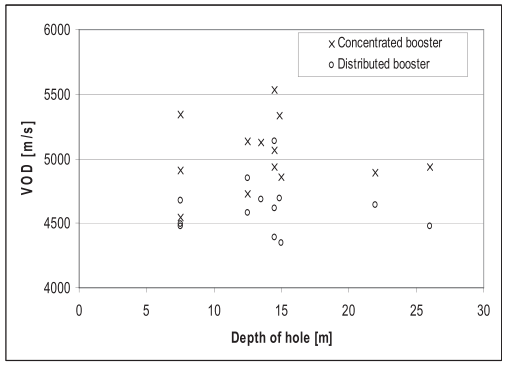

Figure 12. Plot of recorded VODs against depth of hole for concentrated and distributed booster locations.

Table 5. Recorded in-the-hole VOD of explosives at different borehole diameters at Umrer project.

Sl. no.	Hole diameter (mm)	In-the-hole VOD of explosives (m/s)
1	160	4480
2	160	4494
3	160	4565
4	160	4638
5	250	4778
6	250	4820
7	270	4835
8	270	4840
9	270	4911
10	270	5019
11	270	5148
12	270	5155
13	270	5339

Table 6. Recorded in-the-hole VOD of explosives at different borehole diameters at Kusmunda project.

Sl. no.	Hole diameter (mm)	In-the-hole VOD (m/s)
1	160	4498
2	160	4503
3	160	4538
4	160	4599
5	160	4642
6	160	4694
7	260	4778
8	260	4819
9	260	4854
10	260	5058
11	260	5069
12	260	5128
13	260	5138
14	260	5140

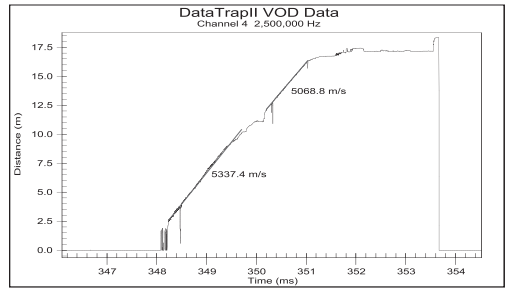

Figure 13. Recorded In-the-hole VOD of SME explosive at bottom and top explosives column charges (the deck length was 10 D i.e. 2.7 m).

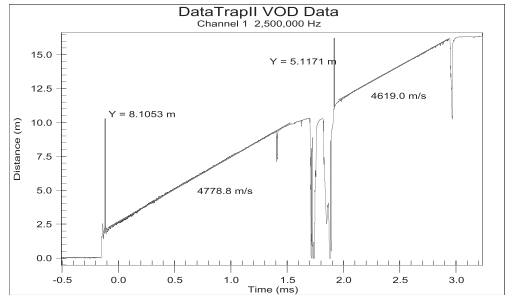

Figure 14. Recorded in-the-hole VOD of explosives in bottom and top explosives column charges.

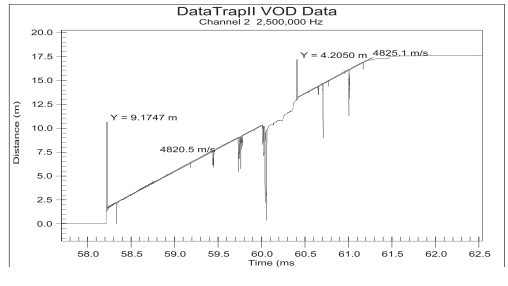

Figure 15. Recorded in-the-hole VOD of explosives in bottom and top explosives column charges.

It has been experimentally shown that the performance of the explosives at the bottom and top of the explosive column is different.The higher VOD at the bottom section of the borehole is attributed to higher density caused by the higher static pressure at the bottom section of the explosive column. The same would apply to the higher VOD observed for longer explosive column.

There exists a positive and significant relationship between in-hole velocity of detonation and borehole diameter. A nearly 24% increase in VOD was observed when the borehole diameter was

increased from 160 mm to 311 mm. However, there is insufficient data to establish a quantitative relationship between borehole diameter and VOD at this stage.

However, the results obtained with distributed boosters yielding lower VOD in the same explosive with all other variables being kept constant must be considered anomalous. Once detonation has been initiated by the booster at the toe, the presence of another booster in the upper section of the explosive column should have no bearing on the VOD, unless the explosive quality in the borehole was non-uniform and degraded towards the collar region. Clearly, additional tests have to be performed to investigate the phenomenon, with better control of explosive compositions.

ACKNOWLEDGEMENTS

The authors express their gratitude to the Ministry of Coal, Government of India for financial support of this study. The support provided by the respective mines during the field studies is much appreciated. The permission of Director, Central Institute of Mining & Fuel Research, Dhanbad, India to publish this paper is also thankfully acknowledged.

REFERENCES

Byers, Brown W. 2002. Critical review of theories of steady non-ideal two-dimensional detonation of condensed explosives. *Swedish blasting research centre (Swebrec) report 2005:1*, 190p.

Cundall, P., Ruest, M., Chitombo, G., Esen, S. & Cunningham, CVB, 2001. The hybrid stress blasting model: A feasibility study. *Confidential Report, JKMRC, ITASCA and AEL*.

Cunningham, CVB. 2001. The energy at detonation: A fresh look at pressure in the blast hole. *Explo 2001, Hunter Valley, NSW, Australia*, pp. 179–189.

Du Pont, 1980. Blaster Handbook, *16th Edition*.

Konya, C.J. & Walther, E.J. 1990. Surface Blast Design, *Prentice Hall*.

Leiper, G.A. & Plessis, M.P. 2001. Describing explosives in blast models.Proceedings of Second International Symposium on Rock Fragmentation by Blasting, Keystone, Colorado, USA, pp. 462–474.

Mohanty, B. 1981. Energy strength and performance and their implications in rating commercial explosives, Proc. 7th Ann. Conf. On Explosives and Blasting Tech., *ISEE,* pp. 293–306.

Mohanty, B. 2009. Intra-hole and inter-hole effects in typical blast designs and their implications on explosive energy release and detonator delay time-A critical review. *Proc. 9thInt. Symp.on Rock Fragmentation by Blasting;Sanchidrian, ed.CRC Press*, pp. 23–31.

Downloaded by [Visvesvaraya Technological University (VTU Consortium)] at 21:55 01 March 2016

Performance of Explosives and New Developments – Mohanty & Singh (Eds)
© 2013 Taylor & Francis Group, London, ISBN 978-0-415-62142-7

Studies into firing accuracy of some Indian permitted electric detonators

S.K. Roy & R.R. Singh
Explosive & Explosion Laboratory, CIMFR, Dhanbad, India

ABSTRACT: Permitted detonators are approved by Directorate General of Mines Safety for use in Indian underground coal mines if they meet the statutory requirements related to their safety, sensitivity and performance parameters. Only seven series of delay detonators with delay nos. 0 to 6 having 25 ms difference in their nominal delay timings are approved in India. Pyrotechnic delay elements used in permitted electric detonators are intrinsically limited in precision and have inherent scattering. Researchers have observed that actual firing timing of detonators differ from their nominal firing times and it can be analysed using statistical concepts. Scattering in delay timings of permitted delay detonator may cause out of sequence firing of holes in underground coal mines which is undesirable from productivity and safety point of view. Firing accuracies of permitted delay detonators marketed by two domestic manufactures were evaluated. Different statistical parameters were calculated to determine the central tendencies and scattering in observed delay timings of different delay detonators. Winzer Index was also calculated to predict the overlapping possibilities. Statistical analysis of delay timings revealed significant probability of overlapping. This study highlighted need for statutory regulation on delay timing of permitted delay detonators and development of permitted electronic detonators in India.

1 INTRODUCTION

Detonators used in underground coal mines in India are required to meet stringent statutory requirements with respect to their incendivity, electrical characteristics, handling safety, water resistance, performance parameters, etc. The Directorate General of Mines Safety (DGMS) is the statutory authority for mines safety in India and regulates the use of explosives and detonators in underground coal mines. As electric detonators contain highly sensitive explosives materials, it should possess adequate handling safety characteristics so that it does not get initiated inadvertently during manufacture, handling, transport, storage and usage. Whereas, electrical detonators should possess uniform electrical characteristics for their satisfactory initiation when used in series, they should be safe against a stray currents defined as their no fire current limit. These detonators should be sufficiently strong to initiate cap sensitive explosives and their crimping should be tight enough to resist any ingress of water when used in watery holes. Moreover, permitted electric detonators should possess satisfactory non-incendive characteristics in inflammable atmosphere in laboratory when checked as per IS 6609 (Part III) (1973) simulating the worst conditions which may prevail during their actual use in underground coal mines.

Two types of permitted detonators are commonly manufactured and approved for use in Indian underground coal mines. These include: (1) instantaneous electric detonators; and (2) delay electric detonators. Only seven series of delay detonators with delay nos. 0 to 6 having 25 ms difference in their nominal delay timings are approved in India. Permitted instantaneous electric detonators are generally used with permitted (ordinary) or P_1 explosive and permitted (equivalent to sheathed) or P_3 explosive. Permitted delay electric detonators can be used only with permitted (for solid blasting) or P_5 explosives in India (Roy & Singh, 2011). Permitted detonators are designed to initiate multiple charges of permitted explosives with a single application of firing current in the blasting circuit. In the solid blasting method, a free face is created by blasting a few holes and then blasting the remaining holes into this opening in a single round using a suitable combination of delay detonators.

Downloaded by [Visvesvaraya Technological University (VTU Consortium)] at 21:56 01 March 2016

Important conditions governing usage of permitted delay electric detonators in solid blasting in Indian underground coal mines include (Prasad and Rakesh, 1992):

i. no detonator other than a 'non-incendive' short (millisecond) delay detonator shall be used in solid blasting.
ii. the estimated period of delay between the first and the last shot of the round in degree I and II gassy coal mines, calculated by the reference to the marking on the detonators, shall not exceed 0.15 seconds.
iii. the estimated period of delay between the first and the last shot of the round in degree III gassy coal mines, calculated by the reference to the marking on the detonators, shall not exceed 0.10 seconds.
iv. the estimated period of delay between any two consecutive shots with different delays shall not exceed 0.06 seconds.

Presently, permitted electric detonators of ten different Indian manufacturers have been approved by the statutory authority for use in Indian underground coal mines. In all these permitted delay electric detonators, delay timing is provided using delay elements made up of pyrotechnic compositions. Delay detonators made with pyrotechnic delay compositions are intrinsically limited in precision and have inherent scattering. For successful and efficient blasting, delay detonators should get fired in the sequence as they are intended. Winzer (1978) completed a study of initiator firing times. He clearly showed that considerable scatter existed and that in some cases the variability was so great that firing times of initiators from adjacent period were reversed. Winzer (1978) and subsequently many researchers pointed that inaccuracies in delay timings of permitted electric detonators may result in out of sequence firing (i.e. overlapping), blown out shots, fly rock, uneven back break, increased ground vibration and air blast, etc. Blowing out of shots holes in underground coal mines is considered to be hazardous as the explosive flame may ignite the possible inflammable mixture of coal dust or firedamp—air mixture likely to be present in underground coal mines. Many researchers and industry have demonstrated advantage of using precise delay timing detonators in improving blast performance and reducing side effects of blasting such as vibration, noise, back break, fly rock, etc. Therefore, overlapping in delay firing of permitted delay detonators is undesirable from production as well as safety point of view. Manufacturing of delay detonators demand high level of quality control in order to keep the scatter within a limit so that overlapping could be avoided. Therefore, in addition to the other statutory requirements, measured delay timing of permitted delay detonators should be within a narrow range to avoid overlapping possibilities. In India, permitted detonators are evaluated in respect of their incendivity, handling and electrical safety, performance and water resistance characteristics as per IS 6609 (Part III) (1973) and DGMS guidelines (Verma et al. 2003). But, present approval practices followed by Indian statutory authority do not emphasize on accuracy of delay timing of permitted electric delay detonators.

The paper presents statistical analysis of measured delay timings of permitted delay electric detonators (0 to 6 delays) of two Indian manufacturers. Overlapping and crowding possibilities amongst different delays were evaluated by calculating Winzer index and graphical methods. Analysis of results revealed significant overlapping between different delays and thus statutory authority should consider results of measurement of delay timings of permitted detonators along with other results related to incendivity, handling safety etc. before granting approval of permitted detonators for use in Indian underground coal mines. Considering inherent limitations of pyrotechnic delay elements and consumption of about 55 million permitted detonators in India, authors feel that development of cost-effective electronic permitted detonators should be considered to eliminate overlapping and crowing of delay timings of permitted detonators.

2 EXPERIMENTAL TECHNIQUE

Schematic diagram of a setup used for measurement of delay timing of permitted electric delay detonators has been shown in Figure 1 which is similar to the set-up used by Harsh and Thote (2006).

It consists of a constant current generator unit, a two-channel oscilloscope, a microphone, a resistance etc. Constant current generator unit used in

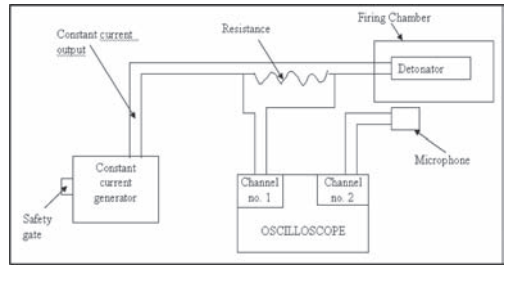

Figure 1. Schematic circuit diagram of set-up for measurement of delay timing of electrical detonator.

Downloaded by [Visvesvaraya Technological University (VTU Consortium)] at 21:56 01 March 2016

the set-up was designed to provide a constant current pulse of amplitude ranging from 0.2 to 3.0 A and duration from 1 to 10 ms, which can be preset by user. The instrument was provided with a safety gate to protect against the inadvertent firing of the detonators. Moreover, detonators are inserted into a firing chamber made of 8 mm thick iron plates before connecting to the terminals of constant current generator unit. Two channel digital oscilloscope having real time sampling rate of 2GS/s was used in the set-up. Microphone, kept at 5 cm from the firing chamber in all the trials, generated an electrical pulse by receiving the sound generated from detonation of detonator inside the firing chamber.

Delay timing of detonators were measured one by one. The intended detonator, whose delay timing was to be measured, was kept inside the firing chamber. Two lead wires of the detonator were connected to the constant current generator unit. Microphone, resistance and oscilloscope were connected as shown in Figure 1. A direct current of 1.20A and duration of 4 ms was set in the constant current generator unit as per statutory guidelines for successful firing of Indian permitted detonators. After necessary connections and safety checks, firing button in constant current generator unit was pressed. Channel 1 of oscilloscope records the firing pulse generated by constant current generator unit as shown in Figure 2.

Sound generated by detonation of detonator was recorded by the microphone connected in channel 2 of the oscilloscope. The time interval between the start of current supply through the detonator and the time when detonator detonated has been taken as delay timing. This timing can be found out by moving cursors between the peaks as shown in Figure 2.

Delay timing of twenty detonators of each delay (i.e. 0 to 6 delays) of two different Indian manufacturers, coded as Manufacturer-A and Manufacturer-B, were measured one by one using this set-up.

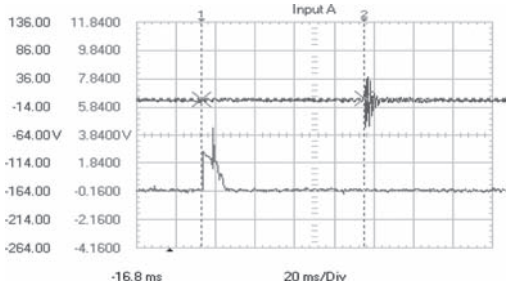

Figure 2. A typical recording of delay timing in oscilloscope.

3 ANALYSIS OF RESULTS

Measured delay timings of the detonators were analysed statistically. Different statistical measures to qualify their central tendencies and scattering in values were calculated. Tables 1 and 2 summarise the nominal delay timing (Tn), average of twenty measurements (A), standard deviation (σ), lowest (T_e), and highest (T_h) measured delay times for each delay period. Table also presents ratio of standard deviation to average value (100 σ/A) (an estimate of dispersion of the observed data with respect to average value), and $(T_h–T_e)/\sigma$ (an indication of the spread in delay times, relative to standard deviation) (Bajpayee et al., 1985). Winzer index (S) (Winzer, 1978; Winzer et al., 1979, Bajpayee et al., 1985), described below in Equation 1, with τ = 0 and τ = 8 ms for consecutive delay periods are also shown in the tables.

$$S = [A_{(n+1)} - A_n - \tau] / [\sigma_{(n+1)}{}^2 + \sigma_n{}^2]^{1/2} \quad (1)$$

Where $A_{(n+1)}$ = Average delay time for period (n+1) detonators; A_n = Average delay time for period n detonators; $\sigma_{(n+1)}$ = standard deviation for period (n+1) detonators; σ_n = Average delay time for period n detonators; and τ = required time interval between the firings of adjacent holes.

Bajpayee et al. (1985) used τ = 0 for mathematical convenience but indicated that τ are about 10 ms for explosives to significantly move the burden typical to underground coal mines. 8 ms criterion is well known and applied rule for defining "separate" charges for predicting vibration amplitudes (Singh, 2004). Initiator crowding occurs when initiators of adjacent periods fire in proper sequence but the interval between the firing times is not long enough. Winzer et al. (1979) and Rholl & Stagg (1988) used τ = 8 to calculate the crowding possibilities. Initiator crowding becomes initiator overlap as τ approaches zero. Winzer Index (S) of less than 3 indicates significant probability of overlap (if τ = 0) or crowding (if τ = 8) between two selected delay periods.

In order to assess overlapping possibilities, recorded delay timings of different delays were anaysed graphically. Figure 3 shows average (A) of each delay and 3σ spread of delay times on both sides of the average (i.e. A ± 3σ) for manufacturer—A. Similarly, Figure 4 shows A and A ± 3σ of each delay for manufacturer—B. In Figures 5 and 6, maximum value of measured delay timing of a delay period (i.e. T_h of delay period n) was plotted against the minimum value of measured delay timing observed with next higher delay period (i.e. T_e of delay period n+1) for manufacturer-A and manufacturer-B respectively.

Downloaded by [Visvesvaraya Technological University (VTU Consortium)] at 21:56 01 March 2016

Table 1. Summary of detonator delay measurement of manufacturer—A.

Delay period (n)	Delay values, ms: Nominal (T_n)	Average (A_n)	Low (T_e)	High (T_h)	Std. dev. (σ)	100 σ_n/A_n	$(T_h–T_e)/\sigma$	Winzer index (S) with τ = 0	Winzer index (S) with τ = 8 ms
0	0	5.73	3.2	8.0	1.24	21.64	3.87		
1	25	25.61	21.1	35.2	3.51	13.69	4.02	5.34	3.19
2	50	68.59	63.1	73.5	2.44	3.56	4.26	10.06	8.18
3	75	86.04	73.1	95.7	6.07	7.05	3.72	2.67	1.44
4	100	114.84	101.1	124.5	5.56	4.84	4.20	3.50	2.50
5	125	131.76	120.5	139.1	4.05	3.07	4.59	2.46	1.30
6	150	151.14	137.9	167.5	7.75	5.13	3.81	2.21	1.30

Table 2. Summary of detonator delay measurement of manufacturer—B.

Delay period (n)	Delay values, ms: Nominal (T_n)	Average (A_n)	Low (T_e)	High (T_h)	Std. dev. (σ)	100 σ_n/A_n	$(T_h–T_e)/\sigma$	Winzer index (S) with τ = 0	Winzer index (S) with τ = 8 ms
0	0	6.46	3.7	9.9	1.66	25.76	3.73		
1	25	34.59	21.8	60.0	10.51	30.38	3.64	2.64	1.89
2	50	63.41	43.3	91.3	12.09	19.06	3.97	1.80	1.30
3	75	87.05	66.9	126.7	12.04	13.83	4.97	1.39	0.92
4	100	115.71	91.0	148.9	16.83	14.54	3.44	1.39	1.00
5	125	134.12	105.9	169.0	15.30	11.41	4.12	0.81	0.46
6	150	144.71	110.6	177.4	19.03	13.15	3.51	0.43	0.11

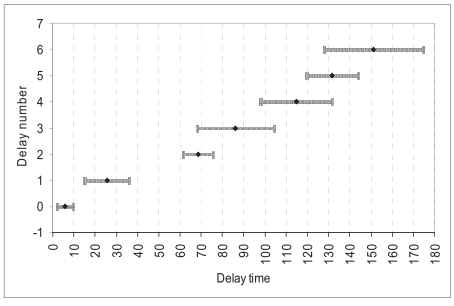

Figure 3. Average and spread of delay timings of manufacturer-A.

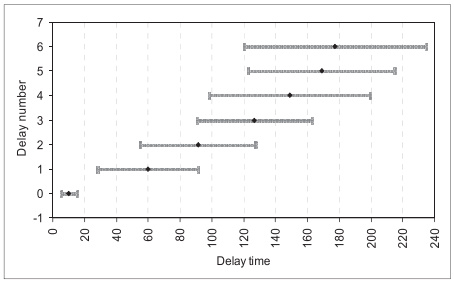

Figure 4. Average and spread of delay timings of manufacturer—B.

4 DISCUSSION ON RESULTS

Summary of data given in Table 1 and their analysis in Figures 3 and 5 for measured delay timing of permitted electric delay detonators of manufacturer-A indicate that

a. Detonators of delay periods 0, 1, and 2 show a Winzer index with τ = 0 as well as with τ = 8 greater than 3 and thus have negligible probability of overlapping and crowding.
b. Detonators of delay periods 3 and 4 also show a Winzer index greater than 3 with τ = 0 but have Winzer index less than 3 with τ = 8 and thus they have negligible probability of overlapping but have chances of crowding (i.e. firing within a delay interval less than 8 ms).
c. Average delay time of delay number 2 detonators (68.59 ms) is higher than its nominal value and is close to nominal value of delay number 3 detonators which is evident from figure 3 and 5 also. Delay periods 2 and 3 have a Winzer index less than 3 and thus have chances of overlapping and firing out of sequence.
d. Detonators of delay periods 4, 5, and 6 show a Winzer index less than 3 and thus have significant probability of overlapping which is evident from overlapping of expected delay timings plotted in Figure 3.

Downloaded by [Visvesvaraya Technological University (VTU Consortium)] at 21:56 01 March 2016

e. Average delay times of delay period 2 to 5 detonators of manufacturer-A were found to be higher by 6.76 ms to 18.59 ms from their nominal values.
f. The highest firing time (T_h) measured with delay period 2, 4 and 5 detonators were found to be higher than the lowest firing time (T_e) observed with delay period 3, 5 and 6 detonators respectively as evident from Table 1 and Figure 5 and thus they have chances of overlapping which was evident from Winzer ratio.
g. The (100 σ/A) and $(T_h–T_e)/\sigma$ ratios for different delay period detonators of manufacturer-A were found to vary from 3.07 to 21.64 and 3.72 to 4.59 respectively. These values of (100 σ/A) and $(T_h–T_e)/\sigma$ ratios for Indian manufacturer—A was found to be similar to that observed by Bajpayee et al. (1985) for permissible detonators in USA.

Similarly, summary of data given in Table 2 and their analysis in Figures 4 & 6 for measured delay timing of permitted electric delay detonators of manufacturer-B indicate that.

a. Detonators of delay periods 0 and 1 have a Winzer index of 2.64 with $\tau = 0$ but have Winzer index of 1.89 with $\tau = 8$. Thus, they have low probability of overlapping, but have significant probability of crowding. From Figure 3 also it is evident that they have very low probability of overlapping. None of twenty detonators of delay period 1 were found to have their delay timing lower than the highest value of delay time observed with delay period 0 detonators as shown in Figure 6.
b. Detonators of delay periods 1 through 6 of manufacturer-B show a Winzer index less than 2 and thus have high probability of overlapping. With increase in delay numbers, Winzer index decreased which shows that possibility of overlapping is more with higher delay period detonators.
c. Inferences drawn from Winzer index for different pairs of adjacent delays of manufacturer-B is also evident from the overlapping of the lines drawn for expected range of scatter of delay timings (i.e. $A \pm 3\sigma$) in Figure 5.
d. Average delay times of delay 1 to 5 detonators of manufacturer-B were found to be higher by 9.12 ms to 15.71 ms from their nominal values. Similar differences were also observed with delay detonators of manufacturer-A. But, as the standard deviation of delay timings of detonators of manufacturer-A was lower in comparison to that of manufacturer-B, overlapping possibilities with delay detonators of manufacturer-B were more.
e. The highest firing time (T_h) measured with delay number 1 through 6 detonators were found to be higher than the lowest firing time (T_e) observed with consecutive higher delay number detonators as evident from Table 2 and Figure 6.
f. As evident from Figures 3 & 5 for manufacturer-B, delay period 2 detonators have overlapping delay timings with delay period 3 as well as 4. Similarly, delay period 3 detonators have delay timings overlapping with not only delay period 4 detonator but also with delay period 5 and 6 detonators. Like wise, delay period 4 detonators have overlapping delay timings with delay periods 5 as well as 6. Such overlapping possibilities were not observed with permitted delay detonators of Manufacturer-A.
g. The (100 σ/A) ratio for different delays detonators of manufacturer-B were found to vary from 11.41 to 30.38 which is higher than that observed with manufacturer—A.
h. The $(T_h–T_e)/\sigma$ ratio for different delays detonators of manufacturer-B were found to vary from 3.44 to 4.97 which is similar to that observed for Indian manufacturer—A and also by Bajpayee et al. (1985) for permissible detonators in USA.

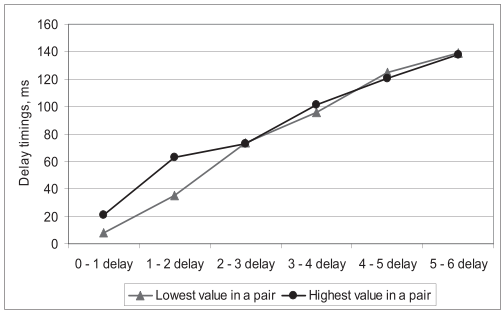

Figure 5. Overlapping of delay timings of two consecutive delays of manufacturer-A.

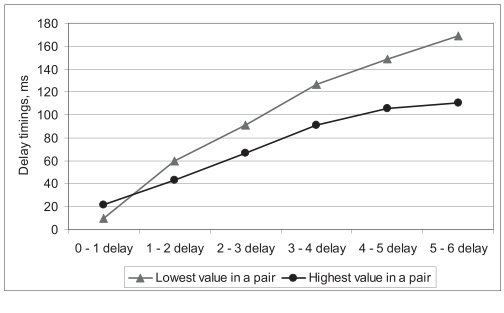

Figure 6. Overlapping of delay timings of two consecutive delays of manufacturer-B.

Downloaded by [Visvesvaraya Technological University (VTU Consortium)] at 21:56 01 March 2016

5 CONCLUSIONS

Results of assessment of firing times of two indigenous manufacturers revealed that actual delay timings of detonators vary from their nominal declared values and have significant chances to get fired out of the sequence. Overlapping possibilities were found to be more with higher period delay detonators of both manufacturers. Scattering in measured delay timings of permitted detonators of manufacturer-B were found to be higher than that of manufacturer-A. Although, permitted electric detonators of manufacturer-A were found to have overlapping possibilities with consecutive higher delays, that of manufacturer-B were found to have overlapping possibilities with even non-consecutive higher delays also. Winzer index calculated for different pair of delay detonators were found to have good correlation with overlapping possibilities inferred from other statistical and graphical methods. Although, this study does not present a critical evaluation of quality control of permitted electric detonators of two indigenous manufactures, results reported here corroborates the results reported by Nabiullah et al. (1988) on some Indian commercial delay detonators which points out that there has not been much improvement in this regard over last two decades. If similar scattering is prevailing with permitted delay detonators of all other manufacturers, statutory authority needs to look into the matter seriously.

As out of sequence firing of detonators, especially in underground coal mines, is undesirable as well as unsafe, Indian manufacturers need to review design and quality control of their permitted delay detonators so that overlapping possibilities is minimised. Moreover, the study has been helpful in highlighting the need for stricter statutory control on delay timings of permitted delay detonators in India. Development of cost-effective permitted electronic detonator may eliminate overlapping possibilities observed with present pyrotechnic permitted delay detonators.

REFERENCES

Bajpayee, T.S., Mainiero, Richard J. & Hay, J. Edmund. 1985. Overlap probability for short-period-delay detonators used in underground coal mining. *Bureau of mines report of investigation 8888,* 18p.

Becker, Karl R. & Hay, J. Edmund. 1985. Effect of direct-current firing levels on detonator delay times. *Bureau of mines report of investigation 8613,* 13p.

Indian Standard IS: 6609 (Part III) (1979). Methods of test for commercial blasting explosives and accessories, Part III: Detonators, general and permitted', *Indian Standard Institutions,* Manak Bhawan, New Delhi, India, 1973, 21p.

Nabiullah, Md., Gupta, R.N. & Singh, B. 1988. Investigation on delay period of some commercial delay detonators. *Journal of Mines, Metals and Fuels, July 1988,* pp. 363–367.

Prasad, S.D. & Rakesh. 1992. Legislation in Indian mines: a critical appraisal, *Vol. II, 1420–1421; Tata Printing Works,* Varanasi, India.

Rholl, Stephen A. & Mark S. Stag. 1988. A computer program to predict the probability of overlap or crowding of adjacent period-period millisecond-delayed initiators. *Fourth mini-symposium on explosives and blasting research, Anaheim, CA, February 4–5, 1988,* pp. 91–105.

Roy, S.K. & Singh, R.R. 2011. Use of spacer aided initiation technique in solid blasting in Indian underground coal mines. *Trans. Inst. Min. Metall. Sec. A, 120 A, (1)*, pp. 25–35.

Singh, P.K. 2004. CMRI report on study on the effect of delay timing, total charge and direction of initiation on blast induced ground vibration. *Submitted to Department of Coal, Ministry of Coal and Mines, Government of India*. New Delhi, pp. 12–13.

Verma, H.K. & Thote, N.R. 2006. Delay precision in permitted copper delay detonator. *Journal of Mines, Metals and Fuels,* 54 (10 & 11), pp. 226–230.

Verma, H.K., Roy, S.K., Singh, R.R. & Bhattacharyya, M.M. 2003. A report on advice on suitability of solar copper delay detonators for use in underground coal mines, *Unpublished CMRI report,* 8p.

Winzer, S.R. 1978. The firing times of millisecond delay blasting caps and their effect on blasting performance. *Nat. Sci. foundation, Washington, DC 220550.* Contract DAR-77–05171, Martin- Marietta Laboratories, 36p.

Winzer, S.R., Furth, W. & Ritter, A. 1979. Initiator firing times and their relationship to blasting performance. *Proceedings of 20th US symposium on rock mechanics,* Austin, June 4–6, Texas, USA, pp. 461–470.

Performance of Explosives and New Developments – Mohanty & Singh (Eds)
© 2013 Taylor & Francis Group, London, ISBN 978-0-415-62142-7

Detonation behavior of bulk emulsion explosive in water filled blast holes

M. Pradhan & R.K. Jade
National Institute of Technology, Raipur, India

ABSTRACT: This paper describes a study carried out to investigate the performance of bulk emulsion explosive in watery blast holes by measuring its continuous in-hole velocity of detonation (VOD). Ten watery blast holes were monitored in a limestone mine. VOD was successfully recorded in seven blast holes. In three of the seven blast holes which successfully recorded the events, full column detonation did not take place and in the remaining four, a large reduction in VOD of the explosive was observed. Through this study an attempt is made to determine the possible causes of malfunctioning of the explosives in the watery blast holes.

1 INTRODUCTION

Water is often encountered in blast holes during and after rainy seasons, especially in lower benches of deep open cast mines. An explosive should have two important properties to be used in watery blast holes. First, it should be able to withstand exposure to water without any detrimental effect on its performance *i.e.* it should be water resistant. Second, it should not float over the water present in the blast holes *i.e*. its density should be higher than the density of the water present in the blast holes. Generally, a density of 1.10 g/cc is considered to be sufficient for an explosive to sink quickly in the clear water having density around 1.0 g/cc. But water in the blast holes is generally not clear; a large amount of silt is mixed in the water—as a result its density is higher than the density of clear water. Under such conditions, an explosive having a density higher than 1.10 g/cc is required.

ANFO, slurry and emulsion are the three explosives commonly used in commercial blasting. Among these commercial explosives ANFO is not considered water resistant. The ammonium nitrate prills used in ANFO explosive are highly hygroscopic. When used in watery conditions, ANFO absorbs the water and gets desensitized. The VOD of ANFO decreases with increase in water content. It has been found that VOD of ANFO decreases sharply, when the water content of ANFO increases to more than 4.0% and at 9.0% of water content the explosive fails to detonate (Bhandari 1997). The density of ANFO is also less than the density of the water. The density of ANFO varies from 0.8–0.9 g/cc.

Both slurry and emulsion explosive were developed to make ANFO water résistant. Unlike ANFO, in slurry explosives both oxidizer and fuel are in liquid form and cross linked to give gel consistency. The gel structure of an explosive prevents the intrusion of water and makes it water resistant. A large reduction in the VOD, vibration and burden velocity of site mixed slurry explosive (SMS) was observed when these were used in wet holes (Cameron & Grouchel, 1990). The performance of SMS in a blast hole, which was full of water, was evaluated by National Institute of Rock Mechanics, India. The VOD at the bottom was found to be 4036 m/s, while at the top it was only about 1000 m/s, indicating deflagration of explosive (NIRM 2001). The density of slurry explosive varies from 0.7 g/cc to 1.15 g/cc.

Like slurry explosive, both oxidizer and fuel in emulsion explosive are also in liquid form. The emulsion explosive is generally water-in-oil type. The tiny droplets of oxidizer salt solution provide the dispersion phase whereas the fuel forms the continuous phase. Each fine droplets of oxidizer salt solution is coated by a thin film of fuel. When the explosive is immersed in water, the oil film prevents the water from entering into the emulsion matrix and thus makes it an excellent water resistant explosive. An emulsifying agent is added to increase the stability of the emulsion. The water resistance of an emulsion explosive depends on the emulsifying quality of emulsion explosive matrix. The better the quality of emulsifying agent, the greater is its water resistance. Density of emulsion explosive varies in a wide range from 0.9 to 1.35 g/cc. In case of bulk product, the density variation is also possible at site as per the requirement. The perform-

Downloaded by [Visvesvaraya Technological University (VTU Consortium)] at 21:56 01 March 2016

ance of bulk emulsion explosive of seven different manufactures has been examined by some previous researchers. Fresh VOD, VOD under shallow water (USWVOD) and VOD under Hydrostatic Pressure (UHPVOD) were determined. USWVOD was determined after hanging the explosive cartridge in a water bath at a depth of 0.5 m for 24 hours with top end open. A fall of about 6.0% to 10.0% in VOD was observed (Nabuiullah et al. 2005). Similarly, Pradhan (2007) evaluated the performance of bulk emulsion explosive in laboratory environment. The VOD of emulsion explosive was observed to fall by 8.0%–10.0% when suspended in water over a time period of 15 days.

Because of its excellent detonation characteristic and water resistance emulsion explosive has become the market leader of commercial explosives in India. Earlier, its use was restricted only to large mines having high explosive consumption. Indigenous development of low cost pump trucks and price war among explosive manufacturers has now made it possible for small mine operators to use bulk emulsion explosive. Many small mines having explosive consumption as low as 500 tpa or even less are now switching over to bulk emulsion explosive from ANFO.

In spite of having excellent water resistance it is observed that the performance of bulk loaded emulsion explosive in watery holes is not satisfactory. Blast jamming (tight muck) and poor fragmentation were found very frequently during and after the monsoon season which lasts for about three to four months in most parts of India.

2 EXPERIMENTS

2.1 *Field details*

Experiments were carried out in a limestone mine. In all ten experiments were conducted in watery blast holes out of which seven were successful. In all the blastholes, the water was static and there was no flow of water through it. VOD could not be recorded in three experiments because either the readings were not picked up by the instrument due to cut off of connecting cable by fly rock or the records of VOD signals were not satisfactory due to insufficient shorting of cable. VOD in two dry blast holes was also recorded for comparison of results. All the experiments were conducted in 152 mm diameter watery blasthole except one, which was performed in 115 mm diameter blasthole. All the blast holes were bottom charged. The depth of the blastholes varied between 8.00 m to 12.30 m. This relatively shallow depth is considered to have negligible effect on the in-hole density of the explosive.

The emulsion explosive used in the study was a double salt explosive. The oxidizer blend (OB) comprised of an aqueous solution of 73.0% ammonium nitrate (AN), 3.0% of sodium nitrate (SN), 0.1% thio-urea (TU) and 17.7% of water. The fuel bend comprised of 2.0% of high speed diesel (HSD), 2.9% furnace oil (FO) and 1.3% of sorbitol mono oleate (SMO). The emulsion matrix was blackish in colour having an initial density of 1.32–1.35 g/cc and temperature of 70–75°C. The viscosity was 80000–100000 cP. Aqueous sodium nitrite solution comprising 20 kg sodium nitrite in 80 litres of water was used as gassing agent.

2.2 *Measurement of VOD*

Velocity of detonation is an important indicator of the performance of an explosive. It is the rate at which detonation wave travels through the explosive column. It is influenced by a number of factors including explosive formulation, degree of confinement, charge diameter, density, primer type, presence of water, etc. (Chiapetta 1988). A number of VOD measurement systems are available today. These can be classified into two broad categories—Point-to-point VOD measurement systems and continuous VOD measurement systems. Point-to-point VOD systems gives the average VOD of the explosive between the two discrete points where the sensor probes are placed. This system has limitation in providing information for critical experimental measurements when trying to detect the degree of malfunctioning of the explosives and transit VOD's within the explosive column. Continuous VOD systems overcome the limitation of the point-to-point VOD measurement systems. By this system, it is possible to measure the VOD between any two points in the explosive column (Crosby et al. 1991, Mishra & Sinha 2003, Harsh et al. 2005).

In the present study, Continuous VOD of the bulk emulsion explosive was measured in-the hole. The well-known resistance wire method was used. The recorded data are linearised for presentation in displacement versus time form with the help of a personal computer. The slope of curve gives the VOD of the explosive.

VODMate instrument (manufactured by Instantel) was used to measure the VOD of the explosives. It has a 14 bit resolution and the sampling rate could be up to 2 MHz.

Due care was taken in the selection of the blast hole for experiments. The blast holes from the production blast were so chosen that there was least possibility of disruption of cable by ground movement and fly rock. The end of the cable to be placed in the blast hole was shortened and insulated by an electrical insulating tape. The shortened end of the cable was taped to the cast booster

Downloaded by [Visvesvaraya Technological University (VTU Consortium)] at 21:56 01 March 2016

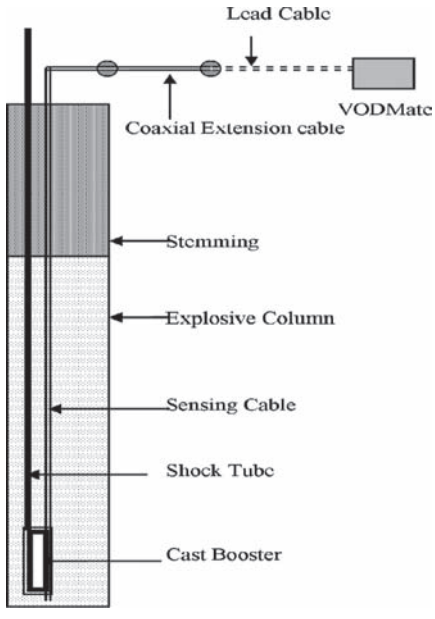

Figure 1. Field setup of in-hole VOD measurement.

and lowered into the blast hole along with shock tube. The primer was placed at the bottom of the hole. Due care was taken that primer should not rise with the product. Also, it was ensured that primer did not sit in the mud. The sensing cable was kept taut when fully lowered into the hole. The emulsion matrix was then pumped into the hole keeping the sensing cable stretched tight to avoid slackness in the cable. All the watery blast holes were bottom charged. The field set up for VOD measurement is shown in Figure 1. The density variation of the emulsion matrix was monitored. When the explosive attained the desired density, the blasthole was stemmed and fired. The recorded VOD data was then transferred to the computer and analyzed.

3 OBSERVATIONS AND RESULTS

As stated earlier, the experiments were carried out in 10 watery blast holes. Out of the 10 experiments, VOD could not be recorded in three blast holes. For comparison of the results VOD was also recorded in two dry blast holes. The summary of the observations is presented in Table 1 and corre-

Table 1. Summary of field observations.

Blast hole no.	Blast hole dia. [mm]	Depth, [m]	Water column, [m]	Charge [kg]	Cast booster [g]	Matrix temp. [°C]	Matrix Density, [g/cc]	Explosive density, [g/cc]	VOD [m/s]	Remarks
1	152	12.30	5.7	175	400	63	1.34	1.14	4535	Sharp downward spikes throughout the column
2	152	8.20	7.0	105	200	62	1.34	1.16	fail	Explosive initiated with a run-up VOD of 3619 m/s and failed to detonate after 0.1 ms.
3	152	8.30	4.2	105	200	62	1.33	1.20	fail	Explosive initiated with a run-up VOD of 3463 m/s and failed to detonate after 0.26 ms
4	152	8.50	6.0	105	200	62	1.34	1.18	fail	Explosive deflagrated with a VOD of 3122 m/s up to 0.38 ms and after that failed to detonate
5	115	9.20	4.7	70	200	60	1.34	1.18	4150	Extremely stable detonation occurred up to 0.8 ms. A wide spike is observed between 0.8 and 0.9 ms.
6	152	9.00	4.0	110	200	58	1.34	1.20	4291	Fair detonation with some spikes between 0.2 and 0.3 ms., and at 0.9 ms.
7	152	9.00	2.0	110	200	48	1.32	1.16	4399	Fairly stable detonation
8	152	10.00	Dry	125	300	60	1.32	1.12	5063	Stable detonation throughout the column
9	152	8.00	Dry	105	200	61	1.34	1.16	5135	Stable detonation except between 0.22 and 0.36 ms

Downloaded by [Visvesvaraya Technological University (VTU Consortium)] at 21:56 01 March 2016

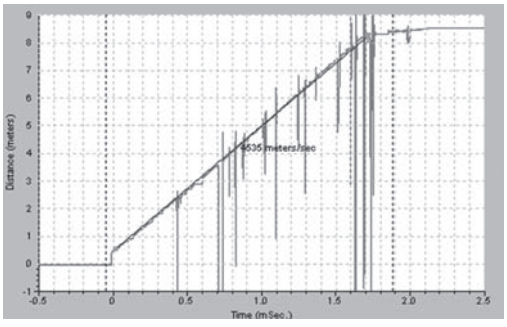

Figure 2. Time distance graph for blast hole no. 1.

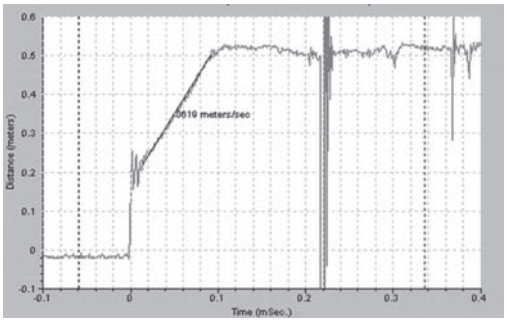

Figure 3. Time distance graph for blast hole no. 2.

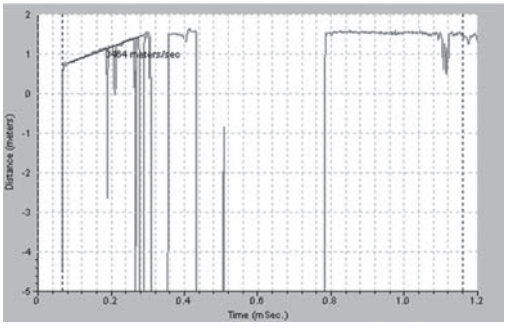

Figure 4. Time distance graph for blast hole no. 3.

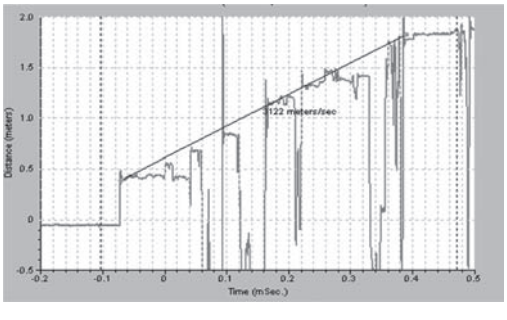

Figure 5. Time distance graph for blast hole no. 4.

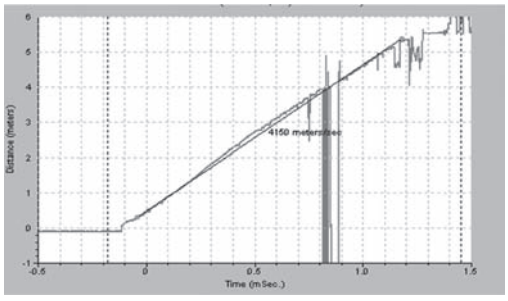

Figure 6. Time distance graph for blast hole no. 5.

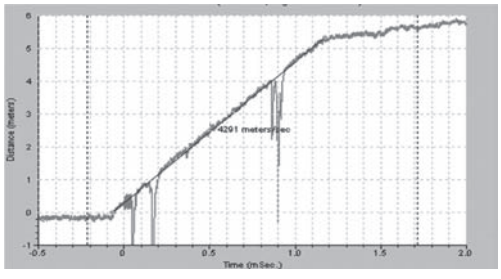

Figure 7. Time distance graph for blast hole no. 6.

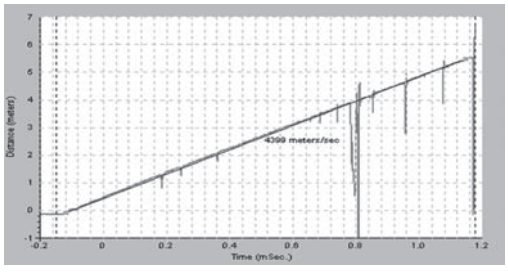

Figure 8. Time distance graph for blast hole no. 7.

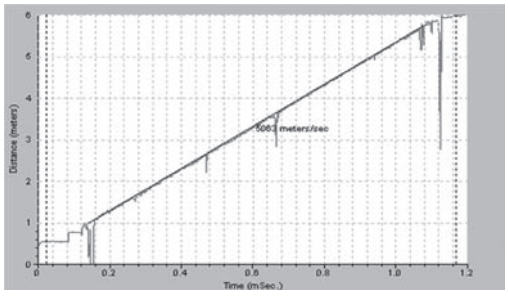

Figure 9. Time distance graph for blast hole no. 8.

sponding distance versus time graph are shown in Figures 2–10. Blast hole no. 1 to 7 are watery blast holes and no. 8 and 9 are dry blast holes.

In blast hole no. 2, 3 and 4 full column detonation did not occur. In rest of the watery blast holes

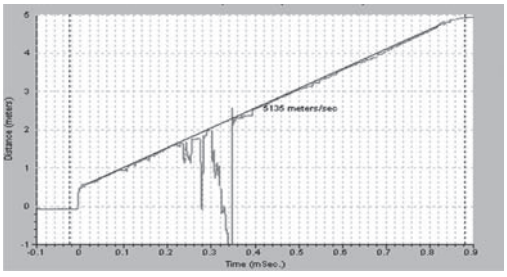

Figure 10. Time distance graph for blast hole no. 9.

no. 1, 5, 6 and 7 full column detonation took place. The explosive detonated with a VOD of 4150 m/s to 4535 m/s. In dry blast holes the explosive detonated with much higher VOD. The VOD in dry blast holes no. 8 and 9 was measured as 5063 m/s and 5135 m/s respectively.

4 DISCUSSIONS

Water is known to have detrimental effect on all explosives. The water resistance of an explosive is assessed on laboratory scale by exposing the explosive to water for 24 hrs and then measuring its detonation velocity in atmosphere. However, real blast environment for watery holes incorporates diverse factors that would alter the performance of the explosive. In the field, the explosive column in watery holes is surrounded by wet walls when detonated. Also in the process of bulk loading, the explosive column may have water pockets entrapped within if not charged properly. Contamination of explosive during charging also produces a similar effect. The influence of each of these probable factors contributing to lower performance of explosives is elaborated as under.

4.1 *Influence of improper charging*

The watery holes are bottom charged to ensure compact charging, so that as the explosive is loaded in the hole the water therein is displaced upward to the near collar region. In spite of bottom charging of the holes, many a times, the withdrawal of the hose is faster than the charge column rise. As a result, the hose does not remain inserted in the explosive column, and the rapid influx of fresh charge traps the water column within (Fig. 11a,b).

The explosive column with entrapped water pocket will behave as two coaxial cylindrical charges, separated by an inert barrier of water. During detonation, the shock passing through the water barrier will get attenuated. For the lengths below certain critical value, the shock wave transmits sufficient energy across the water barrier to initiate the explosive column beyond it, thus resulting in full column detonation (Fig. 11a). If the length of the water barrier is above critical value as shown in Figure 11b, the attenuated shockwave becomes incapable of initiating the explosive column beyond the water barrier, thus inhibiting the full column detonation.

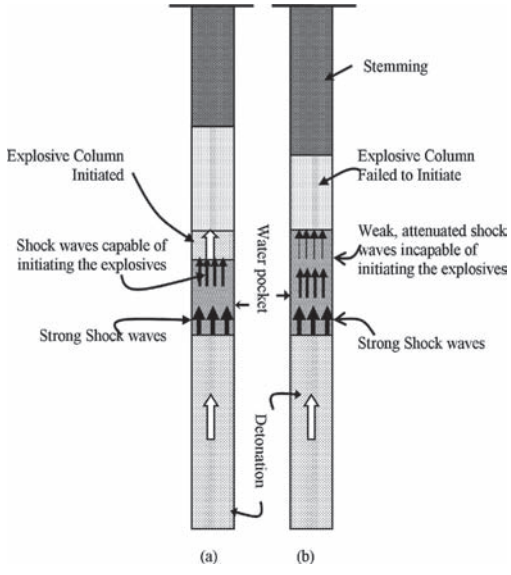

Figure 11. (a) Full column detonation in explosive column having water pockets of length below a critical value (b) Failure of explosive column to detonate fully in a hole having water pocket of length above a critical value.

The presence and formation of water pockets is a possible cause of underperformance of an explosive.

4.2 *Influence of wet walls of the blasthole*

In watery blastholes, the explosive column is surrounded by wet blasthole walls. During detonation, the reaction takes place in a thin zone called reaction zone. The leading face the reaction zone is called shock front and the rear face is called Chapman-jouguet (C-J) plane. A part of the heat released in reaction zone is consumed by the hot gasses behind the C-J plane and a part is lost side way into the surroundings. The remaining heat reaches the shock front and governs the VOD. In case of watery blast holes the explosive column is surrounded by moist blasthole walls. A significant amount of heat produced in reaction zone is absorbed by the surrounding moisture. Hence, less heat is available at shock front and the explosive detonates with a lower VOD.

Downloaded by [Visvesvaraya Technological University (VTU Consortium)] at 21:56 01 March 2016

4.3 *Influence of contamination*

Contamination of explosive may occur due to various reasons. Water in the blast holes generally has silt suspension. Concentration of silt is high at the bottom of the hole. During pumping of explosive, a sudden input of pressure into the blast holes creates sufficient turbulence and formation of sludge. When the suspended silt comes in contact with viscous emulsion matrix, it gets mixed, making it contaminated. Also, the drill cuttings from the collar are dislodged and get added with the explosive. Contaminated explosive detonates at a lower VOD. It is evident that contamination of explosive coupled with other factors may have possibly led to malfunctioning of explosive.

5 CONCLUSIONS

Due to its physical water-in-oil structure emulsion explosives have excellent water resistance. Laboratory studies by researchers reveal a change of up to 10% in VOD because of contact with water. In real blast environment the performance of bulk loaded emulsion explosive in watery blastholes was found to be unsatisfactory. Problems like reduction in VOD (i.e. from 5063 m/s to 4150 m/s), low order detonation, and failure of explosive column to detonate fully were observed. Partial jamming of blast, a phenomenon very frequent during monsoon is one of the manifestations of malfunctioning of explosive in watery holes. In addition to the presence of water, other factors also contribute to affecting performance of bulk explosives. The main causes of unsatisfactory performance of bulk loaded emulsion explosive in watery blast holes are, poor charging practice, contamination of explosive by silt present in water, presence of moisture around the explosive column, and increase in the compressibility of the strata around the explosive charge.

For better blast results in watery holes, the bottom charging of the holes should be practiced. During loading of the explosive, special care must be exercised to keep the hose inserted in the explosive column until full column height is reached. The blast holes should be plugged after drilling so that the drill cutting and slush during monsoon cannot enter the blast holes.

REFERENCES

Bhandari, S. 1997. *Engineering Rock Blasting Operations.* Rotterdam, Netherlands, Brookfield VT: A.A. Balkema:17.

Cameron, A. & Grouchel, P. 1990. The effects of the quality of bulk commercial explosives on the blast performance, *Rock Fragmentation by Blasting; Proc. 3rd intern. Symp., Brisbane, 26–31* August 1990: 335–343.

Chiappetta, R.F. 1988. Blast monitoring instruments and analysis techniques with an emphasis on field application, *Fragblast-International Journal of Blasting and Fragmentation,* Vol. 1: 79–101.

Crosby, W.A., Bauer, A.W. & Warkentin, J.P.F. 1991. State of the art explosive VOD measurement system, *Explosive Blasting*, *Proc. 7th Annual Conf.; International Society for Explosives Engineers*: 23–34.

Harsh, H.K., Dwivedi, R.D., Swarup, A. & Prasad, V.V.R. 2005. Velocity of Detonation (VOD)—A review of measurement techniques, *Technological Advancement and Environmental Challenges in Mining and Allied Industries in 21st Century; Proc. Conf.,* NIT Rourkela, India: 169–175.

Mishra, A.K. & Sinha, P.R. 2003. VOD measurement techniques—A review, *Explosive and Blasting; Proc. 15th National Seminar,* Dhanbad: 43–52.

Nabiullah, Pingua, B.M.P., Jagdish, Khan, M. & Emranuzzamam 2005. Study on explosives and their quality performance, *The Indian Mining and Engineering Journal,* Vol. 44(1): 21–30.

National Institute of Rock Mechanics (NIRM) 2001. Evaluation of explosive performance through in-the-hole detonation velocity measurement, *National Institute of Rock Mechanics, KGF, India, S & T project funded by Ministry of Coal, Govt. of India*: 128.

Pradhan, M. 2007. Investigation into the effects of some factors on detonation velocity of chemically sensitized bulk emulsion explosives, *Doctoral Dissertation: Pt. Ravishankar Shukla* University, Raipur, India.: 98.

Downloaded by [Visvesvaraya Technological University (VTU Consortium)] at 21:56 01 March 2016

Performance of Explosives and New Developments – Mohanty & Singh (Eds)
© 2013 Taylor & Francis Group, London, ISBN 978-0-415-62142-7

Experimental research on thermal decomposition character of new coal permitted water gel explosive

Yan Shi-long, Ren Dong-mei & Wu Hong-bo
School of Chemical Engineering, Anhui University of Science and Technology, Huainan, China

ABSTRACT: The thermal decomposition character of new coal permitted water gel explosives, to which was added an inhibitor, was investigated using the C80 micro calorimeter. The initial and peak temperatures of thermal decomposition were measured, and the kinetic parameters were calculated. These were compared to the temperature of actual production and use. Results show that this explosive has excellent thermal stability.

Keywords: water gel explosive, inhibitor, thermal decomposition

1 INTRODUCTION

The thermal stability of the existing three level coal permitted water gel explosive in our country is good [Wang, Ma, Liu, 2007]. However, large quantities of inhibitor marble powder in the explosives decrease explosion energy greatly, which makes gradually reduces the ability of explosives satisfy the actual requirement [Han, 2009]. Sodium chloride was used as an inhibitor in order to improve explosion properties of explosives in the experiment because its chemical restraining efficiency is higher than marble [Zhao, 2007]. Water gel explosive would decompose under thermal energy, and in rising temperatures, this decomposition would turn more severe [Wang, 1985]. Thus, it becomes crucial for research to investigate whether or not the addition of the inhibitor sodium chloride can keep quondam excellent thermal stability. It is thus very important to research the thermal decomposition character of new coal permitted water gel explosives.

2 EXPLOSIVE PREPARATIONS

Based on the formula design principle of high safety water gel explosive, the new water gel explosive formula was adopted to make explosive samples which referred to the existing process of coal permitted water gel explosive, and used sodium chloride as inhibitor. The major component of formula is shown in Table 1.

Preparation process: ammonium nitrate and water were added into MMAN solution successively at 60–80°C, and PH value was adjusted to 4.5–6.5. Premixing of sodium nitrate and sesbania gel was added to the solution, and stirred for 3–5 minutes. The mixture was heated using a water bath to maintain the temperature at 35–45°C. After the sesbania powder swelled and hydrated fully, the inhibitor, perlite, foam and stabilizer were added successively, at the same time, and stirred into the solution. After the mixture was uniform, the temperature was controlled at 35–45°C. A cross-linking agent was added. When stirred uniformly, it was made explosive an sample. At last, after the temperature was maintained for 10–40 hours, a gelatinous water gel explosive was obtained, with a very good elasticity was very good.

Table 1. Major components and contents of explosive.

MMAN	AN	SN	SC	Sp	Water
31–37	26–31	14–18	5–10	0.8–1.0	10–13

Note: line 1 is component, line 2 is percent content; SN is sodium nitrate; SC is sodium chloride; Sp is sesbania powder.

3 THERMAL DECOMPOSITION CHARACTERACTERISTICS DETERMINATION

3.1 *Experimental condition*

Instruments: micro calorimeter C80, made in France SETARAM.

Condition: sample 100 mg;
Heating rate: 0.2 K min^{-1};
Heating range: room temperature-300;
Reference objects: air.

Downloaded by [Visvesvaraya Technological University (VTU Consortium)] at 21:57 01 March 2016

3.2 *Results and discussion*

Thermal decomposition experiments were made with the C80 micro calorimeter. Figure 1 shows the relationship between heat flow and temperature.

From Figure 1 it can be seen that thermal decomposition of the sample has an obvious exothermic peak, before which is shows a weak endothermic. The endothermic process of the sample was amplified and shown in Figure 2.

Endothermic rate reached maximum (point S) at 112.12°C, which was 1.01 mW. The result can be regarded as live ammonium nitrate. This endothermic quantity of heat included two parts. One was ammonium nitrate vapor volatilized to absorb heat, and the other was ammonium nitrate decomposed into ammonia and nitric acid at 110°C. The reaction is also endothermic. This lead to endothermic rate of the gelatinous system reaches maximum at this point. Sample temperature continued rising because of calorimeter heating at constant rate and reactant exothermic quantity of heat.

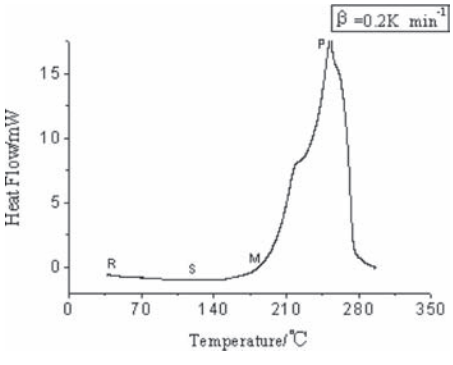

Figure 1. Relationship between heat flow and temperature (β-heating rate).

When temperature reached 183.07°C, the exothermic reaction of the sample began, heat flow rate of pure ammonium nitrate rose slowly to 190°C [Sun, Sun, Lu, et al, 2005], which fits this stage. Sample finished transition from endothermic stage to exothermic stage (point M).

The endothermic process was divided into three stages (shown in Fig. 3). The first stage, that is initial stage (M-O stage), reaction heat flow increases slowly, with the calorimeter's heating to sample, when temperature rose to 170–190°C. Ammonium nitrate begins the second decomposition. The products of decomposition are nitrous oxide and water. This reaction is exothermic, especially as the presence of inhibitor sodium chloride acts as a catalyst, causing the exothermic rate of the sample to becomes strenuous at 185–220°C. The second stage, the acceleration (O-P) stage, the thermal decomposition velocity rises rapidly, but the existence of terraces in the curve shows that the thermal decomposition velocity undergoes some changes, where it increases rapidly in the O-A and B-P stages. However, its speed gradient decreases gradually in A-B. Heat flow increases in B-P stage. It can be regarded that the thermal decomposition of MMAN and ammonium nitrate (thermal flow of pure ammonium nitrate increases rapidly at 232°C), heat flow of the sample reaches its maximum when the temperature reaches 252.39°C.

The heat flow is 17.87 mW. The third stage, the attenuation stage (P-N stage), the reactants and reaction velocity. The exothermic peak of the reaction stops at 296.04°C, the characteristic parameters of the sample were shown in Table 2.

The data of initial reaction stage in Figure 2 were treated with C80 [Sun, Ding, 2005], and the relationship curve of $\ln((dH/dt)/\Delta HM_0) \sim (-1/T)$ (shown in Fig. 4) was drawn, Meanwhile, the linear fitting curve was drawn in Figure 4.

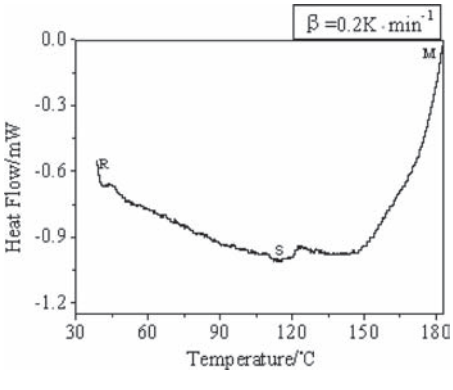

Figure 2. Relationship between heat flow and temperature in the initial reaction stage (β-heating rate).

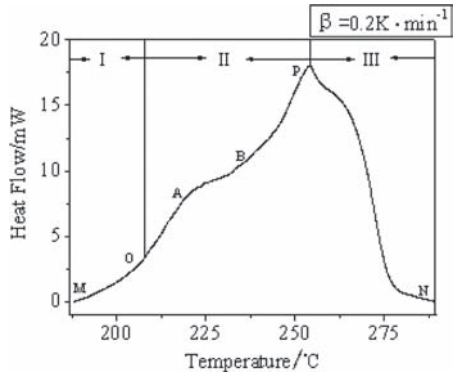

Figure 3. Relationship between heat flow and temperature.

Table 2. Exothermic characteristic parameters of the sample.

T_I/°C	T_F/°C	T_P/°C	H_M/mW	θ/min
183.07	296.04	252.39	17.87	8.56

Note: T_I is initial temperature; T_F is finishing temperature; T_P is peak temperature; H_M is maximum heat flow velocity; θ is exothermic time consuming.

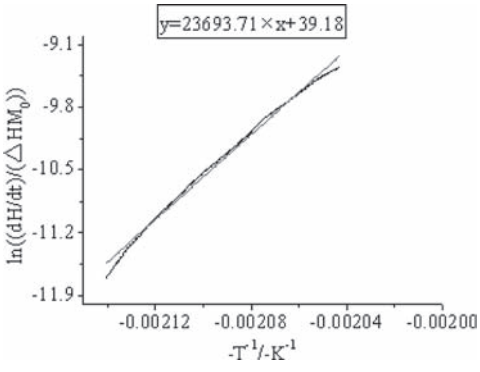

Figure 4. Relational curve between $\ln((dH/dt)/\Delta H \cdot M_0)$ and $-1/T$ in the initial reaction stage.

Table 3. Kinetic parameters in the initial reaction stage of the sample.

ΔH	E_a	ln A	R^2
780.57	197.00	39.18	0.9944

Note: ΔH is reaction enthalpy, $kJ \cdot kg^{-1}$; E_a is activation energy, $kJ \cdot kg^{-1}$; A exponential factor, s^{-1}; R^2 is linear relative coefficient.

Activation energy and exponential factor of the sample can be obtained, which is shown in Table 3.

Apparent activation energy is an important index in measuring high or low of the energy barrier of an explosive reaction. the higher the activation energy, the more difficult the thermal decomposition reaction and the larger the reaction resistance. Activation energy of the explosive sample is up to 197.00 $kJ \cdot kg^{-1}$, thus boasting excellent thermal stability.

4 CONCLUSIONS

1. The initial reaction temperature of the sample is about 183.07°C. Usually, the outlet temperature of the emulsifier is less than 130 °C, and the use temperature is far lower, so the explosive has excellent thermal stability.
2. Crystal change and thermal decomposition lead to endothermic reaction. The activation energy of the explosive is 197.00 $kJ \cdot kg^{-1}$and the exponential factor is 1.04×10^{17}. In order to get more decomposition data to judge thermal stability of materials, further research should be carried out investigating the complicated heterogeneous material.
3. Sodium chloride is cheap, and causes little pollution, so it is an ideal choice for an inhibitor.

REFERENCES

Han Ti-fei. 2009. Study on colloid stability of water gel explosive. Huainan, Anhui University of Science and Technology.

Sun Zhan-hui, Sun Jin-hua, Lu Shou-xiang, et al. 2005. Study of the influence of inorganic acid on the thermal stability of ammonium nitrate. *China Safety Science Journal.* 15(9):57–62.

Sun Jin-hua, Ding Hui. 2005. *Thermal danger evaluation on chemical materials*. Beijing: Science Press.

Wang Jin, Ma Zhi-gang, Liu Zhi-bing. 2007. The thermal decomposition kinetics of water gel explosive. *Chinese Journal of Explosives & Propellants*. 30:52–54.

Wang Xu-guang. 1985. *Theory and practice of slurry explosive*. Beijing: Metallurgical Industry Press.

Zhao Yun-xiang. 2007. Influence and prevention for underwater in process of coal mining. *Chinese Businessman.* 243.

Downloaded by [Visvesvaraya Technological University (VTU Consortium)] at 21:57 01 March 2016

Performance of Explosives and New Developments – Mohanty & Singh (Eds)
© 2013 Taylor & Francis Group, London, ISBN 978-0-415-62142-7

Study and performance of low density emulsion explosive

A.K. Singh, B.M.P. Pingua, Nabiullah, M.K. Panda & S. Akhtar
CSIR—Central Institute of Mining & Fuel Research, Dhanbad, India

ABSTRACT: The ammonium nitrate fuel oil mixture was considered as low density explosive. It was only possible by using low density ammonium nitrate prill 850 kg/m^3. Due to poor behavior of ammonium nitrate in watery hole or moist hole, it could not be popular in India. The problem was solved by using low density emulsion explosives. Low density emulsion explosive was developed and explosive behavior was measured. The energy fuel used in preparation of emulsion explosives was measured by using bomb calorimeter. The explosive properties of ANFO, emulsion explosive such as density, velocity of detonation were measured in unconfined condition. Low density emulsion was found booster sensitive up to 650 kg/m^3 and velocity of detonation was 3000–3050 m/s in 100 mm diameter in unconfined condition. The field trials at limestone and coal mines were found satisfactory.

1 INTRODUCTION

Low-density explosive products were reported throughout the last decades (Silva and Seherpanisse 2010) by manufacturers, researchers and users alike (Heltzen & Kure1980, Moxon & Armstrong 1990, Hunter et al. 1993, Harries & Gribble 1993 & Hunsaker 1950).

The main application of low density explosives (LDE) deals on wall control, to reduce over break, increase slope stability, improve safety and reduce overall costs. Although studies have continually stated the positive benefits of using LDE, the uptake from industry has been slow—partly because of fear of an unknown product (Rock, Maurer & Pereira 2005), and a perception that LDE were only suitable for 'weak strata'. Hopler (1993) makes mention of the low cost of AN (Ammonium Nitrate) following the end of world war II during which ten ammonia plants were built for the munitions industry to support the war. By mid-1956, ammonium nitrate was being mixed with fuel oil (diesel), and poured from the bag into the drill hole. Early references to LDE date back to the late 1960s with the Blasters' Handbook from Du Pont (1969) referring to a Du Pont product named 'Nilite ND' (ND meaning 'no-deck') with a density range from 450 kg/m^3 to 550 kg/m^3 as poured. This product has proven successful in vertical holes when it has been used as a top load. It has successfully replaced decking in quarry shots and is used where the total charge per borehole must be kept below a maximum weight. Heltzen and Kure (1980), showed that a low-density product could be mixed with minimal segregation that was very effective for contour blasting, but its drawback was the additional handling costs associated with the product, they highlighted that an effective low-density product could be delivered that sustained minimal segregation along with no static effects and similar CO and NOx outputs. Wilson and Moxon (1989) conducted extensive trials diluting ANFO with various low-density bulking agents including polystyrene, bagasse (sugar cane waste) and sawdust. The main aim of these trials was to develop a low-shock energy ammonium nitrate based explosive which could be used to fragment weak overburden materials & found that low-density explosives can lead to significant cost saving without compromising fragmentation & production.

Hunter, Fedak and Todoeschuck (1993) used an ANFO based LDE in wall control applications in the range of densities form 360 kg/m^3 to 450 kg/m^3. Jackson (1993) has used emulsion based LDE in field trail, was a combination of chemical gassing agents, glass micro balloons and polystyrene beads & he found that powder factors could be reduced by as much as 30 per cent, while at the same time producing similar results in terms of fragmentation, breakage, better wall stability, reduced fines, also commercially viable. Grouhel and Hunsaker (1995) have found same result as Jackson (1993). Johnson (1996) has also done several trails in the Bowen Basin with limited acceptance of an ANFO/sawdust mix and described significant cost savings over ANFO while providing comparable results. Brent and Armstrong (1998) conducted trials for pre-split applications in large diameter blast holes (311 mm) using a very low-density product (200 kg/m^3) at depth of 45 m. Rowe et al. (2001) have studied with a variable density product to determine its suitability in soft to medium strength

Downloaded by [Visvesvaraya Technological University (VTU Consortium)] at 21:57 01 March 2016

rock types. Beach et al. (2004) have utilized wheat husks as the bulking agent with ANFO base. Rock (2004) highlighted the strengths of lower density products and the techniques to use when designing blasts. This paper deals development and performance of low density emulsion explosive in the field condition.

2 LOW DENSITY EMULSION EXPLOSIVE

The present work relates to an improved non permissible explosive composition. Particularly, a permissible water-in-oil emulsion explosive i.e. shock-resistance and has a relatively low density (less than 1000 kg/m^3). The water-in-oil emulsion explosives contain a water-immiscible organic fuel as the continuous phase and an emulsified inorganic oxidizer salt solution as the discontinuous phase. These oxidizer and fuel phases react with one another upon detonation by a blasting cap or other initiator to produce rapid release of energy & very high pressure.

2.1 *Distribution of energy*

When an explosive detonates in a blast hole, the sudden and rapid release of energy produces very high pressures which initiate a fracture network around the blast hole. As this network expands, the pressure in the blast hole subsequently reduces according to the P-V relationship. Lownds (1986) proposed a simple, idealized, static energy release model in which the zones are partitioned into the commonly known components—shock, heave and energy losses. As can be seen in Figure 1, the pressure following detonation rapidly drops off rapidly as explained below:

- Potential shock energy—area 1,
- Strain energy around the borehole—area 2,
- Fragmentation and heave—area 3a,
- Strain energy in burden at escape—area 3b,
- Lost energy—area 4,

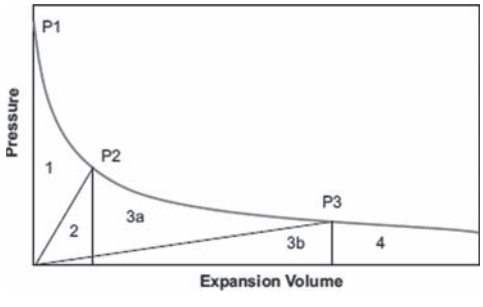

Figure 1. Partition of energy model (Lownds, 1986).

- Initial detonation pressure—point P1,
- Pressure at end of shock phase—point P2 &
- Pressure after which no further work is done on the rock-point P3 (cut-off pressure, usually 100 MPa).

Rock will break far more effectively in tension than in compression. Sequencely energy is utilized in crushing and fracturing the area immediately surrounding the blast hole, Initiating and extending the predominantly radial fracture network away from the blast hole, then opening up both the natural joints and cracks in the rock mass as well as the fractures developed by the earlier high pressures prior to the bulk motion or heave which is manifest as kinetic energy.

The requirement for high initial pressures is minimal in rock types that display jointing and inherent cracking (such as that found in the majority of coal mining overburden). Lownds (1991) has described pressure & volume relationship in gas & stress due to the compression and crushing around the blast hole shown in Figure 2. The tapering off of the stress in rock is caused by the initial compression and crushing around the blast hole followed by growth of the fracture network and then the movement of the rock mass. The actual interaction point is further along the expansion curve than if it were a purely elastic reaction.

Once this interaction point is reached, the heave phase of the process takes over and further fragmentation and breakage is caused by this movement of the rock. As low-density products have a lower VOD, the explosion expansion curve has a lower starting pressure. This lower VOD and initial pressure translates into an increased percentage of the available energy applied during the heave process. A low-density product will still utilize some of its available energy during the initial expansion process, however this is a smaller percentage when compared to ANFO or higher density products.

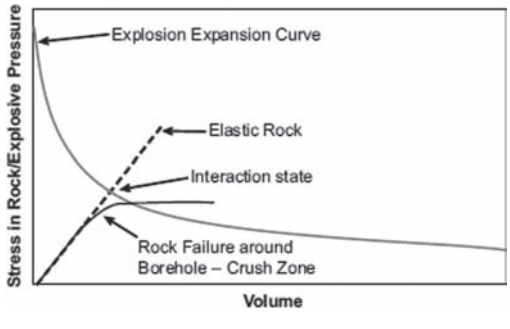

Figure 2. Plot of pressure in gas and stress in rock versus volume (Lownds, 1991).

Downloaded by [Visvesvaraya Technological University (VTU Consortium)] at 21:57 01 March 2016

Low density emulsion explosive was found to be booster sensitive up to 650 kg/m^3 in 100 mm diameter. The velocity of detonation was 3000–3050 m/s. The trial blast in coal mine and limestone mine was satisfactory.

2.2 *Experimentation*

2.2.1 *ANFO*

Ammonium nitrate and fuel oil mixture (ANFO) was prepared by using ammonium nitrate prill and fuel oil. The density of ammonium nitrate was in between 700 and 900 kg/m^3. Ammonium nitrate and diesel were mixed in ratio 94 and 6 percent by weight. The density, velocity of detonation was measured. The energy of explosion was calculated and results are shown in Table 1.

2.2.2 *Low density emulsion*

Emulsion matrix was prepared by mixing of (a) oxidizing solution (b) reducing solution (c) density modifier solution. The oxidizing solution containing ammonium nitrate, sodium nitrate, water and thio-urea was mixed together and heated upto 80–85°C and pH was maintained by using acid. The pH watery solution was between 3.5 and 4.5. The fuel solution contain diesel oil, furnace oil, SMO were mixed slowly at temperature 45–50°C. The oxidizer solution was mixed with fuel solution in high speed mixer. The emulsion matrix was prepared and gassed by using sodium nitrite solution and formaldehyde solution (Fig. 3). The energy of fuel was measured by using bomb calorimeter and explosion energy was calculated and results are shown in Table 2.

2.3 *Performance behavior*

Trial blast of low density emulsion explosive was carried out in limestone and coal mines, where burden, spacing and hole depth were 2.5, 3.0 and 7–8 m. respectively. The blasthole diameter was 110 mm. The result of blast is shown in Figures 4 & 5. The induced ground vibration was measured and results are shown in Tables 3 & 4.

Table 1. Explosive properties of ANFO.

	Low density ANFO		
S. No.	Density, kg/m^3	Velocity of detonation, m/s	Explosive energy kj/m^3,10^5
1	900	4300–4200	34.23
2	850	3900–4100	32.32
3	800	3850–4000	30.42
4	700	3500–3700	26.62

Figure 3. Low density emulsion matrix.

Table 2. Explosive properties of low density emulsion.

Low density emulsion explosives		
Density, Kg/m^3	Velocity of detonation, m/s	Explosive energy kJ/m^3, 10^5
1100	4350–4450	39.08
1050	4150–4250	37.30
1000	4000–4125	35.53
900	3600–3700	31.98
850	3500–3600	30.20
750	3100–3200	26.64
700	3050–3100	24.87
650	3000–3050	23.09
550	Failed	–

Figure 4. Low density emulsion blast result.

The blast results showed that the performance of low density emulsion explosive was good as compared to ANFO.

2.4 *Segregation behavior*

Segregation behavior of matrix was studied. The matrix was kept in 1000 ml measuring cylinder and

Table 3. Ground vibration at different distance with ANFO.

Dia. of hole (mm)	Max. charge/ delay (kg)	ANFO (Low density) Loading density (kg/m)	Dist. (m)	Peak Particle (mm/s)	Frequency (Hz)
110	40	8	100	5.0	15–20
110	42	8	110	5.25	15–25
110	40	8	75	7.0	15–25
110	40	8	65	8.0	15–25
110	40	8	50	10.0	15–25

Table 4. Ground vibration at different distance with low density emulsion.

Diameter of the hole (mm)	Max. Charge kg/ delay	Low density emulsion matrix Loading density (kg/m)	Distance (m)	Peak particle (mm/s)	Frequency (Hz)
110	35	7.0	100	3.2	13.25
110	38	7.1	110	3.1	12.90
110	35	7.0	75	3.2	13.25
110	35	7.0	65	3.2	13.25
110	38	7.1	80	3.5	13.80

Figure 5. ANFO blast result in jointed fractured sandstone overburden coal mines.

shown in Figure 6 and 7. No leaching of water was recorded for fifteen days.

3 RESULTS AND DISCUSSION

The results shown in Table 1 indicates that ANFO could be prepared in density range from 700–900 kg/m^3 keeping its velocity of detonation and energy in the range of 3500–4300 m/s and 26 × 10^5–34 × 10^5 kJ/m^3 respectively.

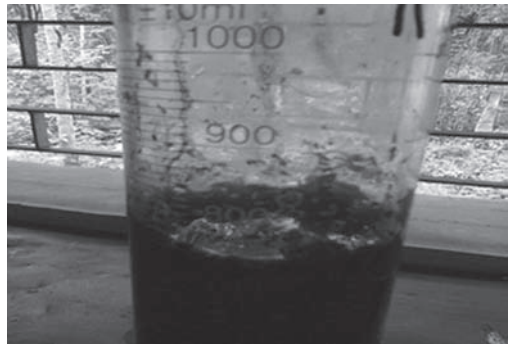

Figure 6. Water leaching test.

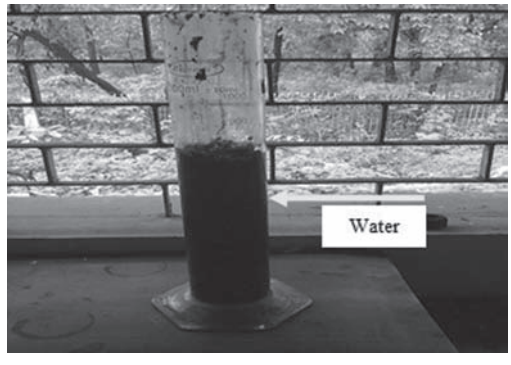

Figure 7. No leaching of water.

The results shown in Table 2 for low density emulsion could be prepared as low as 650 kg/m^3 maintaining the velocity of detonation in between 3000 and 4450 m/s and explosion energy was in the range of 23.09 × 10^5 kJ/m^3 to 39.08 × 10^5 kJ/m^3. Blast outcome with low density emulsion explosives was found to be comparatively better than ANFO. The recorded blast induced ground vibration in case of low density emulsion was lower in comparison to those of ANFO (Tables 3 & 4). This may be due to low energy and low velocity of detonation of emulsion explosives.

4 CONCLUSIONS

- The energy, velocity of detonation and density of low density emulsion explosive was suitable for soft/medium and fractured hard rock blasting.
- The charging with bulk matrix delivery (BMD) vehicle could be used safely in low density emulsion explosives.
- Energy could be altered in blast hole as per geo-mining condition in low density emulsion explosives.

Downloaded by [Visvesvaraya Technological University (VTU Consortium)] at 21:57 01 March 2016

ACKNOWLEDGEMENT

The authors express their thanks to the various sites that have contributed feedback on the application of low-density based emulsion explosive on previous work published by various authors, to the member of ERL of CIMFR for their continued support and assistance in the preparation of this paper & to the Director CIMFR for his support.

Downloaded by [Visvesvaraya Technological University (VTU Consortium)] at 21:57 01 March 2016

REFERENCES

Beach, F., Gribble, D., Littlefair, M., Rounsley, R., Testrow, I. & Wiggin, M. 2004. Blastlite–the practical low-density solution. *Proceedings Explo 2004*, *(TheAustralasian Institute of Mining and Metallurgy: Melbourne),* pp. 147–152.

Brent, G.F. & Armstrong, L.W. 1998. Large diameter presplitting improved through two novel techniques. *Proceedings of ISEE Annual Conference 1998*, *(The International Society of Explosives Engineers: Cleveland),* pp. 511–520.

Dupont. 1969. Blasters' Handbook, (*E I Du Pont de Nemours and Co, Inc: Wilmington*), 57p.

Grouhel, P.H.J. & Hunsaker, R.D. 1995. An introduction to volutionary low density bulk explosive for surface blasting operations. *Proceedings Explo '95, (The Australasian Institute of Mining and Metallurgy: Melbourne),* pp. 67–71.

Harries, G. & Gribble, D.P. 1993. Development of a low shock energy explosive- ANRUB. In H.P. Rossmanith(ed.). *Proc. 4th Int. Symp. On Rock Fragmentation by Blasting, Vienna, 5–8 July,* pp. 379–386. Rotterdam: Balkema.

Heltzen, A.M. & Kure, K. 1980. Blasting with ANFO/ polystyrene mixtures. *Proceedings ISEE Annual Conference 1980, (The International Society of Explosives Engineers: Cleveland*), pp. 105–116.

Hopler, R.B. 1993. History of the development and use of bulk loaded explosives, from black powder to emulsions. *Proceedings ISEE Annual Conference 1993, (The International Society of Explosives Engineers: Cleveland),* pp. 177–198.

Hunsaker, R.D. 1995. An introduction to a revolutionary low density bulk explosive for surface blasting operations. *Proc. Explo. 95. Brisbane, Australia, 4–7 September, Carlton, VIC: Australasian Institute of Mining and Metallurgy*, pp. 67–71.

Hunter, C., Fedak, K. & Todoeschuck, J.P. 1993. Development of low density explosives with wall control applications. *Proceedings ISEE Annual Conference 1993, (The International Society of Explosives Engineers: Cleveland),* pp. 549–554.

Jackson, M.M. 1993. Low strength water gel explosive. Proceedings ISEE *Annual Conference 1993, (The International Society of Explosives Engineers: Cleveland*), pp. 493–499.

Johnson, R.J. 1996. 'SANFO' 'The missing link' in explosives technology. *Proceedings ISEE Annual Conference 1996, (The International Society of Explosives Engineers: Cleveland)*, pp. 242–252.

Lownds, C.M. 1986. The strength of explosives, in The Planning and Operation of Open Pit and Strip Mines. *South African Institute of Mining and Metallurgy: Johannesburg (ed: J P Deetlefs),* pp. 151–159.

Lownds, C.M. 1991. Energy partition in blasting. *Third High-Tech Seminar on Blasting Technology, Instrumentation and Explosives Applications (Blasting Analysis International: San Diego)*.

Moxon, N. & Armstrong, L. 1990. Low shock energy emulsion based wet hole explosives. *Proc. 3rd Int. Symp. On Rock Fragmentation by Blasting, Brisbane, Australia. 26–31 August, Carlton, VIC: Australasian Institute of Mining and Metallurgy*, pp. 45–53.

Rock, J. 2004. Improving blasting outcomes using Softload low-density explosives. *Proceedings Explo 2004, (The Australasian Institute of Mining and Metallurgy: Melbourne),* pp. 153–158.

Rock, J. Maurer, A. & Pereira, N. 2005. Coming of Age for low density explosives. *Underground coal operation conference paper–126*.

Rowe, J.L., Goodridge, R., Stow, D. & Molloy, K.J. 2001. Variable energy explosives for soft ground blasting. *Proceedings Explo 2001, (The Australasian Institute of Mining and Metallurgy: Melbourne),* pp. 111–113.

Silva, G. & Scherpinisse. 2010. Development of low density reacting agents. *Rock fragmentation by blasting–Sanchidrian (ed) Taylor @ Fracis group London ISBN 978-0-415-48290-7*, pp. 117–126.

Wilson, J.M. & Moxon, N.T. 1989. The Development of a low shock energy ammonium nitrate based explosive. *Proceedings ISEE Annual Conference 1989, (The International Society of Explosives Engineers: Cleveland)*, pp. 297–308.

Performance of Explosives and New Developments – Mohanty & Singh (Eds)
© 2013 Taylor & Francis Group, London, ISBN 978-0-415-62142-7

PANFO: A novel low-density dry bulk explosive

G. Silva
GeoBlast S.A., Santiago, Chile

C.P. Orlandi
Enaex Servicios S.A., Santiago, Chile

ABSTRACT: Low-density products allow for better distribution of the explosive's energy within the blasthole, a reduction of vibration levels and the generation of a more uniform and even fragmentation, providing a wall damage control tool contributing to achieve safe walls and mine planning objectives.

This paper presents a novel blasting agent, PANFO, based on PAN (AN coated expanded Perlite) and FO, as to ensure oxygen balance for proper detonation. A Pilot Plant was assembled to scale-up laboratory work, understand both the manufacturing process and product performance under real operational scenarios and, finally, validate the product in real-size blasts in large open pit mines. The most outstanding features shown by PANFO relate to the lack of segregation, the elimination of potential afterburn and the ability of being mixed and loaded on-site using standard ANFO trucks used in the industry. In addition, ingredient composition of PANFO is such that oxygen balance can be easily achieved.

1 INTRODUCTION

The main application of low-density mixtures is focused on wall control, the broad objectives being to reduce overbreak, increase slope stability, improve safety and reduce overall costs.

Economical implications of reducing overbreak are best illustrated in Figure 1, whereby a decrease in overall pit slope angle of 3° for a 100 m wall height will result in 676 m^3/m of extra volume to be removed. Assuming a 1000 m pit circumference and a rock density of 2.5 t/m^3, will result in an extra 676,000 m^3 * 2.5 t/m^3 ~ 1.7 million tons of waste material to be loaded and hauled.

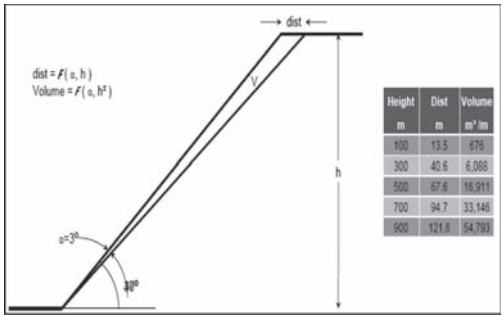

Figure 1. Overbreak volume as a function of wall height.

Research & Development of low-density explosive mixtures has been well documented in the literature. Isanol (Heltzen, 1980), Dynolite (Hunsaker, 1995), Softload (Rock, 2004), LDRA (Silva, 2009), Novalite (Rowe, 2001), Blastlite (Beach, 2004), Flexigel (Lamadrid, 2006), etc; are just some examples of these mixtures. Most of these products have experienced limited success due to ingredient segregation effects, field performance characteristics and/or logistical issues regarding manufacturing, handling and storing.

PANFO, a recently developed low-density, bulk—loaded mixture, fills in most of the previous shortcomings, presenting itself as a sound alternative product for damage control and bench stability. This paper describes the main characteristics of the novel mixture, the basic design of a pilot-plant assembled for manufacturing larger quantities of product for evaluation in open pit mining operations, followed by a summary of field application results.

2 PANFO: INGREDIENT DESCRIPTION & MIXTURE CHARACTERISTICS

PANFO is a bulk loaded low-density Blasting Agent, best described as a two-component system, namely PAN and Fuel Oil (FO). PAN in turn,

Downloaded by [Visvesvaraya Technological University (VTU Consortium)] at 21:58 01 March 2016

consists of an intimate mix of two ingredients, an inert volcanic mineral called Perlite (P) in its expanded form, and Ammonium Nitrate crystals (AN), the latter being the most economical and widespread oxygen supplying agent used in the explosive industry at present.

(i) Expanded Perlite granules: The core of the new explosive concept relates to the use of Perlite in the form of expanded granules. Perlite granules are manufactured via a thermal process requiring temperatures of up to 800° C in order to soften the crude mineral and vaporize water pockets contained within, generating an expanded granule that characterizes itself for its lightness, high porosity and high capacity to absorb and retain liquids. Being a chemically inert ingredient, it will not contribute energy during the reaction process of detonation. The left picture depicted in Figure 2 illustrates a microphotograph of an expanded Perlite granule showing the intricate labyrinth of open pores characterizing its inner structure while the right photograph illustrates the volume change expected when going from crude to crushed to expanded mineral forms.

The size, density, porosity and mechanical strength that expanded Perlite granules attain will depend to a great extent in the source of the crude mineral (geology of deposit) and the expansion process itself. It is obvious that the four mentioned characteristics are intimately interconnected, that is to say: the lower the granule density, the higher its porosity (therefore its absorption capacity) and the lower its mechanical strength. Typical bulk densities of expanded Perlite granules range between 50 kg/m^3 (0.05 g/cc) and 250 kg/m^3 (0.25 g/cc).

Selection of an appropriate Perlite granule density will need to balance opposing requirements, for on one hand there is a need for a light absorbent product (i.e. low-density, high-porosity, high-absorption granules) while at the same time the need for a product having sufficient mechanical strength in order to withstand typical levels of stress occurring during handling and manufacturing.

As an ingredient in the PAN mixture, the expanded Perlite granules provide two main functions. First, they are the density reducing agent of the mix and second and most important, they provide the substrate to hold the AN crystals within their open pore structure, producing therefore a mixture whose ingredients will not segregate upon mixing, handling and loading as it usually happens with typical low density dry mixtures consisting of ANFO prills and diluting agents such as expanded Perlite fines, expanded Polystyrene beads, oat/rice hulls and similar products.

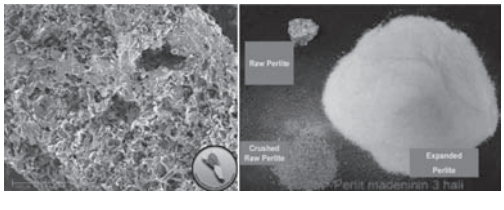

Figure 2. Perlite overbreak volume as a function of wall height.

(ii) Ammonium Nitrate: The second ingredient composing PAN relates to AN crystals. These crystals are supplied to the Perlite granules in the form of a hot concentrated solution. Absorption of this solution within the pores of the expanded Perlite and their subsequent precipitation upon cooling and drying will generate a product (PAN) whose ingredients will not segregate when subjected to handling, mixing and loading forces.

Temperature of the concentrated AN solution is an important issue to consider during the absorption process into the Perlite granules. In order to ensure a proper absorption of the hot liquid within the deeper pores of the expanded mineral, preventing the formation of undesired crystal layers by cooling upon contact, it was deemed convenient to raise the working temperature of the AN solution about 20 °C above its corresponding crystallization temperature. In addition, delaying the time to reach crystallization temperature will facilitate the elimination of excess solution from the granules, which in turn will reduce the formation of AN layers coating the granules and facilitate handling and drying process.

Given its ingredient composition (inert mineral and AN), the resulting granules of PAN classify as an Oxidizing Agent for handling, storage and transportation purposes, in exactly the same manner as standard ammonium nitrate prills do. Moreover, PAN granules and AN prills compare favorably in another important operational aspect, they can be mixed with Fuel Oil (FO) to produce PANFO in the same bulk mixing trucks normally used to manufacture standard ANFO, the only difference being the calibration of the mixing auger and FO injection to the lower density explosive product.

(iii) Fuel Oil Addition: All that is required to transform the granules of Oxidizing Agent (PAN) into the Blasting Agent (PANFO) relates to the addition of Fuel Oil. Contrary to those low-density explosive mixtures using Expanded Polystyrene beads (EPS) as their density reducing agent (such as Isanol and the LDRA previously mentioned), where the chemical incompatibility of napthens based fuels with polystyrene required the use of mineral based oils as fuel; the chemically inert expanded Perlite granules used in the PAN mixtures allows for the use of the regular less expensive Fuel Oil.

(iv) The FO: AN stoichiometric ratio of ~6% weight should prove sufficient to produce an

Downloaded by [Visvesvaraya Technological University (VTU Consortium)] at 21:58 01 March 2016

oxygen-balanced composition. However, tests conducted at the Canadian Explosives Research Laboratories (CERL) in Canada (Silva, 2007), indicated that a slightly higher fuel percentage (~6.8%) minimized the generation of Nitrogen Oxide (NO_x) at the expense of a slight increase of the less toxic Carbon Monoxide (CO) and Carbon Dioxide (CO_2) fumes. Figure 3 next, summarizes toxic fume results obtained at CERL.

In addition, VOD measurements conducted at CERL laboratories with PANFO confined in 50 mm steel tubes also indicated an improvement in explosive performance with the increase of fuel oil content, thus density, as Figure 4 clearly illustrates.

(v) Explosive Characteristics: As illustrated in Figure 5, the physical characteristics of PANFO are

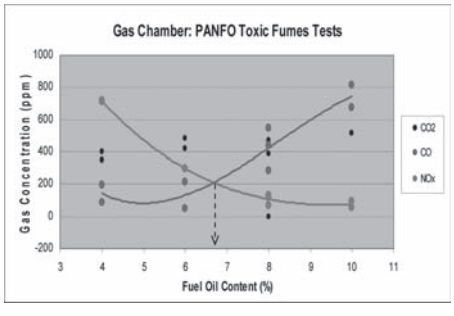

Figure 3. Toxic fumes experiments at gas chamber (CERL).

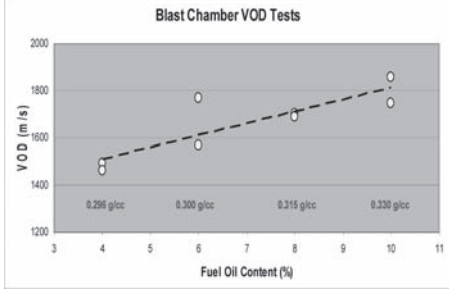

Figure 4. VOD test results at gas chamber (CERL).

Figure 5. Physical aspect of PANFO granules.

those of irregular granular particles. The purplish color observed is just the consequence of dyeing the fuel oil to enable a visual evaluation of the quality of the mix.

The final density of PANFO will depend on various aspects, being the bulk density of the Perlite granules themselves and the AN concentration of the solution the most important ones, followed by the presence of Perlite fines, the use of surface active agents in the solution (surfactants) and the drying process itself (time and temperature).

During last stages of development and field application experiments, where Perlite granules from various sources and ammonium nitrate solutions with different concentrations were used, the density of PANFO ranged from 0.32 g/cc to 0.45 g/cc. Table 1 presented next, summarizes the main physical and thermochemical properties of PANFO, which were calculated at a bulk density of 0.40 g/cc, assuming a density of Perlite granules of 0.14 g/cc and considering a 7% wt. fuel oil addition.

The VOD range included in Table 1 corresponds to measured experimental values for blastholes ranging from 150 mm to 270 mm diameter. These VOD values were then used to calculate the corresponding detonation pressures based on well established formulae. In addition, thermochemical values for absolute and relative strengths were calculated using Cheetah 2.0 code.

The fragility index and maximum fuel oil absorption values were both determined in accordance to standardized laboratory procedures established at Enaex S.A.[1] For comparison purposes, it is worth mentioning that the AN prills manufactured by Enaex recorded a fragility index value of 35% and a minimum fuel oil absorption of 12%, both values

Table 1. PANFO physical and thermochemical properties.

Properties	Units	PANFO
Density	(g/cc)	0.40
VOD	(m/s)	1800–2000
Detonation pressure	(kbar)	3.4–4.0
Gas volume	(lts/kg)	827
Weight strength (WS)	(cal/g)	595
Bulk strength (BS)	(cal/cc)	238
Relative weight strength (RWS)	–	64
Relative bulk strength (RBS)	–	32
Critical diameter	(mm)	50
Minimum primer	(g)	40
Fragility index	%	38
Maximum fuel oil absorption	%	13.5
Classification (PAN)	–	UN 1942 class 5.1
Classification (PANFO)	–	UN 0331 class 1.5

Downloaded by [Visvesvaraya Technological University (VTU Consortium)] at 21:58 01 March 2016

comparing extremely well with those tabulated above for the PAN/PANFO granules.

It is worth restating the fact that PAN ingredients are amenable for an oxygen-balanced composition, an important consideration given that having a balanced explosive mixture opens a window of opportunity for applications in both, surface and underground mining operations.

The high capillary forces characterizing Perlite have proven in the past capable of breaking-down several types of standard emulsion explosives or its blends with ANFO (Heavy ANFOs). Tests conducted within Enaex laboratories, mixing PAN/PANFO granules with two different explosive emulsion matrices (EL-928 oleic acid/caustic soda emulsifying system, and AE-59, PIBSA based emulsifier), proved physical and chemical compatibility between both products. Moreover, successful preliminary VOD experiments were conducted in a 50/50 volumetric mix of PANFO and an emulsion matrix, using Enaex standard testing procedures (150 mm diameter cardboard tubes initiated with a 450 g Pentolite primer). The possibility of mixing these two products presents a window of opportunity for diluting emulsion explosives and/or providing water resistance to the low-density product.

Alike standard ANFO prills, PANFO has null water resistance. However, if required, it can be treated with guar-gum or commercial additives such as Adtec®, where an immediate physical barrier upon contact with water is created. Said additive is used in the established commercial product called WR-ANFO. Figure 6 next, best illustrates the results by comparing the effect on PAN granules placed on top a colored water, with (left) and without (right) the additive. It is worth noting that if PANFO was to be loaded into a blasthole in the presence of static water at the bottom, it will create a floating plug with only a section getting wet due to column weight. Standard ANFO prills on the other hand, will enter into solution indefinitely upon contact with water.

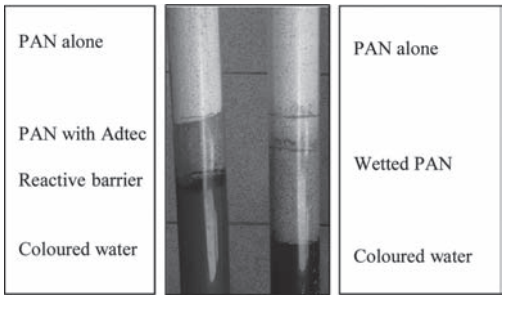

Figure 6. Water protective barrier for PAN granules.

3 PILOT PLANT DESIGN

Once the research and development stages of the novel product were accomplished, efforts were directed towards designing and assembling a manufacturing plant at a Pilot scale.

This decision was deemed necessary in order to satisfy two main goals; first, to enable the manufacturing of larger quantities of the low-density explosive in order to conduct validation experiments at an industrial level, that is, intervening blastholes in operating open pit mines and second, to advance in the learning process related to the equipment involved in the various manufacturing stages, all of which would be put to good use when taking the plant design to higher engineering levels as it is being done at the present.

The Pilot Plant was designed in-house by Grupo Latino S.A. (GLSA) and assembled within the R&D facility at the Enaex Rio Loa Plant, Calama, northern Chile, where explosives are manufactured and delivered to the important mining district existing in the area.

Essentially, the Pilot Plant consists of the following stages:

- Initial screening stage
- Temporary storage tank
- Absorption or wetting stage
- Drying stage
- Bagging stage

A layout of the Pilot Plant showing the basic stages of the process as it was assembled at Enaex explosive facility in northern Chile, is illustrated in Figure 7 next.

(i) Screening stage: The initial screening stage of the process was implemented to reduce the volume of Perlite dusts and fines usually present in the bags due to the fragile nature of the expanded mineral itself and the unavoidable particle breakdown taking place during handling and transportation of

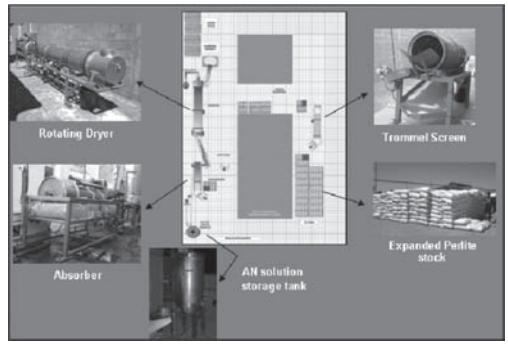

Figure 7. Pilot plant layout.

Downloaded by [Visvesvaraya Technological University (VTU Consortium)] at 21:58 01 March 2016

the bagged product. Reducing the presence of these undesirable particle size range (<0,5 mm) will not only create a better working environment but also facilitate the subsequent wetting and drying stages, reducing agglomeration effects due to the high hygroscopic behavior characterizing AN crystals.

The equipment designed for the screening stage, consisted of a rotating drum (trommel) constructed with perforated stainless steel sheets using 0.5 mm hole diameters, later changed to a 1.0 mm diameter to increase screening efficiency. Figure 8 next, depicts a view of the trommel drum from the feeding (left) and discharge (right) ends.

(ii) Storage Tank: This cylindrical tank, illustrated in Figure 9, was entirely constructed in stainless steel sheets and piping, had a capacity to hold and maintain the temperature of 700 liters of hot AN solution, which was pumped from a special container provided by Enaex. The tank has an impeller built inside to agitate the solution and help maintain a uniform temperature. Electrical heaters and thermostats to adjust and control the solution temperature, fluid level controllers and pumps to deliver the solution to the absorber stage were part of the storage tank system.

(iii) Absorption/wetting stage: The absorber equipment, illustrated in Figure 10, which was also fully constructed in stainless steel, consisted of a perforated screen drum with a fixed helicoidal impeller/turbine fitted on its inside.

Figure 8. Rotating trommel used to screen Perlite dust & fines.

Figure 9. Insulated AN solution tank reservoir.

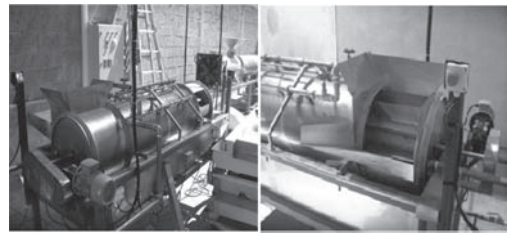

Figure 10. Absorber designed to wet Perlite with AN solution.

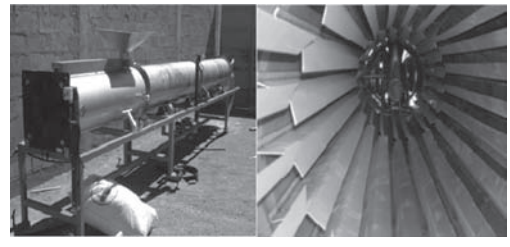

Figure 11. Oven with fins designed for drying PAN granules.

This arrangement was mounted on a tub holding the hot ammonium nitrate solution delivered from the storage tank. Upon rotation, the perforated screen/turbine system, which was partially immersed in the hot AN solution contained in the tub, would force the Perlite granules into the solution for the absorption process to take place. The rotational speed could be adjusted to control residence time of the Perlite in the solution. The end products of this stage were the granules of PAN in a wet state.

(iv) Drying stage: As shown in Figure 11, the equipment for the drying stage of the Pilot Plant consisted of a two-part oven, a rotating drum section of about 4 m long where the actual drying process takes place. An additional 2 m long stationary section contain the feeder port and the electric fan and heaters required to generate and control air flow and temperature (left).

The rotating section of the oven was fitted inside with a series of welded fins (right) in order to promote a cataract effect of the PAN granules and enhance the drying process.

(v) Bagging stage: Expanded Perlite, one of the two main consumables of PAN, was delivered in ~11 kg bags, which were stockpiled as shown in Figure 12.

These same bags were later used to store the PAN mixture after the drying process was completed. Later on in the project, the dry product was transferred to 1 m^3 maxibags and stored outdoors as is usually done with standard AN prills prior to being loaded into the mixing truck for delivery into the operating mines for field evaluation.

Figure 12. Stockpile of expanded Perlite bags.

4 INDUSTRIAL SCALE EXPERIMENTS

A total of 40 tons of PAN was manufactured at the Pilot Plant for use in Buffer rows at several open pit operations in the mining district around Calama, northern Chile. Some of these operations included Chuquicamata, Minera Gabriela Mistral (Gaby), Mina Sur and Radomiro Tomic (RT) all from Codelco Norte, as well as Mina Esperanza and El Tesoro from AMSA. About 6 tons of explosives were tested in each operation.

Delivery of the Oxidizing Agent PAN from the Pilot Plant to the operating mines for testing was done in 1 m^3 *maxibags*, which were later transferred to the mixing truck for fuel oil addition and loading.

The first and most important test was implemented at Mina Esperanza and consisted of a special trial configuration that allowed direct comparison of near-field vibration levels generated by PANFO versus those produced by standard ANFO.

Preparation of PANFO required calibration of the feeding auger and fuel injection system of the mixing truck in order to ensure the appropriate percentage of fuel is being added to the PAN granules. The calibration process is conducted on a regular basis onsite, in the exact same manner as it is done for standard AN prills.

In view of the highly absorbent characteristics of Perlite, it was decided to conduct most field experiments in large open pit operations using 7.5% weight of FO in the PAN mixture to ensure enough fuel will be present in intimate contact with the AN crystals and not dispersed within unoccupied Perlite pores. It is worth noting that the FO percentage refers to the weight of fuel relative to the weight of AN crystals contained in the PAN mixture and not to the weight of PAN (Perlite + AN).

Figure 13 next illustrates the mixing truck specially assigned for the trials at Esperanza Mine to prepare the PANFO mixture. Figure 14 following, shows the mixing truck in the process of discharging the low density product into a blasthole.

The special trials conducted at Esperanza Mine consisted of two very similar tests, the main difference between them being the explosive load. Figure 15 shows the loading configuration of both tests, consisting in nine 270 mm (10⅝ inch) holes, the first three loaded with standard ANFO prills followed by three holes containing one triaxial geophone each, cemented at about 13 m in depth and the last three holes loaded with PANFO.

The same initiation sequence was implemented in both trials, with the PANFO blastholes detonating first, at delays of 200 ms from each other, followed by the regular ANFO blastholes also delayed 200 ms from each other. In this manner, each of the three the geophones will be able to capture for analysis the signature waveforms originating from each of the six loaded blastholes.

Figure 13. PANFO truck used at Esperanza Mine trials.

Figure 14. Discharging PANFO into a blasthole.

Downloaded by [Visvesvaraya Technological University (VTU Consortium)] at 21:58 01 March 2016

Downloaded by [Visvesvaraya Technological University (VTU Consortium)] at 21:58 01 March 2016

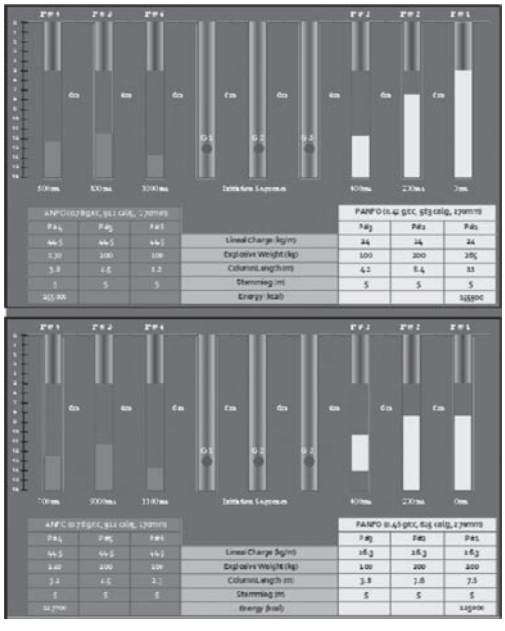

Figure 15. Configuration for Esperanza Mine PANFO trials.

Three VOD monitors were used during the two trials at Esperanza, all of them monitoring the performance of PANFO. Each monitor chain linked the three blastholes containing PANFO in an effort to ensure recording enough VOD information of the explosive of interest.

Table 2 next, summarizes the VOD records obtained in each individual blasthole and the resulting average values for the two trials conducted at the mine.

VOD results indicated average values of 1860 m/s for the first trial at of 0.42 g/cc while the second trial averaged 2000 m/s for a PANFO at 0.45 g/cc.

The above velocities of detonation and corresponding densities can be used to estimate explosion pressures based on approximate formula:

$$Pe(MPa) \sim \rho(g/cc) \times VOD^2(m/s)/8$$

Table 3 compares the explosion pressure of PANFO, as calculated by the previous equation, versus that developed by the standard ANFO manufactured by Enaex (0.78 g/cc) using an experimental VOD of 4391 m/s, an average from various measurements conducted at Esperanza mine under the same hole diameters.

Low explosion pressures are a direct measure of the capacity of an explosive to reduce/control damage. As shown in the table above, when compared to standard ANFO prills, the lowest density explosive industrially available, a reduction ratio of about 10 is to be expected when using PANFO as compared to ANFO.

Table 2. VOD results for both PANFO trials at Esperanza.

Trial #	VOD monitor	Hole 1	Hole 2	Hole 3	Average VOD
Special trial # 1 0.42 g/cc	1	1830	1895	n/r	1863
	2	1825	1925	n/r	1870
	3	1855	1842	n/r	1849
	Average of special Trail #1				1860
Special trial # 2 0.45 g/cc	1	2035	n/r	2115	2075
	2	1960	n/r	n/r	1960
	3	1950	n/r	1976	1963
	Average of special Trail #2				2000

Table 3. VOD results for both PANFO trials at Esperanza.

Explosive	Density (g/cc)	VOD (m/s)	Pe (MPa)	P_{ANFO}/P_{PANFO}
PANFO	0.42	1860	182	10.3
PANFO	0.45	2000	230	8.2
ANFO	0.78	4391	1880	1

The other important indicator used to assess the potential for damage of an explosive refers to the ground vibrations generated upon detonation, which are obviously connected to the borehole pressure, thus to the explosive VOD. The trials conducted at Esperanza mine allowed the direct comparison of vibration levels of both explosive products under similar of rock and explosive load conditions.

Figures 16 and 17 that follow, illustrate the near-field vibration models generated by PANFO and ANFO respectively, defined by the Holmberg & Persson equations, which are in turn identified by their corresponding k and α factors. As expected, the slope of the fit line to the experimental data for either explosive is basically the same given that the measurements were taken under the same rock conditions, however, the resulting difference in vibration levels is considerable.

Figure 18 next, compares the fits to experimental data for both products PANFO and ANFO, where the difference in expected vibration levels generated between them can be easily interpreted. As shown in the graph, for a given H&P factor, a reduction

Downloaded by [Visvesvaraya Technological University (VTU Consortium)] at 21:58 01 March 2016

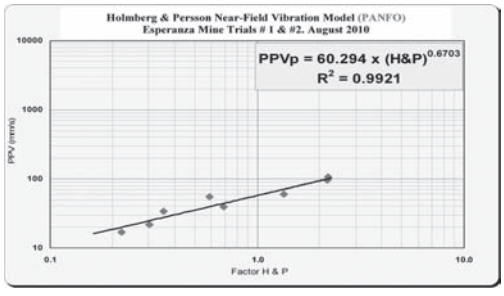

Figure 16. Near field vibration results for PANFO trials.

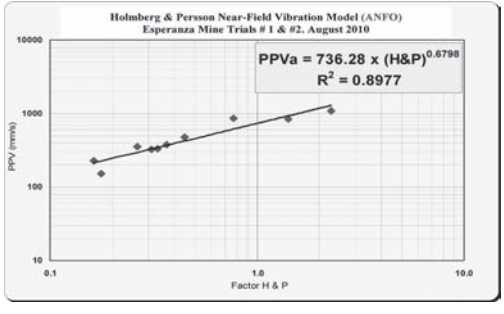

Figure 17. Near field vibration results for ANFO trials.

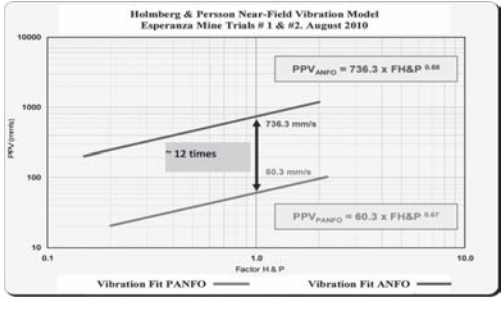

Figure 18. Comparison, PANFO/ANFO near field vibration.

in vibration levels of more than 12 times is to be expected when using PANFO instead of standard ANFO prills. This magnitude of vibration level reduction will certainly have a great impact on wall control and slope stability.

Trials at Esperanza provided the tools to estimate vibration levels and set up a baseline to which to compare tests at other mining operations. Results of the tests conducted at two such operations, Chuquicamata and Radomiro Tomic of Codelco Norte, and Tesoro from AMSA, will be briefly described next.

4.1 *Chuquicamata Mine*

The test at this particular mine was implemented in an area where results of the Acceptability Criteria for single benches established at the operation scored 49%, mostly as a consequence of overbreak due to the presence of a non-competent rock formation.

The experimental blast intervened the Buffer rows by substituting Emultex-N (1.32 g/cc), the emulsion explosive typically applied, with PANFO at a density of 0.45 g/cc.

As Figures 19 and 20 illustrate, the controlled section of the experimental blast was divided into three sectors, the first one consisting of a single Buffer row loaded with PANFO, the second and middle sector consisting of a single row loaded with Emultex-N and the third and final sector with two Buffer rows loaded also with PANFO.

The trials at Chuquicamata mine considered not only the control of damage to the pit walls, but also the requirement of maintaining the rock fragmentation distribution of the ore. Figures 21 and 22 show the results of the fragmentation

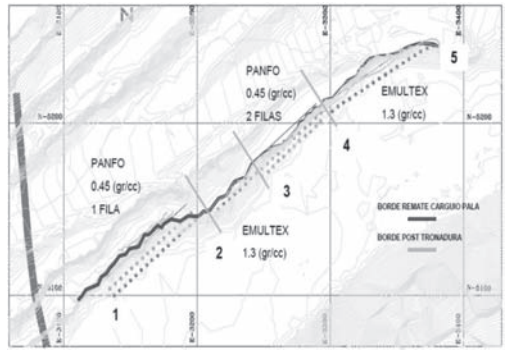

Figure 19. Sectors of the PANFO blast at Chuquicamata.

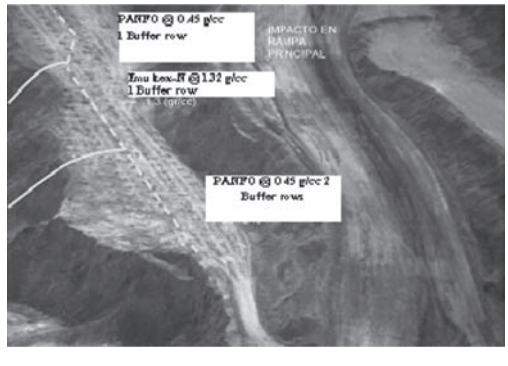

Figure 20. Sectors of the PANFO blast at Chuquicamata.

Downloaded by [Visvesvaraya Technological University (VTU Consortium)] at 21:58 01 March 2016

Setting	Tamaño (")
P25	10,1
P50	12,6
P80	15,7
P90	22,8

Tamaño (")	%
Menor a 2	0,0%
Entre 2 y 4	0,2%
Mayor a 4	99,8%

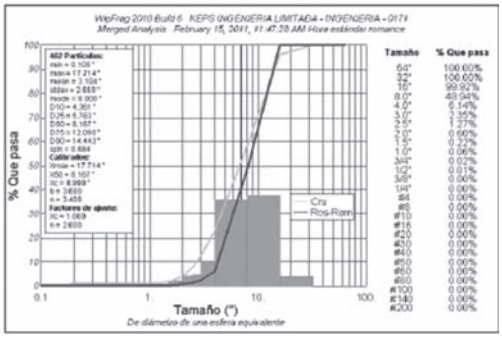

Figure 21. Fragmentation results in the PANFO sector.

Setting	Tamaño (")
P25	5,8
P50	8,2
P80	12,9
P90	14,4

Tamaño (")	%
Menor a 2	0,6%
Entre 2 y 4	5,5%
Mayor a 4	93,9%

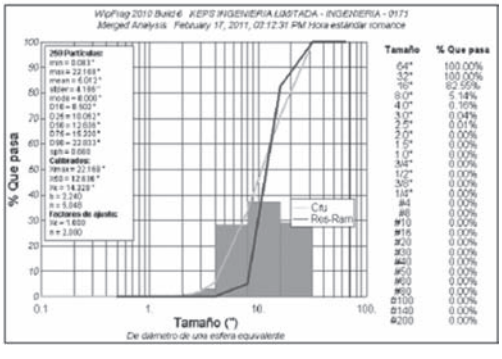

Figure 22. Fragmentation results in the heavy ANFO sector.

assessment using WipFrag for the PANFO and the Heavy ANFO sectors, respectively. Powder factor for PANFO was 98 gr/Ton and for the Heavy ANFO, 293 gr/Ton. Stemming was 4 and 6 m, respectively. Drilling pattern was 5 m × 5 m, hole length 17 m and diameter 165 mm.

Finally, Figure 23 shows the face angle obtained with PANFO and the one with their previous technique using Heavy ANFO (labeled as "normal").

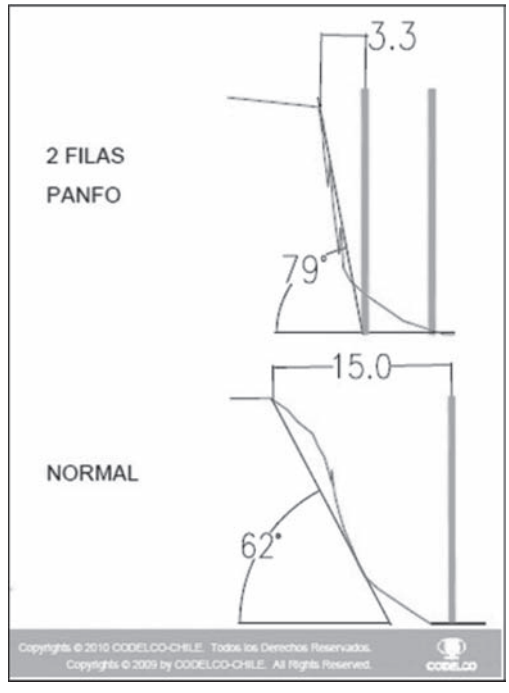

Figure 23. Face angle, PANFO vs "Normal".

5 CONCLUSIONS

Low-density explosive have been used for many years as a tool to reduce damage and, consequently, overall mining costs. In most instances, they comprised of ANFO or Emulsion explosive mixed with a bulking agent. Segregation in these mixtures is sure to occur, limiting the level to which density can be reduced without risking detonation failure. The concept of PANFO was introduced in FragBlast 9, when the laboratory work was presented. At this time, product manufacturing at an industrial scale proved to be successful, simple and flexible.

Furthermore, the logistics, storage, transportation and delivery to the mine sites have demonstrated that this novel solution has important operational advantages, compared to the products in the world market. Especially, it has to be pointed out that the use of standard ANFO and Heavy ANFO trucks is an important advantage.

Finally, PANFO can also be treated as reactive bulking agent in a wide range of desired densities or dilution degrees, eliminating the possibility of propagation failure. Moreover, the product has shown outstanding detonation capabilities when mixed with emulsion matrix in a 50/50 volume basis, therefore, opening a window of opportunities for using the product under wet conditions.

Based on the industrial trials presented in this paper, a high capacity plant is being built in Chile, to be in production in 2013.

REFERENCES

Beach, F; Gribble, D; Littlefair, M; Rounsley, R. (2004). BlastLite-The Practical Low-Density Solution. Proceedings EXPLO 2004, Perth, Western Australia; pp# 147.

Heltzen, A.M. (1980). Blasting with ANFO/Polystyrene Mixtures. Proceedings of the 6th Conference of Explosives and Blasting Techniques (ISEE); pp# 105.

Hunsaker, R.D. (1995). An Introduction to a Revolutionary Low Density Bulk explosive for Surface Blasting Operations. Explo 95. AusIMM Proceedings.

Lamadrid, M.A.; Arellano, M. (2006). Variable Density Explosives. Fragblast-8. Santiago, Chile. Pag. 35.

Rock, J. (2004). Improving Blasting Outcomes Using SoftLoad Low Density Explosives. Proceedings EXPLO 2004, Perth, Western Australia; pp# 153.

Rowe, Goodridge, Stow and Molloy. (2001). Variable Energy Explosives for Soft Ground Blasting. Explo 2001. AusIMM Proceedings. Hunter Valley, NSW. Oct. pp# 28–31.

Silva, Guillermo. (2007). Development, Characterization and Application of a Reactive Bulking Agent for Wall Control. PhD Thesis. Department of Mining Engineering, Queen's University, Kingston, Ontario, Canada.

Silva, Guillermo; Scherpenisse, Carlos. (2009). Development of Low Density Reactive Agents. Fragblast 2009. Granada, Spain.

Silva, Guillermo; Carrasco, José; Orlandi, Carlos. (2010). PANFO, Explosivo a Granel de Baja Energía y Baja Densidad, ASIEX Conference, Santa Cruz, Chile.

Downloaded by [Visvesvaraya Technological University (VTU Consortium)] at 21:58 01 March 2016

Performance of Explosives and New Developments – Mohanty & Singh (Eds)
© 2013 Taylor & Francis Group, London, ISBN 978-0-415-62142-7

Underground cavern excavation using underground bulk explosives—an Indian case study

A.K. Mishra
Indian School of Mines, Dhanbad, India

K.V. Ramana Rao & B. Eswara Rao
Hindustan Construction Company, India

Deepak Joshi
Keltech Energies Limited, India

ABSTRACT: The rapid strides made by the Indian economy in the last decade have resulted in tremendous pressure on the demand for oil and gas. In the recent past ways and means were envisaged to look for the environmentally and strategically safer storage methods for oil and gas. To fulfill these requirements underground gas/oil caverns have been conceptualized. India's dependence on oil imports is expected to be 92% by the year 2020. The Energy Security is paramount for the country's economic development. Keeping in view of the security of supplies, Government of India has planned construction of underground strategic crude oil storage cavern at Mangalore (1.5 Mt), Vizag (1.33 Mt) and Padur (2.5 Mt).

The construction of cavern project always faces the daunting challenge of being completed on or before time. One of the most critical constraints of any construction project is the cycle-time and performance of drilling and blasting operation. The conventional method of blasting poses inherent inefficiencies and limitations. This paper describes a comparative study between conventional cartridge explosives and bulk explosives in terms of cycle time, rate of excavation, half barrel factor and advance rate conducted at Padur cavern project.

1 INTRODUCTION

India's dependence on oil imports is expected to be 92% by the year 2020. The Energy Security is paramount for the country's economic development. Keeping in view of the security of supplies Government of India has planned construction of underground strategic crude oil storage caverns at Mangalore (1.5 Mt), Vizag (1.33 Mt.) and padur (2.5 Mt).

2 SITE LOCATION

The study was conducted at Padur, a village belonging to Udupitaluka, is located on the west coast in south-western part of Karnataka state. The proposed site, located at 13°13′30″ Nlatitude and 74°47'30"E longitude, is about 5 km east of Kaup, which is locatedon the National Highway-17 connecting Mangalore and Goa at 12 km south of Udupi. Bound inthe east by the Western Ghats and in the west by the Arabian Sea, the locationis about 1000 km south of Mumbai by rail. Location of the site is presented in the Figure 1.

The storage facility will consist of two separate storage units for storage of two types of crude in a ratio of approximately 75:25. The caverns are approximately 20 m wide with a maximum height of around 30 m and are having an approximate 'D' shaped cross-section with a horizontal roof level maintained throughout the cavern length with a length of approximately 700 m. At least one shaft has been provided for each storage cavern.

Indian Strategic Petroleum Reserves Limited (ISPRL) has the ownership and control of the crude oil inventories and would coordinate the release and replenishment of crude oil stock with an empowered committee to be constituted by the Government.

Underground storage of crude oil offers various advantages over above ground storage, which may be enumerated as following:

- Easy operation with economic benefit
- Product storage is located at a depth and is fully isolated

Downloaded by [Visvesvaraya Technological University (VTU Consortium)] at 21:58 01 March 2016

Figure 1. Location map of cavern.

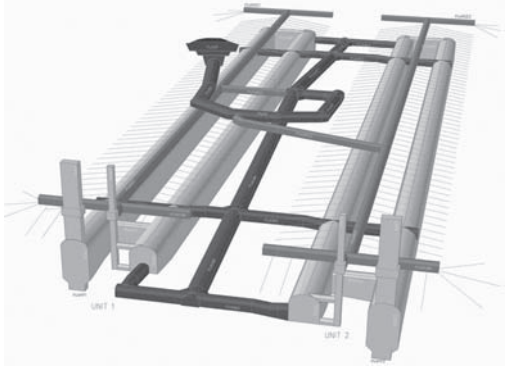

Figure 2. 3-D view of part-A, Padur.

- Technologically proven, environment friendly and safe
- Principle of containment ensures no leakage and contamination
- Safety hazards on account of sabotage, storms, earthquake, and explosions are minimized
- External fires will not affect storage
- Surface land requirement is low
- Cavern by their very nature require very low maintenance and hence safety is in built.

The nature and scope of the excavation work to be done at the site is huge. The Total excavation for the caverns and their connections added up to 1.89 Million cubicmeter (Fig. 2). The caverns themselves are of huge cross-section. The caverns are 20 meters in width and 30 meters in height. The caverns are to be approached by means of access shafts.

Table 1. Geological parameters of the site.

Class	Class-I
Quality	Massive
Dry Density	2863 kg/m^3
Uniaxial Compressive Strength (condition: water saturated)	91–196 MPa
P-Wave Velocity	5.195–5.931 km/s
Young's Modulus	48–75 GPa
Poisson's Ratio	0.26–0.34
Cohesion	5.52–27.52 MPa
Internal Friction Angle	47.81 to 67.04
Porosity	1.42%
Permeability	Zero
Water Content	0.295%

3 SITE GEOLOGY

The predominant rock formation at the site is granitic-gneiss. The salient geo-technical features of the rock formation (by means of sampling done at the given depth of the caverns) are listed in the Table 1.

Major rock type is granitic-gneiss. All the tests were conducted as per the ISRM suggested methods. Triaxial compression test was conducted as per the multiple failure method. Only a limited number of samples were tested for various properties. Uniaxial compressive strength varied from 91 to 196 MPa and cohesion i.e. shear strength of rock varied from 5.52 to 27.52 MPa. The variation in strength is attributed to the orientation gneissic plane to the core axis.

4 PROJECT CONSTRAINTS

The unique nature of the project can be gauged by the constraints placed on the operations:

- Rate of excavation required over the life of the project
- Requirement of smooth blasting
- Limiting the maximum vibration values at crude pipelines
- Importance of limiting over break
- Blasting in accordance with the principles of smooth blasting.
- Excavation of all underground facilities need to be completed in 30 months of award of contract

Looking at the requirement of rapid development at construction site, it was decided to introduce underground bulk explosives instead of packaged explosives.

The technical evaluation was conducted between underground bulk (UG Bulk) explosive and

Downloaded by [Visvesvaraya Technological University (VTU Consortium)] at 21:58 01 March 2016

packaged explosives to understand the efficacy of UG Bulk. It was more important as the basic cost of bulk was 13% higher than that of packaged explosives.

The UG Bulk basically consists of two non-explosive components. The primary component of bulk premix (emulsion) is manufactured at Mother plant and transferred through bulk delivery system to the site. It is carried to the face where it is mixed with sensitizing solution. This sensitizing solution when mixed with the premix produces gas bubbles that lend the sensitivity to the explosive (Onederra, et. al., 1999; Player, 1998; Sang-lim No, et. al. 2004 & 2006).

The concentration of this solution determines the final density of the bulk explosive. Hence, by simply varying the concentration of the sensitizing solution we can change the final density of the product. This ease of control over the density of the product and hence over its velocity of detonation (VOD) and Relative Weight Strength (RWS) allows it to be used for smooth blasting purpose (Mishra, et. al. 2009).

The UG Bulk can be initiated in blast holes by the means of a small cartridge of packaged emulsion, which in turn is initiated by a non-electric or electronic detonator. The column of this explosive can either be bottom primed or mid-primed. Bottom priming saves time while middle priming may produce marginally better result.

5 CHARGING EQUIPMENT

It is basically an assembly of storage bins for the emulsion, sensitizing solutions and water along with a pump that pumps the emulsion at a definite rate and pressure (Fig. 3).

The pump unit runs on the power take off (PTO) of charging vehicle. Some water (about 40 liters) is also required for flushing the charging hose before and after the actual charging operation (Fig. 4). No electricity is required for running the pump.

Figure 3. Pump truck.

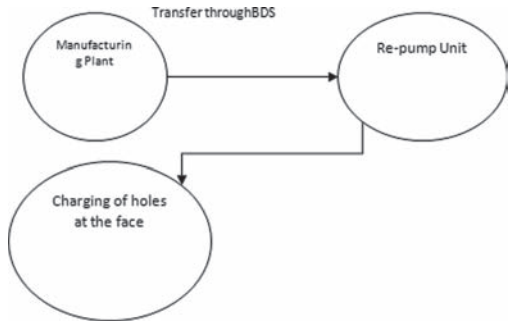

Figure 4. Model of operation.

6 TRIAL BLASTS

Prior to starting trials of UG Bulk at site some statutory approvals had to be taken which were approvals from Chief Controller of Explosives, Petroleum Explosive Safety Organisation (PESO), Government of India.

Charging unit was made by mounting the pump unit on Ashok Leyland underground carrier. This enabled easier and faster movement of the pump to the face.

The trial blasts were conducted at one dedicated face of 20 × 8 m cavern top heading to maintain the consistency, effective monitoring and like to like comparison. The cavern cross section is presented in the Figure 5. Total of 40 blasts were conducted for comparison.

Few blasts with conventional system were monitored to observe the existing practices and get the baseline data.

It was found that for 8.0 m height and 20.0 m width cavern top heading total average number of holes with cartridge explosives were 148 for stage I (i.e. Top heading) and 72 holes for stage II (i.e. slashing) of part-A. Part-B is excavated by another contractor and was not included in study. Average explosive consumption was 567.50 kg for stage I and 142.2 kg for stage II with average advance rate of 3.2 m which was 80% pull.

The cartridge explosive was 32 mm diameter, 235 mm length with 200 gm weight. The relative weight strength and relative bulk strength was 119% and 176% respectively with density of 1.15 g/cc, and velocity of detonation 4000 ± 400 m/s.

Total of 20 blasts were conducted using cartridge explosive. Table 2 represents the blast data recorded with cartridge explosive. Figures 6 & 7 depicts the blast design of cavern top heading. All trails were conducted at stage I while stage II was used for slashing and not included in trails. The charging details are presented in Tables 3 & 4 for stage I and II respectively of the top heading of the cavern.The average hole depth was 4.0 m,

Downloaded by [Visvesvaraya Technological University (VTU Consortium)] at 21:58 01 March 2016

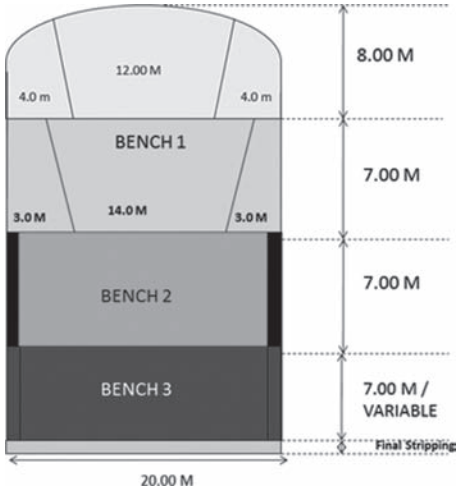

Figure 5. Cross section of top heading and benching for cavern.

Table 2. Results of trial blasts with cartridge explosives.

Blast no.	Total no. of holes	Total charge (kg)	Pull (m)	Powder factor (kg/m^3)	Specific drilling factor (m/m^3)
C1	144	567.50	3.1	2.05	2.08
C2	147	563.83	3.0	2.10	2.19
C3	148	565.50	3.3	1.90	2.01
C4	146	560.63	3.2	1.96	2.04
C5	147	580.82	3.4	1.91	1.94
C6	144	570.65	3.1	2.06	2.08
C7	140	575.50	3.4	1.89	1.84
C8	141	577.53	3.3	1.96	1.91
C9	151	562.50	3.1	2.03	2.18
C10	150	574.50	3.3	1.95	2.03
C11	151	567.50	3.2	1.98	2.11
C12	145	569.50	3.2	1.99	2.03
C13	140	559.86	3.0	2.09	2.09
C14	151	561.50	3.1	2.03	2.18
C15	141	562.35	3.0	2.10	2.10
C16	140	558.15	3.1	2.01	2.02
C17	142	569.39	3.3	1.93	1.93
C18	147	573.27	3.5	1.83	1.88
C19	135	561.49	3.1	2.03	1.95
C20	149	568.17	3.3	1.93	2.02

blast hole diameter of 45 mm and four numbers of reamer holes of 100 mm diameter were used.

6.1 *Methodology of trial blasts*

Required inventory of UG Bulk premix emulsion was maintained at the site in bulk delivery systems.

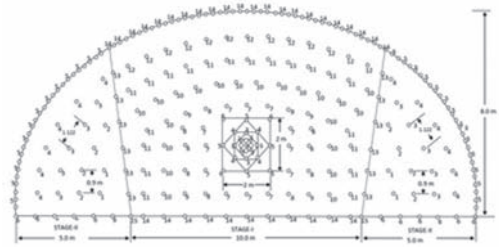

Figure 6. Drilling and blasting pattern for 20 × 8 m cavern top heading.

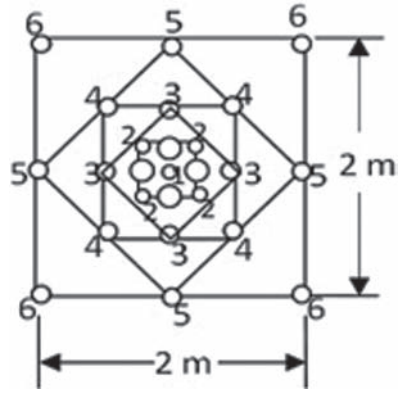

Figure 7. Drilling and blasting pattern of burn cut.

The charging unit was then taken underground upto the face for charging of holes as and when required. The manufacturing plant was located at 50 km from the site. Refilling of bulk delivery system took place as per the requirement.

The whole charging operation consisted of various sub-steps. First of all the hose was laid flat and then it was flushed to clean it completely. The primer cartridge was placed at the mouth of the blast hole and pushed inside the hole with the help of the charging hose. Once it reached the end of the hole requisite amount of explosive was charged into the hole. The hosepipe is pushed out due to the back-pressure exerted by the emulsion coming out of it. The remaining length of the charging hose was pulled out manually.

The UG Bulk explosives properties have been presented in the Table 5.

The charging time taken during trials in a round of charging of 150 holes with UG Bulk explosives are presented in Table 6.

6.2 *Trial blast results*

The following Table 7 represents results of 20 trial blasts conducted with UG Bulk at top heading

Table 3. Summary of charging details for stage I.

Description	Delay no.	No. of holes	Charge/ hole (kg)	Charged length (mm)	Total explosive (kg)
Burn cut holes	1	1	5.20	3200	5.20
Burn cut holes	2	4	5.20	3200	20.80
Burn cut holes	3	4	5.20	3200	20.80
Burn cut holes	4	4	5.20	3200	20.80
Burn cut holes	5	4	5.20	3200	20.80
Burn cut holes	6	4	5.20	3200	20.80
Stoping Holes	7	12	3.95	2140	47.40
Stoping Holes	8	10	3.95	2140	39.50
Stoping Holes	9	4	3.95	2140	15.60
Stoping Holes	10	18	3.95	2140	71.10
Stoping Holes	11	23	3.95	2140	90.85
Stoping Holes	12	13	3.95	2140	51.35
Stoping Holes	13	12	3.95	2140	47.40
Periphery Holes	14	22	3.325	2000	73.15
Bottom Holes	14	11	3.95	2140	43.45
Bottom Holes	15	2	3.95	2140	7.90

Table 4. Summary of charging details for stage II.

Description	Delay no.	No. of holes	Charge/ hole (kg)	Charged length (mm)	Total explosive (kg)
Burn cut holes	1	2	2.07	1300	4.14
Burn cut holes	2	4	2.07	1300	8.28
Burn cut holes	3	5	2.07	1300	10.35
Burn cut holes	4	6	2.07	1300	12.42
Periphery Holes	5	13	2.07	1700	26.91
Bottom Holes	6	6	2.70	1340	16.20

of cavern 20 × 8 m, stage I. The same jumbo was used with same set of operators. The trials were conducted in same cavern top heading with class-I rock mass. The geology was similar to the geology of rock mass encountered during conventional system.

On the basis of results obtained from trial blast using UG bulk and cartridge explosives, the following conclusions may be made:

- Pull per Round—Over the trial period of 20 blasts excellent average advance per round of 90% was achieved against 80% of conventional system. The average advance of 3.6 m per round (for drill hole depth of 4.0 m) as against the average of 3.2 m with conventional system shows the consistency of higher advance achieved with UG Bulk system. This might have been possible due to fully coupled blast holes with UG Bulk as compared to cartridge of 32 mm.
- Over-break—There was significant reduction in over-break. This was achieved with reduction of explosive density in the periphery holes. It was reduced to the level of 0.7 g/cc while with cartridge explosives it was 1.2 g/cc.
- Charging Time—Average charging time per face has been only 140 minutes (including 30 minutes for making connections) compared to 220 minutes of the conventional system, which is almost 36% reduction in charging cycle.
- Labour Requirement—Only 2 labours and one blaster is required for conducting the charging operation compared to 6 blasting crew member required with conventional system.
- Stemming—There was no requirement of stemming material with UG Bulk while we required 15% of stemming in each hole with conventional system. This is a benefit in terms of elimination of cost involved with making, storage, handling and usage of stemming material. UG Bulk explosives have viscosity of more than 80,000 cP. This provided good adhesion with borehole walls and without stemming provided good blast result.

Downloaded by [Visvesvaraya Technological University (VTU Consortium)] at 21:58 01 March 2016

Table 5. Underground bulk explosives properties.

Property	UG Bulk explosives	
Density (g/cc)	1.1	1.2
Critical Diameter (mm)	30	40
VOD (km/s)	4.0	4.5
Relative Weight Strength (RWS)%	85	95
Relative Bulk Strength (RBS)%	105	125

Table 6. Summary of activities associated with charging.

Activities	Time (min)
Flushing of charging hose	2
Initial cup sample taken (after charging 5 holes)	3
Loading face (159 holes)	105
Completing the connections	30
Total Time	140

Table 7. Results of trial blasts.

Blast no.	Total no. of holes	Total charge (Kg)	Pull (m)	Powder factor (kg/m^3)	Specific drilling factor (m/m^3)
B1	144	510.56	3.5	1.63	1.84
B2	147	525.35	3.4	1.73	1.94
B3	148	528.75	3.7	1.60	1.79
B4	146	523.39	3.6	1.63	1.82
B5	147	524.21	3.8	1.54	1.73
B6	144	526.55	3.5	1.68	1.84
B7	140	505.86	3.8	1.49	1.65
B8	141	490.55	3.7	1.48	1.71
B9	151	535.55	3.5	1.71	1.93
B10	150	547.55	3.7	1.66	1.81
B11	151	532.55	3.6	1.66	1.88
B12	145	524.55	3.6	1.63	1.80
B13	140	495.55	3.4	1.63	1.84
B14	151	534.21	3.5	1.71	1.93
B15	141	526.55	3.4	1.73	1.86
B16	140	507.86	3.5	1.62	1.79
B17	142	490.55	3.7	1.48	1.72
B18	147	525.55	3.9	1.51	1.69
B19	135	497.55	3.5	1.59	1.73
B20	149	545.55	3.7	1.65	1.80

UG Bulk did not require the stemming due to good adhesion of explosive and detonation of explosive column was complete in less than 0.6 ms, which was good enough to fragment the rock mass.

7 CONCLUSIONS

On the basis of results we can conclude that UG Bulk system is significantly superior to the conventional system in terms of safety, efficiency and performance in underground cavern excavations. In addition to excellent pull achieved by the system and reduction in charging time, lesser over break and better fragmentation results were achieved. In addition, because of involvement of fewer people at the face during charging operations it adds to the safety, which is always a major area of concern in any underground workings. Moreover with UG Bulk system there is reduction in usage of cap sensitive cartridge explosives up to 93% which eliminates magazine issues, pilferage and other problems.

The system can also prove effective in decreasing the drilling cost by reducing the number of holes per blast which can be effectively done because of better coupling of UG Bulk explosives in the blast holes.

Based on the trial results it can be concluded that UG Bulk is a tailor made product designed to solve most of the blasting related problems and has got a very bright future in underground operations especially in underground cavern excavations.

ACKNOWLEDGEMENT

Authors are thankful to the management of Engineers India Limited for providing support and help during study period. They are also grateful to the management of Hindustan Construction Company Limited for support and permission to publish the paper. Authors would also like to acknowledge the support provided by the management of Keltech Energies Limited.

REFERENCES

Mishra, A.K., Rao, K.V.R. & Triapthi, A. 2009. An Innovative tool for Rapid Excavation of Tunnels and Caverns—Underground Bulk Explosives, *Proc.Of International Symposium on Rock Mechanics & Geo-Environment in Mining and Allied Industries,* IT, BHU, Varanasi, 12–14th Feb, 2009: 200–207.

No, S.L., Moon, S.H., JO, Y.C., Lee. S.P. & Yu, J.Y. 2004. The construction of long and large tunnel using bulk explosives. *Journal of Korean Society & Blasting Engineering*, 22(3): 65–70.

No, S.L., Seung-Hwan Noh, Sang-Pil Lee & Jeong-Woo, Seo. 2006. Construction of long and large twin tube tunnel in Korea-Sapaesan tunnel. *Tunnelling and underground space technology*, (21): 393–393.

Onederra, I., Player, J., Wade, P. & Chitombo, G. 1999. Mass Blast Design, Simulation, Optimisation and Monitoring at Big Bell Gold Mine, *Proc. Fragblast 6*, *1999*, SAIMM.

Player, J. 1998. Big Bell Coming Back for Seconds. *Thirds and Fourths, Proc.Of the UG Operators' Conf., 1998*, Townsville.

Downloaded by [Visvesvaraya Technological University (VTU Consortium)] at 21:58 01 March 2016

Performance of Explosives and New Developments – Mohanty & Singh (Eds)
© 2013 Taylor & Francis Group, London, ISBN 978-0-415-62142-7

Modeling buried explosion in geotechnical centrifuge

Xiangqian Liang, Yikan Fan & Yujing Hou
Department of Geotechnical Engineering,
China Institute of Water Resources and Hydropower Research, Beijing, China

Yi Yang
Guizhou Minghao Blasting Supervision Company, Ltd. Guiyang, China

ABSTRACT: An explosive simulation system was developed in LXJ-4–450 geotechnical centrifuge apparatus. Experimental study of the centrifugal explosive test with this system was carried out. The discussion of scaling laws and test method in centrifugal explosion test is also presented. Centrifuge model tests were completed with a variety of ranges of explosive mass, burial depth and centrifuge accelerations in standard sand. Accelerometers were installed in the model and on the centrifuge arm to monitor blast wave effect on the centrifuge apparatus. The result indicated that centrifugal explosion simulation is safe and feasible with this newly developed system, which provides a new test method for research on dynamic events.

1 INTRODUCTION

Based on the principle that inertial forces are equivalent to the Earth's gravity, a small-scale model at elevated gravity can be used to simulate a corresponding prototype in a terrestrial gravity field. For dynamic testing, a small model at *N*g (*N* times g, which is terrestrial gravity) with energy *E,* is similar to a large event in a terrestrial gravity field with energy equal to N^3E (Schmidt & Holsapple, 1980). In other words, a laboratory experiment with 1 gm of explosives can be used to simulate an event of a few tons in the field if sufficiently high g is provided by some special facilities. For example, a rocket sled was used as a linear accelerator in the former Soviet Union. However, the results were vague (Viktorov & Stepenov, 1960, Schmidt & Housen, 1987). Similarly, a propeller-driven C-131B aircraft was used to provide 0.17 g, 0.38 g, and 2.5 g gravitational fields by flying parabolas and tight turns in the Wright-Patterson Air Force Base, Ohio, USA (Johnson *et al.*, 1969). These two instruments were rarely applied because of potential experimental difficulties. In contrast, the Boeing geotechnical centrifuge apparatus can produce up to 600 g acceleration level. Therefore, the geotechnical centrifuge is an effective tool for modeling large explosion events in the field, including nuclear explosions (Schmidt, 1978; Schmidt & Housen, 1987, Schofield, 1998). The centrifuge model tests are advantageous because of their high efficiency, security, repeatability, and low cost. Consequently, the geotechnical centrifuge model test has been widely used in the past 80 years (Craig, 1989, Taylor, 1995), especially in the former Soviet Union, UK and USA. Based on large sets of experimental data, Schmidt & Housen (1987), Holsapple & Schmidt (1979, 1987), Housen (1983, 2003, 2011), and Piekutowski (1980) introduced "point-source" approximations for the impactor and explosive. A coupling parameter, *C*, was proposed to describe the impactor or explosive. The scaling laws, volume of the crater, and cratering time can be derived by this coefficient using dimensional analysis. Chaun-Ping Lin *et al.* (1994) conducted model tests with small charges, various ranges of burial depth, and centrifuge acceleration levels in lunar soil. The results indicated that there was an optimum depth of burial of eight charge diameters for obtaining the maximum apparent crater volumes. Simpson *et al.* (2005) investigated explosive cratering on earth-filled embankment dams using geotechnical centrifuge model tests. The explosives were placed and detonated on the surface of the dam crest. The reference values of explosive charge, which caused the embankment dam to break, were evaluated based on experimental results. Ma *et al.* (2010) carried out centrifuge model tests for responses of shallow-buried circular structures under surface blasting. These tests were completed at a single acceleration level using the Tsinghua University 50 g-t geotechnical centrifuge.

An explosive simulation system was developed in LXJ-4–450 geotechnical centrifuge at the China (Institute of Water Resources and Hydropower

Downloaded by [Visvesvaraya Technological University (VTU Consortium)] at 21:59 01 March 2016

Research (IWHR)). Experimental studies of centrifuge model tests for buried explosion were carried out with this system (Fan *et al.* 2012a, 2012b). This paper presents the scaling laws, test method, and the main results in the centrifuge model test for buried explosion in sand.

2 SIMILARITY ANALYSES OF CENTRIFUGE MODEL TEST FOR EXPLOSION

Schmidt and Holsapple (1980) considered the crater volume V in the centrifuge model test to be dependent on seven parameters.

$$V = F(g, d, \delta, Y, \rho, a, Q) \tag{1}$$

where g = acceleration level; d = depth of burial; δ = initial density of the explosive; Y = target material strength parameter; ρ = initial density of the target material; a = explosive charge radius; and Q = energy per unit mass of the explosive. The charge mass W can be calculated by:

$$W = \frac{4}{3}\pi\delta a^3 \tag{2}$$

The ρ, a, and Q were chosen as the main variables in dimensionless analyses. Using Π theorem (Buckingham, 1914; Bridgman, 1922), Equation (1) can be written as

$$\pi_1 = F(\pi_2, \pi_3, \pi_4, \pi_5) \tag{3}$$

Where

$$\pi_1 = V\rho/W \tag{4}$$

$$\pi_2 = \frac{g}{Q}\left(\frac{W}{\delta}\right)^{1/3} \tag{5}$$

$$\pi_3 = d\left(\frac{\delta}{W}\right)^{1/3} \tag{6}$$

$$\pi_4 = \rho/\delta \tag{7}$$

$$\pi_5 = \frac{Y}{\delta Q} \tag{8}$$

The specific expression of Equation (3) requires a large quantity of experimental data. If the experiments are conducted with the same explosive detonated at the same depth in the same target, π_3, π_4 and π_5 are constant. Schmidt and Holsapple (1980) concluded that the relationship between π_1 and π_2 is a power regression, expressed as:

$$\pi_1\pi_2^{\alpha} = const \tag{9}$$

3 EXPLOSION SIMULATION SYSTEM

The centrifuge modeling tests were conducted as follows. Firstly, the explosives and sensors were installed in the model. Second, the centrifuge apparatus was started. Then, the explosives were detonated at a scheduled acceleration level. A crater was generated in the target, and the sensors recorded the response; finally, after the centrifuge apparatus stopped, the craters were manually measured. The explosion centrifuge system generally includes a mechanical system, control system, and a monitor system.

3.1 *Mechanical system*

The mechanical system consists of the model container, the model, and the explosive.

In order to sustain the blasting load, the model container was made of thick-walled steel. Taking boundary effects into account, the model container was as large as possible for the swing basket of the centrifuge, and was designed as circular shape with internal dimensions of Φ700 mm × 700 mm.

The model was produced by target materials filled in the model container. No. 8 detonator caps were used as explosive sources.

3.2 *Control system*

The control system includes detonator explosive control and record data control. The duration of explosive loading is very short. Therefore, it is significant that the detonating and recording should be synchronized. Special software was used to achieve this purpose.

3.3 *Monitor system*

The monitor system consisted of sensors, a camera, a floodlight, and so on. This system was used to monitor displacement of the model, and record the response where the sensors were installed. The pictures obtained by camera were monitored in the main control room, and recorded as videos. The data recorded by the sensors were also transmitted to the main control room and analyzed

3.4 *Main technical indexes*

The maximum centrifuge acceleration level for dynamic simulation was taken as 200 g while the

Downloaded by [Visvesvaraya Technological University (VTU Consortium)] at 21:59 01 March 2016

maximum explosive mass in explosion simulation was 5 grams. The number of data acquisition channels was 32 and the sample frequency of the data acquisition system was 1000 kHz per channel.

4 TRIFUGE MODELING TEST FOR EXPLOSION

4.1 *Materials and model preparing*

No. 8 detonator caps and standard sand were used as explosive sources and target materials, respectively. The standard sand was produced in Pingtan County, Fujian Province of China. The grain size distribution of the sand ranged from 0.1 mm to 1.0 mm. The water content of the tested sand measured close to 0%. One cap was equal to 1 gram of hexogen explosives (RDX). 1 and 3 caps were used in these tests.

All 10 tests are listed in Table 1. In the first 7 tests, the explosives were buried at a depth of 100 mm. As is shown in Figure 1, $d = 100$ mm. The last 3 explosions occurred at a depth of 150 mm (d = 150 mm). However, the coordinates of the explosive were not changed because 50 mm depth sand was added to the container. Thus, when d = 100 mm, the sand in the container was filled at 450 mm depth. And, when d = 150 mm, the sand in the container was filled to 500 mm depth. These two cases needed 273 kg and 298 kg of sand, respectively. Thus, there were two values of sand density, 1.58 g/cm^3 and 1.46 g/cm^3 in the second column of Table 1. The explosive was detonated at corresponding acceleration level listed in the fifth column of Table 1.

An accelerometer was installed in the sand to monitor the blast waves in the sand when the explosion occurred, as shown in Figure 1. The accelerometer was at the same depth as the explosive of d in Table 1. The other one accelerometer was placed on the centrifuge arm to monitor blast wave effect on centrifuge apparatus.

Table 1. Main features of the tests.

Test no.	Sand density ρ (g/cm^3)	Charge mass W (g)	Depth of burial (mm)	Acceleration level (×g)
GE	1.58	1	100	1
CE-1	1.58	1	100	40
CE-2	1.58	1	100	70
CE-3	1.58	1	100	100
CE-4	1.58	3	100	40
CE-5	1.58	3	100	70
CE-6	1.58	3	100	100
CE-7	1.46	3	150	40
CE-8	1.46	3	150	70
CE-9	1.46	3	150	100

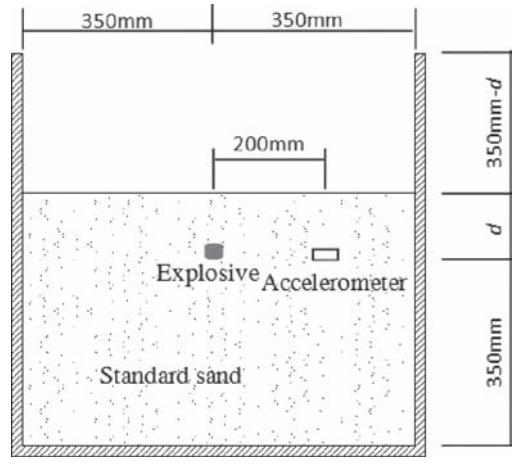

Figure 1. The profile of the test model.

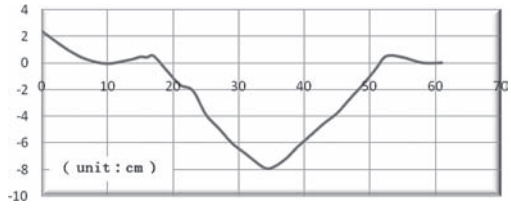

Figure 2. Profile of the apparent crater.

4.2 *Result and discussion*

After the centrifuge apparatus was stopped, the craters were measured with a special vernier caliper. A typical apparent crater profile is shown in Figure 2. The results of all the 10 tests are listed in Table 2.

Figure 3 shows the relationship between π_1 and π_2. There are three lines based on the values of d/a and ρ. Each group is fitted to a straight line in the dual-logarithm coordinate system.

For line No. 1, d/a = 19.6 and ρ = 1.58 gram/cm^3:

$$\pi_1\pi_2^{0.69} = 0.014,\ R^2 = 0.940 \times (\text{Correlation coefficients}) \quad (10)$$

For line No. 2, d/a = 13.6 and ρ = 1.58 gram/cm^3:

$$\pi_1\pi_2^{0.72} = 0.038,\ R^2 = 0.927 \quad (11)$$

Downloaded by [Visvesvaraya Technological University (VTU Consortium)] at 21:59 01 March 2016

Table 2. Crater results of the tests.

Test no.	Volume of crater		
	V (cm^3)	π_1	π_2
GE	2296.50	3622.01	1.39×10^{-8}
CE-1	336.25	530.34	5.55×10^{-7}
CE-2	105.38	165.39	9.71×10^{-7}
CE-3	82.99	130.37	1.39×10^{-6}
CE-4	1903.54	1003.98	8.01×10^{-7}
CE-5	1474.44	776.23	1.40×10^{-6}
CE-6	951.88	503.64	2.00×10^{-6}
CE-7	663.74	322.43	8.01×10^{-7}
CE-8	538.81	262.88	1.40×10^{-6}
CE-9	279.83	137.45	2.00×10^{-6}

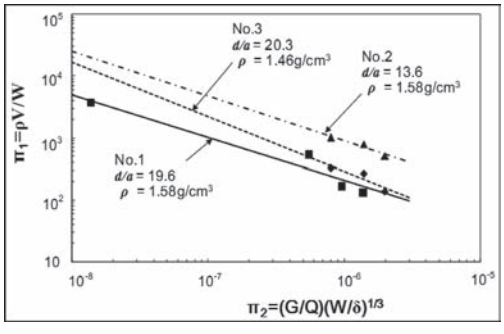

Figure 3. π_1 versus π_2.

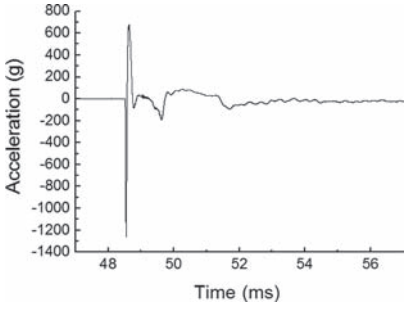

Figure 4. A typical blast wave in sand.

For line No. 3, d/a = 20.3 and ρ = 1.46 gram/cm^3:

$$\pi_1\pi_2^{0.88} = 0.001,\ R^2 = 0.834 \quad (12)$$

Figure 4 shows a typical acceleration wave recorded by accelerometer. This result from test CE-6 showed a pulse with 1250 g peak acceleration. These accelerometers have a large range of ±2000 g, but when positioned near the explosive, the peak acceleration is always out of range. Figure 5 shows the result from the accelerometer on the centrifuge arm in the test CE-6, too. When the centrifuge apparatus was running, the accelerometer recorded the noise made by the tiny vibrations. So, the acceleration in Figure 5 fluctuates around the value of 1.36 g. About a 0.32 g instantaneous increment was recorded because of the blast wave. Compared to the thousands g acceleration in sand, the 0.32 g is very small. In other words, the effect of blast wave on the centrifuge apparatus can be ignored.

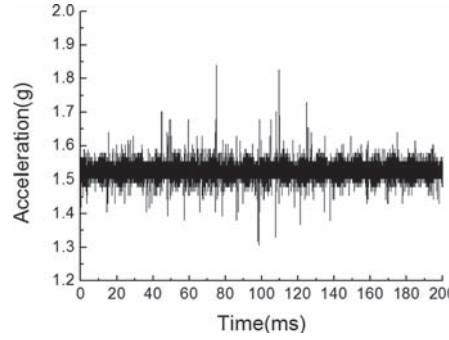

Figure 5. A typical blast wave on centrifuge arm.

5 CONCLUSIONS

This paper presents the explosion simulation system of the IWHR geotechnical centrifuge apparatus, and similarity theory. Ten model tests were conducted to investigate the cratering law and effects of the blast waves on the centrifuge apparatus. The dimensionless parameters, π_1 and π_2, were used to describe the cratering law. Three equations of the relationship between π_1 and π_2 were given by fitting the data of the ten tests. The correlation coefficients R^2 of the three equations are 0.940, 0.927 and 0.834 respectively. Comparing the response between the model and on the centrifuge arm, the negligible effect of the blast wave on centrifuge apparatus can be ignored. These results indicate that the centrifugal explosion simulation is safe and feasible with this newly developed system. Therefore, this test method is advanced for research on dynamic disasters in hydraulics and electric power engineering, transportation engineering and military, national defense engineering, and so on.

REFERENCES

Bridgman, P.W. 1922. Dimensional Analysis. *New Haven: Yale University Press.*

Downloaded by [Visvesvaraya Technological University (VTU Consortium)] at 21:59 01 March 2016

Buckingham, E. 1914. On physically similar systems: Illustrations of the use of dimensional analysis. *Physical Review,* 4(4): 345–376.

Craig, W.H. 1989. Edouard Phillips (1821–1889) and the idea of centrifuge modeling. *Geotechnique*, 39(4): 697–700.

Fan, Y.K., Liang, X.Q., Huang, X., Zhang, X.D. 2012a. Blast wave effect on apparatus and propagation laws in dry sand in geotechnical centrifuge model tests. 2011 Int. Con. on Vibration, Structural Engineering & Measurement, Shanghai, China, October, 2011. Applied Mechanics and Materials, Vols. 105–107, p. 626–629.

Fan, Y.K., Chen, Z.Y., Liang, X.Q., Zhang, X.D. & HUANG, X., 2012b. Geotechnical centrifuge model tests for explosion cratering and propagation laws of blast wave in sand. *Journal of Zhejiang University-SCIENCE A (Applied Physics & Engineering)*, 13(5): 335–343.

Holsapple, K.A., Schmidt, R.M. 1979. A material-strength model for apparent crater volume. Proceedings of the 10th Lunar and Planetary Science Conference, Pergamon, New York, pp. 2757–2777.

Holsapple, K.A., Schmidt, R.M. 1987. Point-source solutions and couplinhg parameters in cratering mechanics. *Journal of Geophysical Research*, 92(B7): 6350–6376.

Housen, K.R., Schmidt, R.M., Holsapple, K.A. 1983. Crater ejecta scaling laws: Fundamental forms based upon dimensional analysis. *Journal of Geophysical Research*, 88(B3): 2485–2499.

Housen, K.R., Holsapple, K.A. 2003. Impact cratering on porous asteroids. *Icarus*, 163(1): 102–119.

Housen, K.R., Holsapple, K.A. 2011. Ejecta from impact craters. *Icarus*, 211(1): 856–875.

Johnson, S.W., Smith, J.A., Franklin, E.G., Moraski, L.K., Teal, D.J. 1969. Gravity and Atmospheric Pressure Effects on Crater Formation in Sand, *Journal of Geophysical Research*, 74(20): 4838–4850.

Lin, C.P., Goodings, D.J., Bernold, L.E. & Dick, R.D. 1994. Modeling studies of effects on lunar soil of chemical explosions. *ASCE Journal of the Geotechnical Engineering*, 120(10): 1684–1703.

Ma, L.Q., Zhang, J.M., Hu, Y. & Zhang, L.M. 2010. Centrifugal model tests for responses of shallow-buried underground structures under surface blasting. *Chinese Journal of Rock Mechanics and Engineering*, 29(S2): 3672–3678 (in Chinese).

Piekutowski, A.J. 1980. Formation of bowl-shaped crater. *Proceedings of the 11th Lunar and Planetary Science Conference, Pergamon, New York*, pp. 2129–2144.

Schmidt, R.M. 1978. Centrifuge Simulation of the JOHNIE Boy 500 Ton Cratering Event. Proc. of the 9th Lunar and Planetary Science Conf. Pergamon, New York-3, pp. 3877–3890.

Schmidt, R.M., Holsapple, K.A. 1980. Theory and experiments on centrifuge cratering. *Journal of Geophysical Research*, 85 (B1): 235–252.

Schmidt, R.M., Housen, K.R. 1987. Some recent advances in the scaling of impact and explosion cratering. *International Journal of Impact Engineering*, 5(1–4): 543–560.

Schofield, A.N., 1998. Geotechnical centrifuge development can correct a soi1 mechanics error. Centrifuge 98, Tokyo, September 1998. Balkema, Rotterdam, pp. 923–929.

Simpson, P.T., Sausville, M.J., Zimmie, T.F. & Abdoun, T.H., 2005. Geotechnical Centrifuge Modeling of Explosive Cratering on Earth Embankments and Dams. *Int. Con. on Energy, Environment and Disasters (INCEED 2005), Charlotte*, North Carolina, USA, July, 2005, pp. 123–124.

Taylor, R.N., 1995. Geotechnical centrifuge technology. Blackie Academic and Professional, London.

Viktorov, V.V., Stepenov, R.D., 1960. Modeling of the action of an explosion with concentrated charge in homogeneous ground. *Inzh. Sb*. 28, 87–96. (English translation, Sandia Report SCL-T-392, Albq., NM, 1969)

Performance of Explosives and New Developments – Mohanty & Singh (Eds)
© 2013 Taylor & Francis Group, London, ISBN 978-0-415-62142-7

Surface coal mines blasting with ANFO in India—a way forward

S.R. Sahay, J.S. Mani, S. Kumar & S. Sengar
Deepak Fertilisers & Petrochemicals Corporation Ltd., Pune, India

ABSTRACT: In India, till now ANFO consumption has been limited to non-coal mining sectors. The paper attempts to address the possible reasons for the neglect so far towards ANFO usage in Indian coal mines in spite of its high potential. An analysis of globally recognized empirical formulas has been done to see the overall economy of ANFO among different strata conditions and charge alternatives in respect of powder factor, blasting costs and mean size fragmentation distribution. Attempt has been made to quantify the contributions of high heave energy of ANFO towards optimum fragmentation from the studies of ANFO performance in similar strata of the non-coal sector. The study has been done for effective blast design and explosive selection for Shovel and Dragline benches of Indian surface coal mines in different geotechnical conditions. The outcomes of results justify the potential of ANFO and its selection by mine operators worldwide.

1 INTRODUCTION

In the year 1954, the first on-site mixed explosives consisting of Ammonium Nitrate (AN) and lamp black was used in Maumee coal company open pit in USA.Since then this class of explosive has made steady progress. Originally it was used in large diameter blast holes only, but today it is also employed in quarrying, construction, mining and elsewhere in blast holes ranging from 311 mm in open pit down to 25 mm diameter size in underground mining. Globally ANFO and blends occupy 70–80% share of open cast Coal mines blasting. This could become possible due to advent of good quality of porous prilled ammonium nitrate (PPAN) worldwide. Though the field performance of ANFO made from PPAN is excellent, we still lack proper tools to quantify the capacity of ANFO.

The blasting performance of explosive depends not only upon the type of explosives but also on the specific partitioned energy requirement of rocks.. Shock Energy and heave energy content of explosive should meet the shock energy and heave energy requirement of the rock. To meet the minimum heave energy requirement of rock sometimes the holes are overcharged using high VOD explosives, generating surplus shock energy which can lead to unwanted effects such as noise, vibrations, etc. In this paper, the applicability of ANFO in different rock types has been discussed. The blast geometry has been calculated to achieve higher powder factor and lower blasting costs targeting same desired fragmentation in hard and medium hard rock with the help of proven empirical equations for Emulsion as well as ANFO explosives. For our analytical study we have considered the standard emulsion explosive composition available for Indian open cast Coal Mines i.e. a standard emulsion doped with 20% PPAN prills. It is pertinent to mention that explosive companies in India have Bulk mixing & delivery (BMD) hardware to handle emulsions with 20% PPAN doping for open cast coal mines and there is no availability of BMD hardware to handle straight ANFO or higher ANFO percentage blends. Fragmentation analysis has been done to see the rock breaking potential with ANFO as well as emulsion with the help of Kuz-Ram fragmentation model. After seeing the outcome of the analysis it was inferred that ANFO Blends are a better choice among bulk explosives for large dia. (>150 mm) in dry and watery holes respectively in Indian surface coal mines.

Advantages of blasting in open cast coal mines with ANFO can go much beyond the tangible benefits and needs the attention of the researchers for measurement/quantification of the parameters such as heave energy, blast hole pressure, volume of gases produced, confinement of gases, partitioned energy requirement of rock for fragmentation etc.

Worldwide, Ammonium nitrate-fuel oil (ANFO) mixture today offers the most cost effective blasting system in every type of rocks and claims dominant share of explosives market in countries like USA, Australia, Canada, South Africa and Brazil.

Downloaded by [Visvesvaraya Technological University (VTU Consortium)] at 22:02 01 March 2016

2 DEVELOPMENT OF ANFO MADE FROM PPAN

The technology of making ANFO started from using AN crystals, and non-absorbent prills for almost a century. It slowly graduated to involvement of leading chemical technology providers such as Stamicarbon (Netherlands), Grande Paroisse (France), Norsk hydro (Sweden) and Uhde (Germany) and others for development of PPAN and other low density AN forms during the last three to four decades.

In India, non-availability of quality PPAN prills in sufficient quantity, non-availability of Bulk ANFO charging hardware, commoditization of explosives procurement process by public Sector units and licensing hurdles restricted ANFO application to non-coal sector. Organized mining sectors such as limestone mining which has strata similar to coal measure overburden strata mostly use ANFO with PPAN for their entire blasting requirement in India.

2.1 *Quality of PPAN and work capacity of ANFO*

The conventional concept of measuring explosive power by using VOD, density, detonation pressure, relative effective energy (REE), available thermo-chemical energy cannot totally quantify the work capability of ANFO made from PPAN. Fragmentation results showed that higher heave energy content of ANFO outperformed the performance parameters for ANFO predicted by the conventional empirical norms. For assessing true work power of explosive, it became necessary to account not only the relative stored energy of a product, but also its rate of energy and gas volume release.

ANFO efficiency increases where prill porosity is higher and consequently loading density of the explosive is lower. This can be argued against generally admitted ideas of measuring explosive power by explosive impedance which is defined as a function of explosive VOD and density, Therefore, the efficiency of industrial explosives related to ANFO (for example "relative weight strength" or "relative bulk strength") is a tool that must be used with caution.

Porous prilled ammonium nitrate (PPAN) is obtained through an original manufacturing process that lends a microcrystalline internal structure to the prills as shown in fig below. In comparison with standard AN, this particular structure gives PPAN an increased total porosity-with pores of smaller diameter, and a lower density. These prills gives a better VOD as compared to the standard prill.

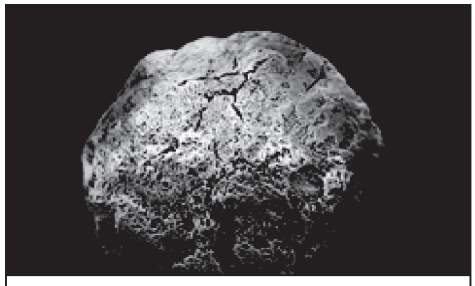

PPAN - Surface features of low density, porous, prill.

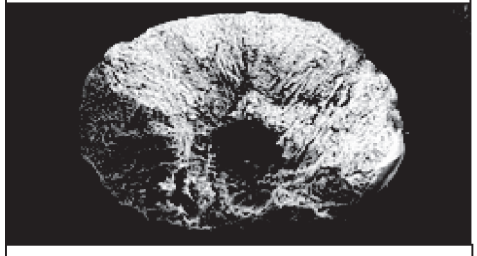

PPAN - cross-section showing internal pores, capillaries, locked-in voids

Tools for measurement of shock energy parameters are somewhat subjective as the measurements depend on the target medium employed.

Similarly, heave energy measured as Bubble Energy in under water test does not give an absolute measure since water does not simulate a rock in terms of resistance or confinement. Similarly other test such as lead block test, crater test has not been able to quantify the heave energy content of the ANFO explosives in absolute terms and the field results have outperformed the predicted results as per the empirical norms.

It is estimated by some that of the explosive energy 20% comes from Shock energy, 60% from heave energy and remaining is dissipated as losses.

This clearly indicates the scope of measurement of absolute heave energy of ANFO made from technically superior grades of PPAN and to develop blast design norms based on their actual work capacity.

3 APPLICABILITY OF DIFFERENT TYPES OF EXPLOSIVE IN DIFFERENT TYPES OF ROCKS

Conventional thinking has stipulated that higher VOD (and subsequently higher pressure) products produce better results in all but weak strata. This

Downloaded by [Visvesvaraya Technological University (VTU Consortium)] at 22:02 01 March 2016

holds true for massive rock formations with minimal and irregular joint and micro-cracking (such as massive granites). In rock types that display jointing and inherent cracking (such as that found in the majority of coal major strata), the requirement for high initial pressures is minimal. As such, a more optimal blast can be provided by products that display significant partitioning towards heave (gas or bubble) energy.

3.1 *Production blasting in various rocks*

The properties of the rock mass have the most important interrelation with blast design variables. Recommended selection criteria of explosives for the four broader classification based on type of rocks can be as follows:

i. Resistant massive rocks—Explosives with high density and high detonation velocity: Slurries, Emulsion.
ii. Highly fissured rocks—Explosives with high gas energy, such as ANFO, HANFO.
iii. Rocks that form blocks—Explosives with balanced Shock & Gas energy, such as AL—ANFO, HANFO.
iv. Porous rocks—Explosives with high gas energy, such as ANFO.

Efficient and successful performance of an explosive in a rock mass requires that its properties be compatible with those of the subject rock mass. An empirical correlation of the preferred explosive type for a range of rock mass properties (Brady & Brown,1993) indicates that ANFO(higher heave energy) is suitable for use in a wide range of rock mass conditions and the application of high energy explosives is justified only in strongest and more massive rock formations (fig 1). Since majority of coal mining overburden (UCS, 20–50 MPa) display jointing and inherent cracks,, correct explosives energy for the rock can be provided by products that display significant partitioning towards heave (gas or bubble) energy.

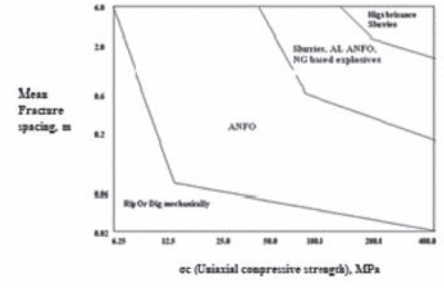

Figure 1. An empirical integration of explosive type and rock mass properties.

3.2 *In deep hole blasting*

In deep blast holes (say >10 m) chemically gassed explosive, settles down with its high weight due to higher hydrostatic pressure & longer sleeping time. This may compress & squeeze the gas-bubbles, particularly in sleeping holes. As the depth increases the size of the air bubbles reduces, also increasing the density of the explosive. If increased beyond certain critical density, explosive loses its sensitivity & reduces to dead-press condition. Due to non-availability of air bubble sensitization this causes poor or no detonation on initiation, mainly at the toe, & might result into partial or complete blast failure with serious toe problems.

However this can be prevented, if hole is charged with ANFO, HANFO or doped (20% AN) Emulsion explosive with porous prills (with adequate voids).This also helps in improved sleeping time for the emulsions in deep holes.

3.3 *In watery holes*

ANFO as such has its inherent limitation of water resistance. However ANFO can be blended with emulsion (30% to 70%) depending on the amount of water present in a hole and the required energy density of the explosives column in a given strata condition.This practice is already proven overseas to provide necessary water resistance to ANFO.

3.4 *Blasting for energy optimisation*

ANFO added to emulsions can increase the energy by about 5% for every 10% increment in AN added. ANFO also has the added advantage of producing more gaseous detonation products, and therefore, an increase in gas volume is also realized. An increase in gas volume usually leads to better heave and throw of the rock being blasted.

In a 70:30 ANFO: Emulsion blend, popularly known as Heavy ANFO, the macropores between particles are partially or completely filled with a high density non—explosives emulsion matrix. This increase the loading density and relative effective energy (REE) in addition to rendering an increased level of water resistance to the product. The higher REE enables expanded blast hole patterns and saves drilling cost if the rock mass permits.

ANFO-Emulsion blends will have to be augured when emulsion content goes below 70% or so; otherwise it can be pumped into the blast holes. ANFO emulsion blend with a ratio of 55:45 offers the best energy maximization package which helps in lowering of drilling cost by expansion in blast pattern.

Downloaded by [Visvesvaraya Technological University (VTU Consortium)] at 22:02 01 March 2016

3.5 *Cast (throw) blasting*

Cast blasting method is used for maximum overburden rock displacement and throw in surface coal mining and has been experimented extensively in open pits in many countries like, USA, Russia, South Africa, Australia etc., It has been found that cost can be reduced considerably in comparison with conventional method of workings. The above countries are using ANFO (in dry holes) and HANFO (wet holes) for cast blasting because of its higher heave energy (higher throw velocity) and lower overall costs.

4 TECHNO-COMMERCIAL ASSESSMENT

Techno-commercial assessment of different charge alternatives has been done to see the blast performances in respect of fragmentation, powder factor and total blasting costs.

4.1 *Prediction of post blast fragmentation size distribution*

There are different types of tools for analyzing the rock fragmentation, like sieving, digital image analysis, monitoring excavator loading cycle time and bucket fill factor and quantifying with the help of empirical models (Kuz-Ram). We have selected the empirical model i.e. Kuz-Ram model for our analysis as the input data consists of the relevant blast design parameters.

A commonly used parameter to quantify fragmentation is to use the mean fragmentation size, often designated by K_{50}. K_{50} is a parameter which represents the screen size through which 50% of the loosened rock would pass if screened.

Three Key equations are the backbone of this model:

i. Kuznetsov's equation,
ii. Rosin-Rammler equation and
iii. Uniformity Index

The formula was originally created by Kuznetsov's and further modified by Cunningham:

$$Xm = A * \left(\frac{V}{Q}\right)^{0.8} * Q^{0.167} * \left(\frac{115}{E}\right)^{0.6333} \quad (1)$$

Where A = rock factor, 7 for medium hard rocks, 10 for hard and highly fissured rock and 13 for hard and weakly fissured rocks; Xm(K_{50}) = mean fragmentation size (cm); V = rock volume per hole; Q = mass of explosives per hole; and E = relative weight strength of explosive.

Rosin—Rammler equation:

$$R = e^{-\left(\frac{X}{Xc}\right)^{N}} \quad (2)$$

Where R = proportion of material retained on screen; X = screen size; and N = Uniformity index.

$$Xc = Xm/(0.693)^{1/N} \quad \text{(Maynard, 1990)} \quad (3)$$

The value of N is dependent on drilling pattern, hole deviation, hole depth, charge length, etc., commonly varies from 0.8 to 2.2 (Cunningham, 1983). Higher value indicates uniform sizing, while a low value indicates higher proportions of both fines and coarse fragments.

Uniformity Index (N):

$$N = \left[2.2 - 14\left(\frac{B}{D}\right)\right]\left[0.5\left(1 + \frac{S}{B}\right)\right]^{0.5} \times \left(1 - \frac{W}{B}\right)\left[\frac{L}{H}\right] P \quad (4)$$

Where B = Burden (m); D = Diameter of explosive (mm); W = standard deviation of drilling error (m); L = charge column length; H = bench height (m); P = Blast pattern factor (i.e. 1.0 for square & 1.1 for staggered).

To achieve desired fragmentation, the number of holes required to be drilled depends on the area of influence of a charge, i.e., the energy factor of an explosive. Optimum energy factor of the selected explosives(s) and blast design parameters makes the decision variables in the program formulation. To see the overall impact of explosives selection on drilling & blasting and fragmentation, studies of optimum blast design was required for different types of benches and with different types of explosives.

Burden and spacing can be calculated by using Konya and Walter (1990) equation (5) for shovel and dragline faces. Blast geometry has been improved on the basis of energy balance by using equation (6).

$$B = 0.038D\left(\frac{\sigma e}{\rho r}\right)^{0.33} \quad (5)$$

$$Be = 0.044F\left[Ch * Eaws * \frac{Vvod}{\sigma r * Vp}\right]^{0.5} \quad (6)$$

$$S - (1.1 - 1.2) * B \quad (7)$$

Downloaded by [Visvesvaraya Technological University (VTU Consortium)] at 22:02 01 March 2016

Where D = Diameter of Explosives (mm); σe = Density of rock (g/cc); σr = Density of rock (g/cc); Ch = Explosives charge (Kg/m); Eaws = Absolute weight strength (Kcal/Kg); Vvod = Velocity of detonation of explosives (m/s); Vp = Primary wave velocity in rock (m/s); S = Spacing (m); F = correction factor for drilling (for staggered pattern F = 0.8–0.9 & for rectangle pattern F = 0.9–1.0).

$$\text{Stemming}(T) = (0.7 \text{ to } 0.9) * B \tag{8}$$

4.2 *Explosives and rock properties*

To carry out blast design in an optimum manner it is essential to fully understand the explosives & rock properties considered for the study. The details are given in Tables 1 & 2.

From the velocity curve of ANFO (Fig. 2), the value of ANFO VOD is taken as 4700 m/s and 4500 m/s for hole diameter of 311 mm and 259 mm respectively.

4.3 *Blast geometry*

Firstly the blast parameters were determined with the help of equation nos. (6), (7) & (8) and data from Tables 1 & 2. The K_{50} values were generated from the design parameters for both explosives. Thereafter nos. of simulations were done to achieve the closest values of K_{50} for different types of explosives in medium hard coal bearing strata for reverse generation of optimized blast parameters for common fragmentation index as shown in Table 4.

The values of K_{50} have been targeted to achieve the optimum fragmentation size as indicated by Jimeno et al. 1995 (Table 5).

Jimeno et al. (1995) recommended that the maximum fragmentation size for the crusher should be 80% of the input size of the crusher, fragment size for loading a bucket should be 0.7 times the bucket size and optimum fragmentation size for a shovel should be 0.125–0.166 times the shovel bucket size. Max. & optimum values for some bucket sizes have been given in Table 2. Majority of the Indian surface coal mines have been using big size of Heavy Earth Mover Machines (HEMM), such as 10/70, 20/70 and 24/96 draglines and 5, 8, 10 m^3 and now 42 m^3 bucket capacity shovels of different boom height. Generally for more than 10 meter bench height, 10 m^3 bucket size shovel are operated and for more than 30 meters dragline bench, 24 m^3

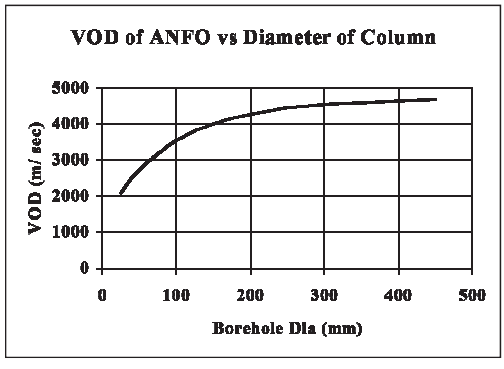

Figure 2. Borehole Velocity of ANFO.

Table 1. Properties of Explosives.

Explosive	Density (g/cc)	Chemical Energy (mJ/Kg)	AWS (Kcal/Kg)	RWS	RBS (%)	VOD (m/sec)
Emulsion (20% AN Doped)	1.3	2.95	702	79	125	5091
ANFO	0.82	3.75	893	100	100	4451

Source: (ISEE Blasters' Handbook, 17th Edition, Table 9.1, page 101).

Table 2. Properties of coal bearing rock.

Rock type	Bench	Density	σc (Kg/cm²)	σt (Kg/cm²)	Vp (m/s)
Fine grain Sandstone	Dragline	2.3–2.4	786	164	2380–2476
Medium grain Sandstone	Dragline	2.25–2.35	495	103	2200–2350
Fine grain Sandstone	Shovel	2.35–2.40	750	166	2450–2630
Medium Grain Sandstone	Shovel	2.25–2.30	421	49	2130–2240

(Nabiullah, Pingua and jagdish, 2010).

Downloaded by [Visvesvaraya Technological University (VTU Consortium)] at 22:02 01 March 2016

Table 3. Optimum & Maximum fragmentation size with respect to Bucket size.

Bucket Size, m^3	6	8	10	15	20	24
Maximum Fragment size, m	1.3	1.4	1.5	1.7	1.9	2.0
Optimum Fragmentation size, m	0.3	0.3	0.4	0.4	0.5	0.5

Table 4. Blast geometry for medium Hard Rocks.

Blast Geometry				
Explosives	Emulsion		ANFO	
Parameter	D/L	S/D	D/L	S/D
Diameter (mm)	311	259	311	259
Hole depth (m)	40	15	40	15
Bench Height (m)	40	14	40	14
Burden (m)	9.8	7.9	9.0	7.5
Spacing (m)	11.7	9.5	11.0	8.8
Volume of rock (m^3)	4574	1056	3960	924
Stemming (m)	6	5.5	6.0	6
Deck (m)	3	0.00	3.0	0
Explosive (Kg)	2962	612	1930	410
P.F(cum/Kg)	1.54	1.73	2.05	2.25

D/L—Dragline Bench & S/D-Shovel Dumper bench.

Table 5. Value of K_{50} & N for (medium hard rock).

Explosives	Emulsion		ANFO	
A	7	7	7	7
K_{50} (mean size fragmentation), in cm	48	40	48	40
N (Uniformity Index)	1.44	1.25	1.47	1.27

bucket size dragline is operated. Herein for determination of blast geometry and prediction of fragmentation size, the optimum fragmentation size has been taken as 40 & 50 cm for 10 m^3 shovel and 24 m^3 dragline respectively.

The commonly used drill diameters are 160 mm and 259 mm for Shovel (for 5 m to 25 bench height) and 311 mm (for >25 m bench height) for Dragline benches respectively in Indian surface coal mines.

The blast parameters have been determined for medium hard rocks and charge alternatives with respect to targeted values of K_{50} (kept same for both explosive**).** Now a days, the surface coal mines are operating with large bucket size excavators (>10 cum). A balanced design has been established to see the economy of blasting costs with Bulk Emulsion and Bulk ANFO.

4.4 *Fragmentation results (K_{50} & Uniformity index (N))*

It is known that explosives energy is not the only factor affecting fragmentation. Rock mass structure, physic-mechanical properties and blast geometry also have influence on fragmentation. The values of K_{50} have been kept same for all charge alternatives, close to optimum fragmentation size given in Table 3 (for 10 to 24 cum bucket size).

From Figures 3 & 4, it is very clear that the fragmentation distribution in blasted muck pile in both

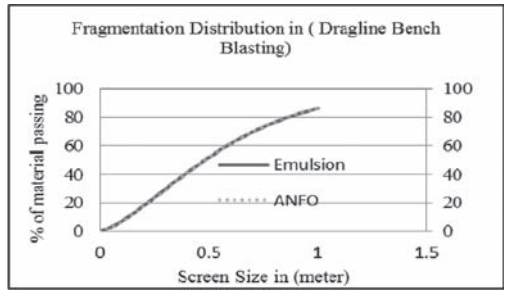

Figure 3. Fragmentation distribution showing nearly common values for Emulsion in ANFO in Dragline bench.

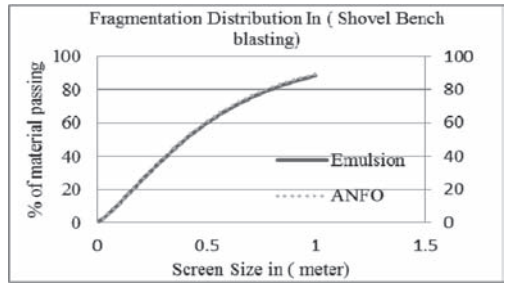

Figure 4. Fragmentation distribution showing nearly common values for Emulsion and ANFO in shovel bench.

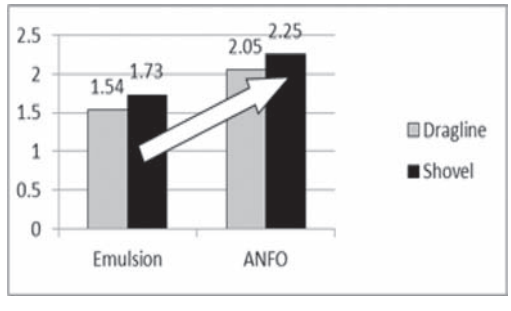

Figure 5. Powder factor in medium hard strata for ANFO and Emulsion.

types of benches are same, therefore it becomes an identical condition for comparative analysis for different types of charge alternatives.

For nearly same fragmentation index, there is a major improvement in powder factor by using ANFO in both Dragline and Shovel bench as shown in Figure 5.

5 COST ANALYSIS

From economical point of view, the best explosives is not always the least cost explosives but rather the one that achieves the lower blasting costs along with better rock fragmentation. On the basis of above blast geometries, blasting costs has been calculated and given in Tables 6 & 7 and Figure 6.

It is seen from the above results that ANFO saves approx. 15% in blasting costs and a sharp improvement (approx. 30%) in powder factor over bulk emulsion explosives while maintaining the same fragmentation index.

In the above analysis Absolute weight strength of explosives, VOD of explosives and density of explosives has been used as the major energy contributing factors for the explosives. The absolute heave energy of ANFO has not contributed to the predicted powder factor based on above norms the empirical norms does not consider the impact of the additional volume of gases and other factors generated by ANFO. The higher content of oxidizer (94%) as compared to nearly 70–75% in Bulk

Table 6. Unit costs of explosive & drilling.

Explosives cost *			Drilling Cost**		
Explosives	ANFO	Emulsion	Diameter (mm)	259	311
Cost (Rs./Kg)	28	28	Cost (Rs./m)	321	695

*Calculated on the basis of current price of Ammonium nitrate in India. For emulsion price good quality emulsion doped with 20% PPAN has been considered. **From a study conducted at Nigahi project, NCL of Coal India Limited in 2008, drilling cost was has been converted into present value).

Table 7. Total costs of blasting in (Rs. per cum).

Explosives	Emulsion		ANFO	
Bench	D/L	S/D	D/L	S/D
Drilling cost (Rs/m^3)	6.08	4.56	7.02	5.21
Explosive cost (Rs/m^3)	18.13	16.23	13.65	12.43
Total blasting cost (Rs/m^3)	**24.21**	20.79	20.67	17.64

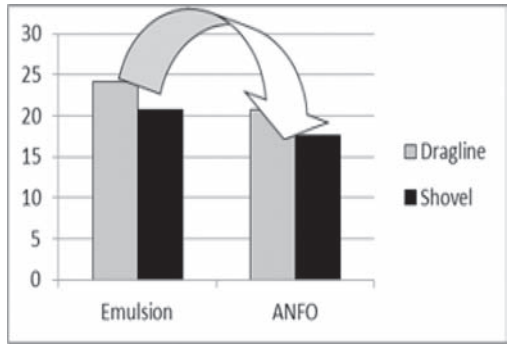

Figure 6. Total blasting costs for different charge alternatives.

Emulsion produces nearly 30% more gases for better fragmentation and displacement of rock.

Some of the other major benefits of ANFO which needs to be additionally evaluated can be summarized as:

- Due to lower loading density, charge per hole will be lower which will result in lower blast induced vibration i.e. lower PPV.
- Reduction of toe in coal mining—being able to drill every blast hole to coal or reduce coal stand-off to ensure all toe material is blasted.
- Protection of coal—comparatively lower shock energy than others explosives prevents the product from damaging the coal roof.
- ANFO offers a very consistent and high quality explosive with negligible chances of a misfire or poor blast.
- Better fragmentation due to higher heave energy helps in improving the loading cost and transportation cost and also helps the mine in reducing the mining cycle time significantly.

6 CONCLUSIONS

ANFO usage in Indian coal mines has been less common so far in spite of its high potential, due to non-availability of right quality porous prilled ammonium nitrate (PPAN) and its delivery units, but now new indigenous plants have come up with high production capacity based on proven technologies. In the coming days all aspects of ANFO performance, safety, convenience to handle and use and benefit to the environment need to be thoroughly evaluated for application in surface coal mine blasting. Surface Coal Mines in India can effect significant saving in explosives, increase the production rate and substantially save on the total cost of operations through better fragmentation by using ANFO.

Downloaded by [Visvesvaraya Technological University (VTU Consortium)] at 22:02 01 March 2016

Mixing AN Prills with emulsions to make ANFO-emulsion blends can help improve water resistance and open the scope for optimized distribution of explosive energies across the explosive column. Surface coal mines in India can have mobile manufacturing units (MMUs) with capabilities to deliver Straight ANFO, Heavy ANFO, Doped Emulsion and Straight Emulsion from a single truck in line with the global practice.

ACKNOWLEDGEMENT

The authors are grateful to DFPCL for allowing this paper to be presented at the International Symposium "Fragblast'10" held in India in Nov'12. The views expressed in this paper are of the authors and not necessarily of DFPCL.

REFERENCES

Adhikari, G.R. & A.K. Ghose. 1999. Various approaches to blast design for surface mines, *Journal of Mines, Metal & Fuels,* January-February, pp. 24–30.

Cunnigham, C.V.B. 1987. Fragmentation estimations and the Kuz-Ram Model-Four years on, in *2nd International Symposium on Rock Fragmentation by Blasting,* Keystone, Colorado, pp. 475–487.

JKMRC. 1998. Optimisation of fragmentation for downstream processing, *AMIRA Final Report*, p. 483.

Konya, C.J. 1995. Blast Design, *Published by Intercontinental Development Corporation*, Ohio 44064, USA.

Kuznetsov, V.M. 1973. The mean diameter of fragments formed by blasting rock, *Soviet Mining Science,* Vol. 2, pp. 39–43.

Manon, J.J. 1997. How to select an explosives or blasting agent for a specific job. *The Indian Mining & Engineering Journal,* May, Bhubneshwar.

Nabiullah, Pingua, B.M.P. & Jagdish. 2010. Study on optimum powder factor and quality of explosives in surface mines, *The Indian Mining & Engineering Journal,* April, Bhubneshwar, pp. 22–30.

Nabiullah, Pingua, B.M.P. & Jagdish. 2010. Study on cost effective bulk emulsion and their performance in different geo-mining condition, *Proceedings of 3rd national seminar on rock excavation techniques*, January 08–09, Nagpur.

Pradhan, G.K. 2002. Changing trends in blasting in open cast mines, *The Indian Mining & Engineering Journal,* Nov.-Dec., Bhubneshwar, pp. 23–28.

Smith, M.L. 1990. A coupled expert system approach to blast design, *Mine planning and equipment selection, Singhal & Varva (eds.),* Balkema, Rotterdam, pp. 481–488.

Wright, K.W. 1986. Effective blast design selecting the right explosive for the right job. *World Mining equipment*, Vol. 10, No. 3, pp. 28–33.

Downloaded by [Visvesvaraya Technological University (VTU Consortium)] at 22:02 01 March 2016

Performance of Explosives and New Developments – Mohanty & Singh (Eds)
© 2013 Taylor & Francis Group, London, ISBN 978-0-415-62142-7

Causes of explosion in a bulk emulsion explosive plant

B.M.P. Pingua & Nabiullah
Central Institute of Mining and Fuel Research, Dhanbad, India

ABSTRACT: Bulk emulsion explosives are used in major coal producing countries like China, Australia, Indonesia, South Africa, India and USA. It is used in India as straight/doped /ANFO. It is understood that bulk emulsion matrix is safe in production, transportation and uses. It is safe as compared to packaged explosive because most of explosive incident occurred in package plants. In recent years, a major explosion occurred in bulk explosive plant at Waidhan, Singrauli District of India, in which 22 persons were killed on spot and three explosive plants were completely demolished on 5th July 2009. A detail study was done to find out the causes on the basis of ground simulation test including thermal test of emulsion matrix, detonating fuse, detonators and hot projectile impact on material. It was found that explosion was occurred in pumping emulsion matrix and hot flying fragment hit the explosive van parked in other explosive plant which enhances the explosion and damage.

1 INTRODUCTION

There are twelve explosive manufacturing units at Singrauli area to supply the Site Mixed Emulsions (SME) to Northern Coalfields Limited. Out of them eight bulk plants are situated in Udyogdeep Industrial Area and distance between any two structures is close to each other.

An explosion was occurred on July 5, 2009 (Sunday) in between 6.40 pm to 6.50 pm in emulsion matrix plant at one of the Bulk plant and Explosive van parked at another bulk plant premises containing detonating fuses. Most of the Bulk Matrix Delivery (BMD) vehicles were damaged due to explosion and their structures were lost. In which about 20 workers were killed and 30 to 40 workers were injured. The Figures 1 & 2 show the damage of Bulk plant showing boiler & pump truck and Industrial Area in Waidhan respectively.

The intensity of the blast was so high that it damaged the other explosive plants in Udyogdeep Industrial Area, Waidhan to varying extent. Two sounds of explosion were heard up to two kilometers distance. This indicates that there were two explosions in the Udyogdeep Industrial Area with a loud bang. The explosion overpressure was experienced by the people up to a distance of 15 to 20 km.

Figure 1. Damaged pump truck.

Figure 2. Damage industrial areas.

1.1 *Description of SME Plants, BP-1 and BP-2*

The explosion occurred in two Site Mixed Emulsion plants, say BP-1 and BP–2. The bulk explosive plants have facility to prepare emulsion matrix by continuous process with ammonium nitrate doping facilities. The BMD parking area and other vehicles of BP-1 plant boundary was close to BP-2 plant. About 50 MT of emulsion matrix in silo and three BMD vehicles were parked in the parking area of BP-1 plant premises along with one explosive van containing about 1, 20,000 m detonating fuse. Bulk

Downloaded by [Visvesvaraya Technological University (VTU Consortium)] at 22:02 01 March 2016

matrix delivery parking area and other vehicles of BP-1 plant boundary were close to BP-2 plant and locations of plants are shown in Figure 3.

The location of BP-2 silo was about 22 m away from the exploded van. About 20 MT emulsion matrix was in Silo. Three BMD vehicles of BP-2 plant were parked in the parking area. Plant production was going on and transfer of emulsion matrix/doped matrix was in one of the BMD vehicle and other vehicles were parked in the parking area. The distance of structures in BP-2 plant is shown in Figure 3.

Hans Perlid (1996) described the safety of emulsion explosives. Dry pumping of emulsion matrix

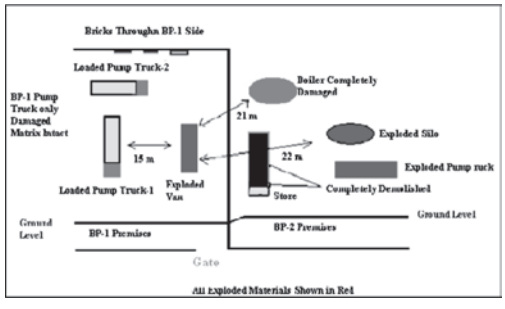

Figure 3. A layout of reconstruction of the scene prior to the incident.

may increase the temperature in the product and lead to explosion.

Pingua and et al. (2008) measured the primary and secondary detonation flame of 10 g/m, 5.5 g/m and 3.5 g/m detonating fuse (DF) by using high speed video technique. They have also measured the flame speed and duration of DF flame. Nabiullah and et al [3] (1989) studied the thermal behavior of DF at elevated temperatures and reported that detonating fuse is safe to use in fiery zone.

Richard J. Mainiero and James H. Rowland III (2009) studied the causes of accident occurred due to collision of ammonium nitrate train wagon and a wagon containing fuel oil. He suggested that flashpoint of fuel was fired by overheating, impact or by other human error.

Dott. Ing Roberto Folchi (1996) studied the explosion and fire hazard assessment for explosives, ammunition and fertilizing agents' facilities after EU directive 96/82/EC "SEVESO II" and reported the impacting factors and damage extension for severity level. Each impacting factor will produce decreasing damages at increasing distance. The iso-damage areas and threshold values for each impacting factor are given for predefined damage severity level shown in Table 1.

This impacting factor is related to the mass explosion of explosive materials. For damage assessments, the relevant parameters are positive

Table 1. Nature of damage due to explosion.

	Damage area				
	1	2	3	4	5
Nature of Damage effect	Highly lethal	Lethal boundary	Irreversible injury	Reversible injury	Domino effect
Peak air overpressure and secondary fragmentation (people in the structures) distance were the positive peak pressure reaches;	55 kpa	24 kpa	16 kpa	8 kpa	2.75 kpa
Primary fragmentations (in open spaces) throw distance of…		1[1]		1[2]	
Ground vibrations (people in non reinforced structures) distances were the peak particle velocity reaches…	300 mm	250 mm	200 mm	100 mm	
Dangerous gas release (absorbed doses) distance were the gas concentration reaches. (in ppm)	LC50 (30 min, hmn) $NO_x = 315$ $CO = 5647$ $CO_2 = 50$ K	-	IDLH $NO_x = 100$ $CO = 1200$ $CO_2 = 40$ K	–	–

[1] Dangerous fragment in an area of 56 m^2

[2] Fragment (maximum fragments throw)

Downloaded by [Visvesvaraya Technological University (VTU Consortium)] at 22:02 01 March 2016

Table 2. Scale distance and peak air pressure.

Scale distance ($D/kg^{1/3}$)	Peak air overpressure (kpa)
1.58	689.5
1.78	551.6
1.98	344.75
2.78	241.3
4.76	40.26
7.14	27.58
7.93	20.68
11.90	1.80

Table 3. Air over pressure at different distance and quantity of explosives.

Distances (m)	Predicted AOP(dB) at different quantity of explosives			
	1000 kg	1200 kg	1400 kg	2000 kg
100	172	173	173	175
500	152	153	154	155
1000	144	145	145	147
1500	139	140	140	142
2000	135	136	137	138
5000	124	125	126	127
10000	116	117	117	119
20000	107	108	109	110

peak overpressure and associated impulse or also energy and duration of the impulsive load on the structure. Peak overpressure and associated impulse at various distances can be calculated, Table 2.

Adhikari and et al. (2007) developed an equation for prediction of air over pressure (dB) due to detonation of explosives. The effective distances with quantity of explosives are shown in Table 3.

The main objective of the study was to find out the causes of incident occurred in bulk emulsion plants. It was found that emulsion matrix can be manufactured by safe process but dry heating in pumping unit may lead the thermal explosion, at the same time explosive van parked in the area causes the major destruction.

2 EXPERIMENTATION

2.1 *Flash point of organic fuels*

The flash point of different fuels and fuel mixtures were measured by using Abel flash point apparatus (closed cup method) and result are given in Table 4.

Table 4. Flash point of organic fuels.

Fuels	% weight	Flash point (°C)
Diesel oil	100	69.8
Furnace oil	100	92.4
Sorbitane monooleate	100	108.2
Diesel + Furnace + SMO	50:35:15	89.2
Kerosene oil	100	48
K-oil+ SMO+FO + Diesel oil	40:10:30:20	67*
K-oil + SMO + FO + Diesel oil + Carbon	20:10:30:20: 20	81*

*Depends upon the% of K-oil in mixture.

Table 5. Physical properties of emulsion matrix.

Properties	Results
Color	Blackish
Density (g/cm^3)	1.40 ± 0.02
Viscosity (cps)	80000 ± 500

Table 6. Sensitivity of AN prills doped emulsion.

AN doped%	Density (gm/cc)	Result
10	1.36	Failed
20	1.34	Failed
30	1.32	Failed
50	1.28	Detonation VOD: 2800–3000 m/s

2.2 *Physical properties of emulsion matrix*

Emulsion matrix was collected from bulk emulsion plant. The physical properties such as viscosity and density were precisely recorded. The results are given in Table 5.

2.3 *Sensitivity of straight emulsion matrix*

The matrix was packed in 83 & 125 mm PVC tubes and fired with 100 g cast booster (PETN + TNT). No detonation results were observed. Matrix was doped with AN prills (0.88 g/cm^3) and placed in 83 mm diameter pipe and fired with 100 g cast booster. The results are given in Table 6.

2.4 *Effect of temperature on detonating fuse in isothermal conditions*

Detonating fuse (DF) contains Penta Erythritol Tetra-Nitrate (PETN) and when PETN is not

Downloaded by [Visvesvaraya Technological University (VTU Consortium)] at 22:02 01 March 2016

encased in the protective wrapping/coating, is extremely sensitive to heat and impact. Because of protective quality of the wrapping and small amount of PETN (9–10 g/m) inside; detonating fuse is remarkably safe against detonation by impact, heat and friction.

Acetylene flame was applied on 10 g/m detonating fuse. The heating of detonating fuse is shown in Figures 4 and 5. Acetylene flame temperature was in between 800 and 1000°C. The time of application on detonating fuse was 2 to 3 minutes. The burning of detonating fuse is shown in Figure 5 and results are given in Table 7.

Figure 4. Heating of detonating fuses.

Figure 5. Burning of detonating fuse.

Table 7. Effect of temperature on detonating fuse in isothermal condition.

Time of application (min)	Results
1	Local burning, no explosion
2	Local burning, no explosion
3	Local burning, no explosion
4	Local burning, no explosion, no detonation
5	Local burning, no explosion, no detonation

2.5 *Effect of temperature on hot emulsion matrix (Isothermal Condition)*

0.02–0.03 kg of emulsion matrix (color: blackish, density: 1.39 ± 0.01 g/cm^3) was placed on acetylene flame and high temperature was applied on matrix. The temperature of burning matrix was measured by IR pyrometer as in Figure 6 and burning of matrix is shown in Figure 7. The temperature effects on emulsion matrix are given in Table 8.

Figure 6. Measurement of temp. by IR Pyrometer.

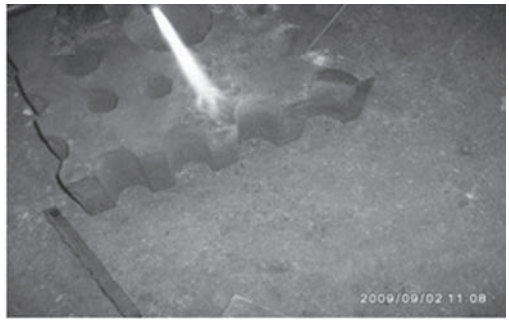

Figure 7. Burning of emulsion matrix.

Table 8. Effect of temperature on emulsion matrix in isothermal condition.

Time of application (min.)	Results
1	Local burning, no explosion/detonation
2	Local burning, no explosion/detonation
3	Local burning, no explosion
4	Local burning, no explosion, no detonation, when matrix taken out, it was quenched
5	Local burning, no explosion, no detonation, when matrix taken out, it was quenched

Downloaded by [Visvesvaraya Technological University (VTU Consortium)] at 22:02 01 March 2016

2.6 *Effect of temperature on detonating fuses (adiabatic condition)*

A coil of 0.10 kg detonating fuses was placed in steel tube and it was heated over 1500 watt heater. It was observed that local explosion occurred and detonation was not continued outside the surface of DF.

2.7 *Effect of temperature on emulsion matrix and AN prill doped matrix (adiabatic condition)*

Emulsion matrix was heated in closed steel pipe. Temperature sensor and heating arrangement were done as shown in Figure 8. The matrix containing pipe was heated electrically. The heating of matrix causes thermal explosion and cap of steel pipe thrown out within 3–4 minutes due to generation of high shock/gaseous pressure and explosion. Blackish/whitish fumes and explosion flame were observed and run away temperature was recorded by using temperature indicator. The test results are given in Table 9.

2.8 *Effect of detonation flame on detonating fuse in isothermal condition*

Cap sensitive emulsion composition was fired in Hard PVC pipe/steel cannon. 0.15 to 0.60 kg of detonating fuse in the form of coil was hung at varying distances from 0.3 to 1.0 m from the mouth of cannon. The cap sensitive explosive was fired and its effect on detonated fuse was recorded. The Z value for different distances was calculated for go or no go tests. The test results are shown in Table 10.

$$Z = D/W^{1/3}$$

where D = distance, m; and W = weight of explosive fired, kg.

Figure 8. Experimental set up for heating of matrix in adiabatic condition.

Table 9. Effect of temperature on emulsion matrix in adiabatic condition (Confined).

Composition	Temperature (°C)	Results
Emulsion matrix	160–170	Black fumes, flame, explosion
Emulsion matrix	170–180	Black fumes, flame, explosion
Emulsion matrix	175–185	Explosion with flame
Matrix with 20% AN prill	160–180	Explosion with flame
Matrix with 30% AN prill	160–180	Explosion with flame

Table 10. Effect of detonation flame on detonating fuse.

Explosive weight as donor (kg)	D (m)	Weight of detonating fuse as acceptor, DF (kg)	Z, (D/kg$^{1/3}$)	Results
0.292	0.60	0.15	0.904	Burnt
0.292	0.60	0.15	0.904	Partial burning
0.292	0.30	0.15	0.452	Burnt with flame
0.292	0.30	0.15	0.452	Burnt with flame
0.375	1.00	0.30	1.38	Failed
0.375	0.80	0.30	1.11	Partial detonation
0.375	0.60	0.30	0.832	Detonation
0.375	0.40	0.30	0.554	Detonation
0.375	0.30	0.30	0.410	Detonation

2.9 *Effect of hot metal projectiles on detonating fuse (isothermal conditions)*

Cap sensitive emulsion composition of 0.292–0.30 kg was fired in hard PVC pipe/steel cannon. About 0.10 to 0.15 kg of nut and bolts were placed inside the cannon/PVC bore. The distance of explosive and nut & bolts was 0.05 to 0.10 m from the mouth of the cannon. The emulsion explosive was fired with electric detonator. Its effect on detonating fuse was recorded.

The Z value for different distances was calculated for go or no go tests. The test results are given in Table 11.

Downloaded by [Visvesvaraya Technological University (VTU Consortium)] at 22:02 01 March 2016

Table 11. Effect of hot metal projectiles effect on detonating fuse.

Weight of donor, cap sensitive emulsion (kg)	D (m)	Weight of acceptor, DF (kg)	Z, (D/kg$^{1/3}$)	Results
0.292	0.30	0.30	0.226	Detonation
0.292	0.60	0.30	0.904	Detonation
0.292	0.85	0.30	1.210	Failed
0.375	0.80	0.30	1.110	Detonation
0.375	0.80	0.30	1.110	Detonation
0.375	1.00	0.30	1.39	Failed

Figure 9. Experimental setup for DF to cartridge with projectile.

Figure 10. Misfired cartridge with hot projectile.

2.10 *Effect of hot metal projectiles on emulsion explosives/emulsion matrix (Isothermal Condition)*

Detonating fuse of 0.30 to 0.31 kg was fired in hard PVC pipe/steel cannon. The nut and bolts of 0.10 to 0.15 kg were placed inside the cannon/PVC bore. The distance of explosive and nut and bolts was 0.05 to 0.10 m from mouth of the cannon. The experimental setup and post detonation results are shown in Figures 9 & 10. The detonating fuse coil was fired with electric detonator. Their effects on emulsion explosives were recorded.

Table 12. Effect of hot metal projectiles on doped emulsion matrix and cartridge emulsion.

Weight of donor, detonating fuse (kg)	D (m)	Weight of acceptor, emulsion explosives/ emulsion matrix (kg)	Z (D/kg$^{1/3}$)	Results
0.30	0.6	2.5	0.944	No detonation
0.30	0.3	2.5	0.226	No detonation
0.30	0.3	0.375	0.505	No detonation
0.30	0.3	0.375	0.450	No detonation
0.30	0.1	0.375	0.150	Partial deflagration
0.30	0.3	6.25	0.450	No detonation
0.30	0.1	6.25	0.150	No detonation

The Z value for different distance was calculated for go or no go tests. The results of tests are shown in Table 12. In experiment no detonation was recorded.

3 EFFECTIVE DISTANCE COMPUTATION

On the basis of simulation technique and Z values (D/kg$^{1/3}$) various effective zones of burnt/high order deflagration/detonation were computed.

Case I: Donor is explosive and acceptor is detonating fuse.

The effective zones were computed by using Z value. The results are shown in Table 13.

Case II: Donor is detonating fuse and acceptor is doped emulsion/AN.

The effective zones were computed by using Z value and results are shown in Table 14.

4 RESULTS AND DISCUSSION

The results shown in Table 6 indicate that emulsion matrix was not sensitive to detonators & cast booster (PETN+TNT) when fired in hard PVC tube. However, it was sensitive to booster when doped with more than 30% ammonium nitrate prills. Results in Tables 7 and 8 shows that emulsion matrix and detonating fuse were not sensitive to flame. They burnt in unconfined condition.

Table 13. Effective zone for different weight of explosive for detonation of detonating fuse as acceptor because DF is sensitive to shock, hot bullet, flame etc.

Explosive weight (kg)	Distance without bullet (m)	Distance with hot bullet (m)
50	3.06	4.08
100	3.85	5.144
150	4.41	5.304
200	4.86	5.84
300	5.56	6.68
500	6.59	7.92
1000	8.30	9.97
1500	9.50	11.42
2000	10.46	12.56
3000	11.97	14.38

Table 14. Effective zone for different weight of detonating fuse for detonation of doped emulsion/AN as acceptor because emulsion explosive is almost insensitive to shock, hot bullet, flame etc.

Weight of detonating fuse (kg)	Distance (m)
100	0.69
200	0.87
300	1.00
400	1.10
500	1.20
700	1.32
800	1.40
900	1.44
1000	1.50
1200	1.60
1400	1.67
1600	1.75

When flame was withdrawn, the burning quenched within, but under confined condition the detonating fuse deflagrated and no detonation recorded. The results shown in Table 9 indicate that the emulsion matrix was not burnt in isothermal condition, but in adiabatic condition it deflagrated at above 160°C and an explosion was recorded.

Doped emulsion was found to be more sensitive as compared to emulsion matrix. The results shown in Table 10 indicated that detonating fuse burnt and deflagrated due to detonation flame. The Z value for each test was computed and it was found that at lowest value 0.41 m/kg$^{1/3}$, the fuse only burnt without explosion.

The results shown in Table 11 indicate that detonating fuse was found sensitive to hot bullet impact at Z value 1.11 m/kg$^{1/3}$. It is found that DF was detonated by impact of hot projectiles and failed at Z value 1.39 m/kg$^{1/3}$.

Emulsion matrix and doped gassed emulsion were sensitive to hot projectiles at minimum value 0.150 m/kg$^{1/3}$ as in Table 12.

It was recorded that matrix become sensitive when it was rubbed in any confined condition.

The effective distances were computed for PETN (as DF) as receptor and results are shown in Table 13. The effective distance for 500 kg of explosive to PETN is 6.59 m without projectiles and with projectiles the distances increases to 7.92 m. Similarly, for 3000 kg of explosive, the effective distances are 11.97 and 14.38 m without projectiles and with projectiles respectively.

The effective distances for emulsion matrix/doped emulsion was computed and results are shown in Table 14. The results indicate that for 1400 kg PETN (as DF) the effective distance was 1.67 m to deflagrate emulsion matrix/doped emulsion.

The Tables and accidental site indicate that most of the damages were due to air overpressure of 30 to 40 m effective zone. The results indicated that there were two sounds, first may be due to thermal explosion of emulsion matrix in loading system and second may be due to detonation/sympathetic detonation/deflagration in detonating fuse.

5 CONCLUSIONS

From the above studies the following conclusions are made:

- Emulsion matrix and emulsion explosives may burnt or explode under the adiabatic condition that depends upon the quantity.
- Detonating fuse gets burnt/deflagrate in isothermal condition due to heat.
- Detonating fuse and other initiating devices viz. detonators, shock tube, MS connectors, etc may be detonated due to impact of hot particles, projectiles or excessive heat in adiabatic condition.

ACKNOWLEDGEMENT

The investigation team is thankful to explosive industries for their co-operation during the investigation period. Thanks are also due to the Director, Central Institute of Mining and Fuel Research, Dhanbad for giving permission to publish this paper.

Downloaded by [Visvesvaraya Technological University (VTU Consortium)] at 22:02 01 March 2016

REFERENCES

Adhikari, G.R., Venkatesh, H.S., Theresraj & Balachander, R., 2007. Measurement and analysis of air overpressure from blasting in Surface Mines, *Visfotak-Explosives Safety & Technology*, vol. 1, No. 2, India.

Folchi, R, 1996. Explosion and Hazard Assessment for Explosives, *Ammunition and fertilizing agents Facilities after EU Directive 96/82/EC " SEVESO II",* download from Internet.

Hans, Perlid. 1996. Pump Safety Tests Regarding Emulsion Explosives, *Notro Nobel AB/Dyno Explosives Group,* Gyttorp, Nora, Sweden.

Mainiero, R.J. & Rowland J.H. 2009. A review of recent accidents involving explosive transport, *International Journal of Explosive Engineers*, USA.

Nabiullah, M.K., Gupta, R.N. & Singh, B. 1989. Studies on the thermal behavior of detonating fuse and detonators, *Journal of thermal Analysis,* vol. 35, page 1166–1172, Budapest.

Pingua, B.M.P., Nabiullah, M.K., Mishra, G.D. & Patel, K.L. 2008. Study on underwater blasting energy and flame characteristics of detonators and detonating fuse, *Sci. Tech. Energetic Materials,* vol. 69, No. 6, Japan.

Downloaded by [Visvesvaraya Technological University (VTU Consortium)] at 22:02 01 March 2016

Energy and Performance

Performance of Explosives and New Developments – Mohanty & Singh (Eds)
© 2013 Taylor & Francis Group, London, ISBN 978-0-415-62142-7

Author index

Boosters and Initiators

Explosives, Explosions and New Developments